The Effects Of Elevated Temperature And Cycle Rate Variations Upon The Low-cycle Fatigue Resistance Of Some Low-alloy Steels.

66–2143

DePAUL, Robert Allen, 1936–
THE EFFECTS OF ELEVATED TEMPERATURE AND CYCLE RATE VARIATIONS UPON THE LOW–CYCLE FATIGUE RESISTANCE OF SOME LOW–ALLOY STEELS.

Lehigh University, Ph.D., 1965
Engineering, metallurgy

THE EFFECTS OF ELEVATED TEMPERATURE AND CYCLE RATE VARIATIONS UPON THE LOW-CYCLE FATIGUE RESISTANCE OF SOME LOW-ALLOY STEELS

by

Robert Allen DePaul

A Dissertation

Presented to the Graduate Faculty

of Lehigh University

in Candidacy for the Degree of

Doctor of Philosophy

in

Metallurgical Engineering

Lehigh University
1965

CERTIFICATE OF APPROVAL

Approved and recommended for acceptance as a dissertation in partial fulfillment of the requirements for the degree of Doctor of Philosophy.

Sept 13, 1965
(date)

Alan W. Pense
Professor in Charge

Accepted, Sept 13, 1965
(date)

Special committee directing the doctoral work of Mr. Robert Allen DePaul.

Alan W. Pense
Chairman

Edward N. Kottcamp Jr

Voris V. Latshaw

George Kramer

ACKNOWLEDGMENTS

The author extends his sincere appreciation to Dean Robert D. Stout and Dr. Alan W. Pense for their technical guidance and encouragement throughout the course of this investigation. Special thanks are also due Mr. David S. Malyevac for supplying the 1100 cycle per hour, "T-1" fatigue data. Mr. Martin Sheska and his entire machine shop staff are to be commended for their willing cooperation and expediency in specimen preparation and equipment maintenance. And finally, the patience and understanding encouragement of the author's wife, Anne, is noted and most sincerely appreciated.

The financial aid granted by the Materials Division of the Pressure Vessel Research Committee of the Welding Research Council made this work possible.

TABLE OF CONTENTS

TABLE OF CONTENTS (cont'd)

LIST OF TABLES

LIST OF FIGURES

LIST OF FIGURES (cont'd)

LIST OF FIGURES (cont'd)

LIST OF FIGURES (cont'd)

LIST OF FIGURES (cont'd)

LIST OF FIGURES (cont'd)

ABSTRACT

The influence of elevated temperature and cycling frequency upon the fatigue behavior of moderate-strength, low-alloy steels was investigated. 5,000 to 100,000 cycle lifetime fatigue tests were performed on A-212,B; A-387,B; and "T-1" steels at cycle rates of 110, 1100, and 12,000 cycles per hour. Temperatures of 400°F, 600°F, 800°F, and 900°F were applied in the reversed bending, constant deflection tests. All three steels were tested in the spray quenched and stress relieved condition, while the A-212,B and A-387,B steels were also tested as normalized and stress relieved.

It was found that in general, the 5,000 and 100,000 cycle life fatigue resistance of the three steels tested was not markedly changed over the temperature range from room temperature to 800°F, except in temperature intervals where strain aging phenomena appear to intervene. There was no predictable influence of cyclic variation noted applicable to all steels and conditions. A series of peaks or maximum allowable strains were revealed when total strain was plotted against testing temperature. The distribution of these peaks indicated a strain-rate sensitive aging phenomenon which became operative at lower temperatures with lower cycle rates. The A-387,B steel seemed to be more sensitive to such a phenomenon than the other two steels tested.

An empirical relationship was developed using Coffin's generalized expression, $\epsilon N^m = c$, where ϵ is a total strain value, N is the lifetime in cycles, m is the absolute value of the slope of the log-strain versus log-cycles curve, and the constant, c, is a material parameter. Fatigue

behavior for similar alloys can be predicted within reasonable error by the relationships presented. In general, $\epsilon_{5,000}$ can be estimated from the steel's reduction in area at the temperature in question and the material parameter can be obtained from the temperature, yield to tensile ratio, and total alloy content of the steel. The 5,000 to 100,000 cycle fatigue curve could be predicted from this information.

The application of the elevated temperatures and cycle rate variations did not alter the basic microstructure of the steels during testing, nor the general transcrystalline crack propagation path as previously noted in room temperature tests. Deformation bands were noted in the normalized and stress relieved A-387,B specimens when tested at temperatures of 800°F and 900°F.

INTRODUCTION

Since the advent of the utilization of metals in machine members or components, certain of these components have been known to fail after being subjected to repeated or varying loads without any plastic deformation to warn of the impending fracture. This, in view of the fact that a static load of equal magnitude was safely carried by a similar component with no apparent difficulty, has led to the concept of fatigue as a mode of failure. Generally speaking, metal fatigue can be defined as a mode of failure associated with an externally applied cyclic load of such a magnitude as to be well within the capacity of the material if applied in a static fashion.

The importance of fatigue as a fracture mode dates back to the early part of the 19th Century when Albert [1] in 1829 proof-tested mine-hoist chain links by repeated loading in tension prior to their being placed into service. Rankine [2], in the mid-1840's, recognized stress raisers in the form of "sharp angles" in machine components as potentially dangerous with respect to fatigue failure. Shortly after this, the expansion of the railway system raised questions on the effect of repeated loading upon axles, wheels, rails, and bridges. The result of such questions was the initiation of several comprehensive studies by Hodgkinson [1], 1849, and Fairbain [1,2], 1864, in Great Britain and Wohler [2], 1852, in Lower Silesia, on the effects of repeated bending and torsion on railroad axles and related equipment.

Much of the European work on fatigue was ignored by most American investigators [3,4] of the late 1800's. However, the discovery, in the

early 20th Century [1,2,5], that slip band formation occurred with the application of a cyclic load changed their way of thinking.

The scientific advances made in the first half of the 20th Century revealed that not only were railroaders to be vitally concerned with fatigue, but the DeHaviland Comet aircraft failures of 1954 [6] proved that fatigue could not be ignored in aircraft design as well.

There has been a vast amount of information published on the subject of fatigue since 1900 as can be witnessed by reviewing the annual bibliographic listings of fatigue published by ASTM since 1950 [7]. The work at Lehigh University, since the early 1950's, has extended this knowledge, particularly of behavioral aspects of steels suitable for pressure vessel application, in low-cycle-life fatigue tests [8,9,10,11,12].

Ultimately, the primary purpose of fatigue testing is to predict the behavior of metals used in service applications in which repeated loads are experienced. To this end, various types of fatigue tests have been developed and are being applied today.

However, as in any type of laboratory mechanical test, the relation between test results and service behavior is always in doubt. In addition to this doubtful relationship in itself, there are further complications due to scatter in the laboratory test [13]. This scatter is due to many causes. Any material which is commercially produced has inherent inhomogenieties which account for a great deal of variance. A major culprit is a local strength differential associated with multiphase structures, grain boundaries, and inclusions, all of which are present in degree in today's commercial steels. A possible cause of scatter

one step removed from the material is the specimen itself. It is difficult to assure oneself that each and every specimen was prepared in such a way that possible variables such as ingot chemistry variations, hot working effects in rolling and forming, and cold working effects in machining were all held constant from specimen to specimen. A third major scatter producer is variation in testing conditions from test to test. Such variables could include precise alignment in specimen set-up, ambient temperature, humidity, and air flow about the specimen in high speed tests. An important variable in testing conditions where elevated temperatures are concerned is the technique of monitoring the temperature [14]. Most experiments, because of inadequate testing procedures, measure only the mean statistical temperature of the specimen. However, local temperatures, especially along slip planes, may increase considerably during deformation in testing. It is clear that predictions of service behavior based upon laboratory fatigue tests cannot be made with 100% certainty.

To avoid the obvious danger of underdesign, a substantial margin of safety must be imposed upon each and every structure experiencing cyclic loading. This safety factor should make allowances for the uncertainties involved in material preparation, component manufacture, and the specific service conditions prevailing.

The best approach to the aforementioned problem is a simple comparison between a large number of laboratory tests and an equally large number of prototype structures to ascertain the character of the relationship between the two types of results. The comparison is simple,

but the approach is not feasible from an economic point of view. (The Appendix of this dissertation includes the results of such a comparison based upon limited data involving prototype pressure-vessels.) As one might expect, the cost of such a comprehensive study would be prohibitive as would be the time involved in gathering data.

The best approximation to such a prototype study is a statistical evaluation of fatigue data generated from laboratory tests which hopefully closely duplicate expected service conditions. However, the use of statistics is not a finite science either. A degree of uncertainty is a "built-in" feature of any statistical technique. Also, statistical evaluations require large populations of data in order to yield results with any reasonable degree of certainty. Depending upon the structure being tested and the type of fatigue test being used, this large number of data points may also be impractical. Fatigue data, especially those from a limited number of tests, cannot be safely generalized into any universal relationships, but conclusions from these tests must be restricted to the materials and conditions to which they directly apply.

Historically, investigators have approached the concept of fatigue through parameters involving, for the most part, the endurance phenomenon. This endurance limit is a stress value determined from a number of fatigue tests, below which it is assumed fatigue failure will not occur over an infinite number of cycles. The stresses involved in such a test are such that the elastic limit of the material is seldom exceeded, thus no generalized material flow or plastic deformation is experienced. The degree of scatter under such conditions is large owing to the dependence

of failure upon the presence, size, and distribution of various imperfections from specimen to specimen. Endurance testing is also very dependent upon surface conditions of the specimen.

Such is not the case in the type of fatigue test utilized in this study. The fatigue lifetimes of interest vary over the range 5,000 to 100,000 cycles to failure, whereas endurance testing involves 10-million or more cycles. This shorter life-span necessitates the use of higher applied stresses to cause earlier failure. As a result of the higher applied stresses, the material's elastic limit is exceeded and one is faced with a complex combination of elastic and plastic strain components as opposed to the simple elastic strain system of endurance testing. The presence of these high strains introduces plastic deformations which tend to relieve the stress concentrating effect of surface flaws. One finds then, that in tests involving these higher stresses, the surface conditions and presence of imperfections are not as critical in determining failure as they were in endurance testing [15]. This factor naturally leads to a smaller degree of scatter.

A schematic representation of the stress distribution for a beam in simple bending is shown in Figure 1 [16]. The common mathematical approach to a bending beam involves the flexural formula for elastic beams

$$\sigma = \frac{Mc}{I} \tag{1}$$

The distribution described by equation (1) is shown in Figure 1(a) where σ is the outer fiber stress, M the applied bending moment, c is the distance from the neutral axis of the beam to the point of interest (in this case the outermost fiber), and I is the moment of inertia for the

beam configuration. Should the testing conditions be such that plastic flow can occur in the outermost fibers of the beam specimen, the stress distribution might look something like that shown in Figure 1(b). As a boundary condition of plastic behavior, the stress distribution would appear as in Figure 1(c). The outer fiber stress in this condition would be given by

$$\sigma = \frac{2Mc}{3I} \tag{2}$$

It can be seen that in the limiting case of all-plastic stress, the maximum outer fiber stress as calculated by equation (2) would be two-thirds that of the pure elastic stress distribution, and one might observe an apparent increase in fatigue strength under such conditions. The presence of such massive plastic deformation could inherently increase the scatter of fatigue results since the degree of plastic deformation could conceivably vary from specimen to specimen. A common concept of such massive deformation would be simply creep. Such creep could be involved in elevated temperature fatigue tests. The subsequent redistribution of stresses to a condition of an elasto-plastic stress system would further complicate the interpretation of the data. In addition, this creep behavior is itself dependent upon a number of variables including composition and microstructure. Thus the occurrence of creep adds to the scatter factors where elevated temperature fatigue tests are involved.

While it is customary to refer to fatigue studies from the standpoint of applied stress to failure, one finds, for the magnitude of stresses applied in this investigation, it is wise to rely upon strain as a primary variable rather than stress. Low [17] noted a continuous

behavior in strain versus fatigue-life plots for lifetimes in the 100 to 1,000,000 cycle range whereas a stress versus fatigue-life plot was not continuous throughout this same range. This can easily be explained by considering the yield point phenomenon. Low concluded that the continuity under strain conditions suggested that strain rather than stress be considered as the cause of fatigue failures. Johansson (18) states that a constant strain amplitude gives more stable conditions when testing in the plastic region than does a constant stress amplitude or a constant bending moment. Thus the results and terms used in the dissertation pertain to allowable total strain, rather than stress, for failure.

The need for further fatigue data concerned with low-cycle lifetimes is necessitated by the many developments in science and engineering in recent years. As more data are gathered and more knowledge gained about material behavior under fatigue loading, the resulting designs more closely approach optimum conditions. With advances in knowledge of plasticity theory and elasto-plastic stress conditions some degree of yielding can be tolerated. Consequently both material and cost can be spared.

While the majority of structures are expected to last indefinitely, there are situations where an assembly such as a missile is expendable after a finite lifetime. There are also those cases where cycle rates are so low that a reasonable lifetime may involve a small number of cycles as opposed to the millions of cycles involved in endurance tests. Such examples as high-pressure vessels, heavy guns, and pipe would fall into this latter grouping. A specific example of such a limited life-

time would be a pressure vessel such as that used in a nuclear reactor which might have a useful lifetime of 100,000 cycles [19].

Recently, several investigators [20,21,22] have developed empirical mathematical relationships in an attempt to characterize the low-cycle fatigue behavior of metals. For the most part, however, these expressions have been based upon room temperature fatigue tests, and are, therefore, limited in their application to the total concept of fatigue.

The form of these expressions is given, in general, by

$$\epsilon N^m = c, \tag{3}$$

where ϵ is a specified strain in the specimen, N is the number of cycles to failure, while m and c are constants. Coffin [20] has suggested that the strain factor be one of plastic strain, the exponent, m, equal to one-half for most materials, and the constant c related to the fracture strain found from a standard tensile test of the material. Others [23,24] have found that for lifetimes in excess of 5,000 cycles, and ranging up to 100,000 cycles, the total strain range value rather than the plastic strain as applied by Coffin is more useful. This is in agreement with some previous work by the writer [25] in which it was found that Coffin's equation and constants did not apply to the data obtained from the materials and type of specimen utilized in the current study for lifetimes in excess of 10,000 cycles.

In addition, the exponent, m was found not to be one-half (m is experimentally determined as the absolute value of the slope of the log-total-strain versus log-cycle fatigue curve). In no case did this value of m reach Coffin's suggested one-half [24].

For many applications, cyclic loading of high strains would not be experienced at a rate of several hundred or thousand a minute, but rather one an hour or even one per day. The low rate of one cycle per hour or one per day experienced in service is the basis for applying a cycle rate variable in this study. As previously stated, regardless of the care exercised in planning an experiment which closely approximates actual service conditions, there are some variables which are not practical to reproduce. Such a variable is an extremely low cycle rate in fatigue tests. It would be out of the question to run tests at one cycle per day and hope to obtain meaningful data within a useful period of time. It is hoped, therefore, that the results of a series of cycle rates ranging from 200 cycles per minute down to 2 cycles per minute may provide the ability to extrapolate to the even lower rates of one cycle per hour or one per day. Naturally, this extrapolation involves some doubt but certainly less doubt than generalizing on the basis of rotating beam fatigue tests at a rate of 5,000 cycles per minute as Waisman[26] proposes. It should be mentioned, however, that Waisman was referring to the endurance limit when he stated that over a wide range, the frequency does not influence the fatigue life at room temperature up to 5,000 cycles per minute.

However, Benham[27] introduces the possibility for an effect of cycle rate when he noted that regardless of the generally accepted theory in conventional fatigue testing, that of a negligible effect on lifetimes for cycle rates between 500 and 10,000 cpm, there is definite evidence to support the contention that a decrease in lifetime may result from a drop in frequency from, say, 500 to 1 cpm.

The above considerations take on added significance when one introduces the influence of elevated temperature upon fatigue behavior. While it is commonly accepted that the tensile properties of most steels deteriorate with increasing temperature, apparently little attention has been paid to the effect of elevated temperature conditions upon fatigue life. Perhaps, since the endurance limit has been found to be related to the ultimate tensile strength of a steel, it has been assumed that if you concern yourself with the breakdown of the tensile properties, the fatigue behavior will follow. This, of course, is true but only to a point. Allen and Forrest[28] have noted a shift in the temperature of peak fatigue strength when compared to a similar peak in tensile properties. They relate this shift to a stress-sensitive change occuring in the fatigue specimen during testing. For want of a better phrase one might apply the term strain-aging to this phenomenon. Coffin[29,30] noted a modification in the fatigue behavior of AISI 1010, 1111, and a 0.1%C - 2.0%Mo steel which appeared as an aging effect. It is suggested that these aging effects may be sensitive to composition and strain range as well as strain rate. It has been observed that a decrease in strain rate accompanied by an increase in strain range induces an aging phenomena to occur at lower temperatures in some cases, while intensifying the effect in others.

For a mild steel the general decline in tensile strength with increasing temperature is interrupted by a maximum strength value at about 485°F[28]. Fatigue resistance in tests at 2,000 cpm varies similarly with temperature. The major exception is a displacement of the maximum from 485°F for tensile strength to 650°F for fatigue strength.[31] Forrest

showed that the temperature of peak fatigue strength is lowered by lowering the cyclic frequency of testing. Tests run at 10 cpm [28] reduced the peak strength temperature to between 400 and 575°F. An increase in the fatigue strength is also noted for the lower speed. These results suggest that strain aging during an entire fatigue test is not sufficient to raise fatigue strength noticeably but that it is necessary to lock dislocations within the period of one stress cycle to obtain an appreciable effect. Baird [32] attributes this behavior to the presence of carbon and nitrogen acting as an obscure dislocation locking mechanism within a single stress cycle and refers to this behavior as dynamic strain aging. The term "dynamic strain aging" is used to denote aging processes occuring simultaneously with plastic strain. Rally and Sinclair [33] have shown that an increase in testing temperature raises the knee of the S-N curve to a higher stress and a lower number of cycles, which is in agreement with the strain aging mechanism.

Since the previous work has been limited substantially to room temperature data, one of the purposes of the present study should be to indicate the feasibility of a mathematical statement, comparable to that of Coffin's, applying to elevated temperature fatigue behavior, covering the low-cycle region and possibly cycle rate variations as well. The financial support for this study was supplied by the Materials Division of the Pressure Vessel Research Committee of the Welding Research Council. A complimentary study, sponsored by the Fabrication Division of this same group, was performed simultaneously at Lehigh and dealt with the creep and stress rupture behavior of a series of steels.

The decision to run fatigue tests over the range of 600 to 900°F for this study was made to ascertain the interplay between fatigue and the onset of creep and to learn more about this strain aging phenomenon with respect to common, moderate-strength, low-alloy pressure-vessel steels. The materials chosen for the study were selected on the basis of their availability to, and potential use by pressure vessel fabricators. All three steels are commonly used today in pressure vessel applications and show some potential for limited elevated temperature service. These steels are described in the materials section.

The goal of this study is to expand the knowledge specifically of the fatigue behavior of the materials chosen with the hope that a more sophisticated design criteria will emerge for elevated temperature applications. That is, it is hoped that the results of the two complimentary programs can be combined such that one can determine at what point in elevated temperature applications one must become concerned with either stress rupture or fatigue failure as a limiting design value as opposed to the one-quarter of the ultimate tensile strength criterion used today. The variation in applied cycle rate should provide a better insight into the effects of extremely slow stress variations in service vessels. To some degree, the variation in testing temperature may expose application limitations pertaining to each specific steel tested. And finally, it is hoped that, should a relationship exist between fatigue behavior and some easily obtainable material parameter, this relationship could be developed in such a fashion as to permit prediction of fatigue behavior with a reasonable degree of confidence.

EXPERIMENTAL PROGRAM

Approach

In view of the ultimate objectives of a comprehensive research program at Lehigh University studying the effects of elevated temperature service upon low-alloy, moderate-strength steels, the following experimental approach was conceived. The entire fatigue research program is easily sub-divided into four basic phases consisting of first, the actual mechanical testing phase involving tensile and fatigue tests at ambient conditions and in the elevated temperature range of 600°F to 900°F. A variation in cycle rate was utilized in the fatigue program in that fatigue curves were generated at 1100 and 12,000 cycles per hour respectively with a limited number of tests at 110 cycles per hour.

The second phase involves a more detailed investigation of some unexpected results of phase one. This work deals basically with the anomalous fatigue behavior exhibited by the "T-1" steel at 800°F and 900°F when tested at 12,000 cycles per hour. This secondary study consisted of aging "T-1" specimens prior to testing at 800°F for various lengths of time. Any change in fatigue behavior as compared to the unaged specimens of phase one was noted. Tensile specimens and charpy bars were cut from the broken "T-1" fatigue specimens in an effort to ascertain the aging effect on the tensile and impact properties.

Part three of the research program involved the mathematical interpretation of the elevated temperature fatigue data from the stand-

point of temperature and cycle rate effects. In all cases a single or double linear least-square analysis was made on each set of fatigue data. There is a set of data for each of the three steels in each heat treatment condition utilized at each of the four testing temperatures and for each of the two cycle rates for a total of forty separate fatigue curves.

Particular emphasis was placed upon the slope of the least squares line and the 5,000 and 100,000 cycle strain values. A multiple regression analysis was performed with the previously mentioned fatigue curve values as dependent variables and the various tensile property values and chemical compositional values as independent variables. The resulting regression equation was applied as an empirical relationship in predicting fatigue behavior from tensile and compositional data.

The fourth phase of the program involved light and electron microscopy in studying the secondary crack morphology of the fatigue specimens tested at each of the four temperatures under low, moderate, and high applied strain levels. A plastic replica technique was employed in the electron microscopy phase using chromium shadowing and a carbon backing to obtain a film for viewing.

Materials and Heat Treatments

As previously mentioned, the materials chosen for study were selected for their potential to be utilized in pressure vessel applications where limited elevated temperature service is anticipated. The steels which were selected are ASTM designated A-212 (Grade B) and A-387 (Grade B), while the third steel is a United States Steel Co. proprietary material labeled "T-1". The A-212,B is a plain carbon

steel with the carbon content in the 0.25% to 0.30% range. The A-387,B is a chromium-molybdenum grade of about 1.0%Cr and 0.5%Mo, while the "T-1" is a complex alloy steel containing restricted amounts of nickel, chromium, molybdenum, copper and vanadium. The chemical analyses for the specific heats of steel used in the study are listed in Table I. It was necessary to use two different heats of each type of steel in the investigation, and this is noted in Table I where both compositions are given. Identical heat treatments were applied to the corresponding heats and room temperature fatigue tests were performed to ascertain any differences in the fatigue characteristics resulting from compositional effects.

The A-212,B and the A-387,B steels were tested in the quenched and tempered, and in the normalized and stress relieved condition. The austenitizing temperature for the A-212,B steel was 1650°F while that for the A-387,B grade was 1675°F. Austenitizing time in all cases was one hour. The tempering and stress relieving temperature for both grades was 1150°F and the time at temperature was one hour. The "T-1" steel was tested in the mill-quenched and tempered condition only. This mill treatment involves an austenitizing temperature of 1700°F with a tempering treatment of 1200°F for a sufficient length of time to produce the prescribed tensile properties.

All heat treatments involved in the study (with the exception of the "T-1" steel" were performed on 3/4" thick plates, 12" in width and 18" long. The normalizing was performed in a still air quench while the spray quenching was performed in accordance with the technique established by Canonico [34].

Four specimens of the geometry shown in Figure 2 were cut from each of the normalized 12" x 18" plates. Stress relieving followed the milling operation but preceded final grinding of the reduced section which took place immediately prior to testing. Three specimens were cut from each of the spray quenched plates following tempering. A larger "waste-piece" was cut from the quenched 12" x 18" plate prior to removing any usable specimens to avoid possible edge-effects resulting from the spray quenching.

Testing Equipment and Procedures

Tension Tests: All tensile testing was performed on 0.252-inch diameter, one-inch gage length specimens. The testing temperature was held to $\pm 5°F$ at temperature levels of 600°F, 700°F, 800°F and 900°F in addition to ambient conditions and all specimens were broken in air. Heating was accomplished by way of a resistance furnace. A strain rate of 0.05 inches per minute was used through the tension tests which were performed on an Instron Tensile Testing Machine. The data recorded and tabulated consisted of yield strength, ultimate tensile strength, elongation, reduction in area, strain hardening exponent, and the yield strength to tensile strength ratio for all steels and conditions.

Fatigue Specimen: The fatigue testing was performed using the standard Lehigh reversed bending cantilever fatigue specimen (R=-1) shown in Figure 2, and a constant deflection type of loading. As can be seen from the specimen geometry, the width to height (or thickness) ratio is 5 to 1 providing for a 2:1 biaxial stress distribution at the center (35). All specimens were cut from 3/4" x 12" x 18" plates with the longitudinal

axis of the specimen parallel to the rolling direction of the plate. The reduced section of the specimen was milled and subsequently ground to an 80-grit finish with the scratches running parallel to the longitudinal axis of the specimen (perpendicular to the plane of fatigue crack growth). A complete description of the test has been published elsewhere [8,9].

Fatigue Testing Apparatus: The fatigue testing apparatus shown in Figure 3 is one of two such units built especially for this investigation to complement a third existing machine described by Laxar [36]. This third testing machine applies a similar load to the specimen but has a different drive mechanism.

Basically the fatigue testing apparatus consists of a fixed support which holds the short end of the specimen rigid and an arm which applies a vertical reciprocating motion to the free end of the specimen during testing. The deflection of the free end of the specimen is varied by means of an adjustable eccentric cam unit mounted on the end of the motor drive shaft. Thus the strain in the specimen can be varied simply by altering the eccentric cam setting prior to each test. Provision is made so that the cycle rate can be varied by means of a more elaborate back-gear arrangement utilizing a chain-sprocket drive for positive action. The standard cycle rate of 12,000 cycles per hour was used for part of the testing program and these resulting fatigue curves were compared with those obtained at 1100 cycles per hour (or a 10 to 1 reduction in cycling speed), and limited data at 110 cycles per hour (or a 100 to 1 reduction).

Complete fatigue curves were obtained for tests at room temperature, 600°F, 800°F, and 900°F in air for the 12,000 and 1100 cycle per hour rates. Also, 5,000 cycle life strain values were obtained at the 110 cycle per hour rate. The elevated temperatures were attained using a resistance-type furnace which enclosed the fixed grip and the specimen length up to within several inches of the movable clamp. Test specimens with embedded thermocouples indicate a temperature variation of ±10°F within the center of the reduced section. The equipment shown in Figure 3 shows the furnace raised to reveal the specimen in testing position.

Strain Measurements: Strain measurements on the room temperature specimens were made with a Tuckerman optical strain gage having a nominal 1/4-inch gage length. The gage-length straddled the midpoint of the reduced section and registered total strain over several complete cycles of reversed bending. Vertical deflection readings at the free end of the specimen were also recorded with the strain readings. By calculation one could ascertain the equilibrium or midpoint deflection of the specimen as indicated by a dial gage. By flexing the specimen to its maximum deflection in one direction and returning to the midpoint position one could obtain a Tuckerman reading. Repeating the process in the reversed direction would result in a second Tuckerman reading. The difference between these two Tuckerman readings is a measure of the plastic strain range imposed upon the specimen in one complete cycle of reversed bending. All strain readings were made and recorded after the tenth cycle to eliminate any possible errors resulting from strain hardening effects (10).

A special mechanical fixture had to be devised for strain measurements at the elevated temperatures. This fixture is in the form of an inverted "U" and is mounted on the specimen by way of a knife edge and a slotted nut, both of which are rigidly attached to the specimen through three threaded studs which are welded to the specimen. The strain in the specimen is transmitted by the fixture to the thin cross-piece of the U-shaped bracket. A foil-type resistance strain gage is mounted on the cross-piece in such a fashion as to experience a flexure whenever the specimen is flexed. Maximum and minimum microinch values of strain in the gage were noted on a Baldwin SR-4 Strain Indicator. These microinch differences yield specimen strain values by way of a room temperature correlation with the Tuckerman strain gage. Effectively the mechanical fixture has a one-inch gage length at its point of attachment to the specimen. The strain readings were made, as in the room temperature tests, after ten complete cycles had been experienced by the specimen.

Failure Criteria: All strain data taken are in the form of percent total strain range and percent plastic strain range to failure. Specimen failure is defined as the point at which the flexed section can no longer transmit a useful load to the fixed end. This point is determined by zero deflection as registered by the Baldwin strain recorder which in this case is connected to an SR-4 type resistance strain gage mounted on the vertical loading arm of the fatigue machine. A no-load condition experienced by the arm dictates failure of the specimen.

PRESENTATION AND DISCUSSION OF RESULTS

Elevated Temperature Tensile Properties

The data from the elevated temperature tensile tests are listed in Table II and are presented graphically in Figures 4 through 6.

Figure 4 reveals the expected drop-off in ultimate tensile strength and yield strength with increasing testing temperature. It is evident that only one steel, the "T-1", shows any marked peak in tensile strength with increasing temperature. The fact that the peak occurs at a significantly higher temperature than that noted by Allen and Forrest[28] for a mild steel may be a consequence of the complex composition of the "T-1" or could possibly be an effect of strain rate. While no tensile tests were performed at 400°F and 500°F, the literature[37] reveals no major maxima or minima within the room temperature to 600°F range. It can be noted that there is a mild decrease in strength for the A-212 steel in both the quenched and tempered, and the normalized and stress relieved conditions to 600°F. From 600°F to 900°F the tensile strength deteriorates at an increasing rate for both conditions as might be expected for a low-strength, plain carbon steel. The normalized and stress relieved condition of the A-387,B also shows this small initial decline in tensile strength, but in this case a slight recovery is noted at 700°F, followed by a drop-off in strength to 900°F. The A-387,B grade differs from the A-212 in that there is a marked separation between the two heat treated conditions of the A-387,B, while the strengths of the two comparable conditions of A-212 differ only slightly at each temperature. This difference is a ramification of the relative hardenabilities of

the two steels. The absence of any substantial alloying elements in A-212 and its low carbon content necessitate a rather poor hardenability as compared with A-387,B. The quenched and tempered A-387,B, while starting at a considerably higher tensile strength at room temperature, shows much the same general effect of increasing temperature as its normalized and stress relieved counterpart; the only difference being that the strength level for the quenched and tempered steel is shifted to higher values throughout the temperature range. The microstructures of the steels in the various heat treated conditions differ by degrees. A later section of this dissertation is devoted to the metallographic aspects of the study, but some distinct characteristics of the structures should be noted at this time. The A-212 steel, due to its relatively poor hardenability, shows only a slight difference between the quenched and tempered and the normalized and stress relieved conditions. Both structures are basically pearlite-ferrite aggregates with the outstanding distinction being the pearlite spacing. The pearlite in the quenched and tempered condition is unresolvable under normal light microscopy conditions while that of the normalized and stress relieved structure is coarse and easily resolvable. The A-387,B, steel shows a marked difference between the two heat treated conditions. The normalized and stress relieved structure is composed of ferrite and blotchy pearlite areas much too fine to be resolved by light microscopy. The quenched and tempered structure is composed of acicular ferrite-carbide networks, vastly different from the normalized and stress relieved structure. The "T-1" which is mill quenched and tempered is very similar in micro-

structure to the quenched and tempered A-387,B, with little significant to distinguish between the two.

As might be expected, the yield strength versus temperature plot of Figure 4 shows the same general effect of increasing temperature as was noted in the tensile strength plot. The same groupings exist for the latter figure in that the two conditions of the A-212 steel show similar strengths for all temperatures. The normalized and stress relieved A-387,B exhibits moderate strength, while the quenched and tempered A-387,B and "T-1" steels possess the highest strengths of the steels tested. The "T-1" and the A-387,B, steels show similar effects of increasing temperature upon yield strength.

The temperature effects upon ductility are shown in Figure 5. It should be noted that the expected increase in ductility associated with the decrease in strength above 700°F is generally exhibited by the two plots of Figure 5. The slight dip observed in the 600°F to 700°F region in the elongation plot is probably associated with a strain aging phenomenon during testing, as the corresponding peaks in the strength curves could also be attributed to a strain aging mechanism.

Figure 6 is a plot of strain hardening exponent versus testing temperature. It can be seen that the strain hardening exponent increases from its room temperature value to a higher value when measured at 600°F or 700°F. A general decrease in the strain hardening exponent is experienced above 700°F. This effect is most pronounced in both conditions of the A-212 steel. It is also interesting to note that the groupings observed in Figure 4 are maintained in this plot in Figure 6 with the only difference being that the order is reversed in that the

A-212 steels show considerably higher strain hardening exponents than do the quenched and tempered "T-1" and A-387,B, with the normalized and stress relieved A-387,B maintaining its central position.

The similar effect of temperature upon both the tensile and yield strengths result in rather constant yield strength to tensile strength ratios throughout the elevated temperature range. The one exception to this statement is the A-212 steel in which the yield to tensile ratios drop considerably from their room temperature values to those at 600°F and 700°F with a slight recovery at 800°F and 900°F. This occurs for both heat treated conditions of the A-212 steel. This same general trend is exhibited by the other steels, but the differences in the yield to tensile ratios throughout the temperature range are slight in these cases. It is this low yield to tensile ratio in the 600°F to 700°F range which causes the apparent marked response to temperature for the A-212 steels in Figure 6. The increase in the strain hardening exponent for the other steels is a combination of the factor previously mentioned combined with a decrease in ductility as observed in Figure 5. These combined effects produce a more steeply rising stress-strain curve, and therefore a larger strain hardening exponent. The increase in ductility in the 900°F region combined with the increase in yield to tensile ratio results in a decrease of the exponent as noted in Figure 6.

Fatigue Properties

All the data used in generating the fatigue curves are given in the Appendix. For ease of discussion and comprehension, only effects pertinent to two fatigue-life levels will be presented and discussed. These two lifetimes involve, essentially, the end points of the fatigue curves.

They are the strain ranges required for 5,000 and 100,000 cycle lifetimes. A third parameter to be presented is the slope of the log-strain versus log-number of cycles to failure plot. The strain ranges for failure at the two previously mentioned lifetime levels for the three steels studied are found in Table III along with the respective slopes of the fatigue curves.

12,000 Cycle per Hour Fatigue Tests

Figures 7 through 11 are the fatigue plots of log-total strain versus log-cycles to failure for the three steels studied in the various conditions of heat treatment. A series of three summary plots found in Figures 12, 13, and 14 reveal the effects of elevated temperature upon the total strain range for the 5,000 and 100,000 cycle ends of the fatigue curves and upon the slope of the respective curves. Figures 12 and 13 substantiate previous work[12] on different steels which indicates that higher strength materials, "T-1" and quenched and tempered A-387,B, in this case, are superior in room temperature fatigue resistance for 100,000 cycle lifetimes to the lower strength materials represented by the normalized and stress relieved A-387,B and both conditions of the A-212,B steel. However, the weaker but more ductile steels show superiority at the shorter lifetime of 5,000 cycles, again when tested at room temperature. This distinction was maintained generally for the 100,000 cycle data as the testing temperature was increased, but the 5,000 cycle data showed considerable variation with increasing temperature. Figure 12 shows that at 600°F, the 5,000 cycle total strain values were about equal to or slightly below the room temperature values for the "T-1" and the A-212,B steels. There was a marked increase

in fatigue resistance for both conditions of the A-387 steel over the same temperature range. While the A-212 steels showed definite increases in total strain at 600°F for 100,000 cycles, the values are still lower than those of the other steels, which remained about the same as at room temperature.

At 800°F, all steels and conditions showed a decrease in total strain range for 5,000 cycles, as did all but one series for the 100,000 cycle strain range. The exception was the quenched and tempered A-212 which recorded a 10% increase in allowable total strain range at 800°F for 100,000 cycle life over the 600°F value.

A testing temperature of 900°F introduces an apparent recovery in 5,000 cycle fatigue resistance in that all but two series show strain ranges approximately equal to, or greater than their respective room temperature values. These exceptions are the two heat treated conditions of the A-212 steel which show considerably less fatigue resistance at 900°F than they exhibited at room temperature. The 900°F recovery is evident for the 100,000 cycle plot also, but it is not as marked. Generally speaking, the effect of temperature seems to be much more drastic on the 5,000 cycle lifetimes as is evidence in a comparison between the spreads involved in Figures 12 and 13. While all the steels appear to have recovered their room temperature fatigue resistance at 900°F for 100,000 cycles, the A-212 steels still show their inferiority to the other materials tested. In fact, with the exception of the marked decrease in allowable strain at 100,000 cycles for the normalized and stress relieved A-387,B steel at 800°F, the plain carbon A-212 shows poorer fatigue resistance "across the board" at 100,000 cycles.

When comparing the effects of elevated temperature upon the fatigue resistances and the tensile strengths of the steels studied, there seems to be some contradiction in the results. Where the fatigue values show a dip in the curves, the tensile values show a peak, and vice versa. This is probably an interplay between strength and ductility and their effects upon fatigue life which also involves differences in strain rates. A later section will explore the relationship between fatigue behavior and tensile properties in more detail.

The fatigue curves in Figures 7 through 11 are linear least square fits to the data with no subjective influences. The data points have been eliminated for clarity. They are all listed in the fatigue data section of the Appendix. Had all the data points been shown for the four curves in each figure the result would have been incomprehensible. By the same token, the showing of selected points for each curve would not have been a fair representation of the true data. Thus, it was decided that no data points be shown on this type of plot. The average deviations in the plots range from 2% to 16% with a median value of 6.4%. It should be pointed out that for fatigue work, especially elevated temperature fatigue tests, the scatter has been kept to a minimum. In most cases, where the average deviation is high it is because of one or two 'bad' points which statistically probably should have been eliminated. There were two plots which demanded some attention from a subjective viewpoint. These were the 800°F and 900°F "T-1" plots at 12,000 cycles per hour. One is shown in Figure 15 with the room temperature plot added to give some indication of the minimal scatter involved in the room temperature tests. The room temperature curve shown on the

plot is what one would consider as normal. The 800°F data seem to indicate an unusual behavior. The sharp decrease in fatigue resistance at 800°F results in a knee in the curve at 50,000 cycles with decreasing fatigue resistance from this point on. The 900°F data show a similar but less marked drop-off occurring at about 20,000 cycles and progressing beyond 100,000 cycles. The doubt as to the real or imaginary effects of such a behavior is further complicated by the fact that should the data for both temperatures be treated as two single straight lines as in Figure 7, the slopes of the four curves differ only slightly. However, the possibility of an aging or embrittling phenomenon exists, and this had to be investigated. The results of the study of this irregularity will be discussed in a later section.

1100 Cycles per Hour Fatigue Tests

As in the previous section, Figures 16 through 20 present the 1100 cph fatigue plots for the three steels studied in the respective conditions of heat treatment. Summary curves can also be found in Figures 21, 22, and 23 showing the effects of elevated temperature upon the total strain range for 5,000 and 100,000 cycle lifetimes and upon the fatigue curve slope.

The superiority of the weaker, but more ductile steels at room temperature in the 5,000 cycle range noted in the 12,000 cph tests was maintained in the 1100 cph tests as well. The same order of merit for the 100,000 cycle values is also displayed in Figure 22 as compared with Figure 13. As in the 12,000 cph tests, the A-212 strain values remained below those of the other steels with increasing temperature at 100,000 cycles.

The 5,000 cycle plot indicates that the effect of increasing temperature varies with the particular steel and condition while, for the 100,000 cycle values, all the steels and conditions react similarly to increasing temperature but the degree of response varies with the steel. The quenched and tempered A-387,B strain ranges remain about the same at 5,000 cycles with an increase in testing temperature. However, the other series react quite differently. Both conditions of the A-212 steel show a decrease in fatigue resistance with increasing temperature. The quenched and tempered series shows an almost linear decline from 400°F through 900°F, while the normalized and stress relieved condition shows about a 20% decrease in allowable strain range from room temperature to 400°F followed by a leveling-off to 600°F, and then a sharp decline through 800°F and 900°F. Both conditions suffer about a 40% loss in fatigue resistance at 900°F for 5,000 cycle lifetimes when compared with room temperature values. The normalized and stress relieved A-387,B reacts strangely in that it experiences a dip at 400°F followed by a sharp recovery at 600°F amounting to a 20% improvement in fatigue resistance over its room temperature value. As would be expected, tests at 800°F cause a drop in allowable strain range for the normalized and stress relieved A-387,B, but the resulting strain value is about the same as the original room temperature value. This is further decreased in tests at 900°F. The "T-1" steel, at 5,000 cycles, shows only a slight decline in fatigue resistance to 600°F followed by a declination to 900°F at an increasing rate.

The general dip and subsequent recovery in 5,000 cycle fatigue resistance observed in Figure 12 for the 12,000 cph tests at 800°F and

900°F does not appear in the plots of Figure 21 for the 1100 cph tests. Rather, the general trend is to continue at 900°F the decline in fatigue resistance experienced at 800°F.

The data from the 100,000 cycle plot of Figure 22 also differ markedly from those of Figure 13. Room temperature to 600°F shows little effect on allowable strain with the exception of the marked increase in fatigue resistance shown by the normalized and stress relieved A-387,B. This is comparable to the similar increase shown in Figure 21 for the same steel at 5,000 cycles. Generally, there appears to be a peak in fatigue resistance at about 800°F for the 1100 cph tests as opposed to the dip noted in the 12,000 cph results for this temperature. The A-212 steel is the exception to this statement in that the quenched and tempered condition displays a mild peak in allowable total strain at 400°F followed by a steady decline in fatigue resistance from that point on. The normalized and stress relieved condition exhibited a similar mild improvement at 400°F followed by a shallow dip in allowable strain at 600°F, a slight recovery at 800°F, and the normal decrease in fatigue resistance at 900°F. All steels and conditions show a decline in fatigue resistance from 800°F to 900°F, but it is notable that the allowable strain value for the quenched and tempered A-387,B at 900°F is approximately the same as its original room temperature value, while that for the normalized and stress relieved A-387,B is actually 25% higher than its room temperature value. The 900°F values for the other steels and conditions were lower than their original room temperature values.

The data from the "T-1" tests at 1100 cph for 800°F and 900°F do not suggest the discontinuous type of behavior noted in the 12,000 cph tests.

The linear least square fits to the fatigue data in Figures 16 through 20 have about the same degree of scatter as those in the 12,000 cph section. The average deviation varied over the range of 3.7% to 18.4% with a median value of 5.8%. As was previously noted, this minimal degree of scatter should be considered quite good when all the variables, as mentioned in an earlier discussion of scatter in this dissertation are taken into account.

Plastic strain values are given with all data points in the Appendix for three cycle rates. Readings were taken as described previously. No use was made of these data in this dissertation since they did not add anything of value to the discussion. The observation that the plastic strain values gradually increase with increasing total strain can be made. However, in the elevated temperature tests, the plastic strain tends to fall off to a point where it is difficult to detect. This is in agreement with that predicted by Forrest and Tapsell[38] as the type of behavior expected where dislocations are slowed down by strain hardening processes until strain aging is able to lock them.

110 Cycles per Hour Fatigue Tests

The application of the 110 cycles per hour testing rate to the entire 5,000 to 100,000 cycle lifetime range was not practical from a time standpoint. For this reason the 110 cph data are limited to the low cycle end of the fatigue curve.

Figure 24 is a summary plot showing the effects of elevated temperature upon the total strain range for 5,000 cycle life when tested at 110 cph. As a point of interest, note the consistent

superiority of the plain carbon A-212 steel at room temperature over the stronger, more highly alloyed A-387,B and "T-1" steels in this low cycle region. As in the faster cycling rates, however, this superiority is soon lost as higher testing temperatures are applied. The series of 110 cph curves of Figure 24 also show some influence of microstructure upon the temperature effects on fatigue behavior. The normalized and stress relieved A-212 steel exhibits a 15% decline in allowable strain range from room temperature to 400°F, while the normalized and stress relieved A-387,B steel maintains a constant fatigue resistance through the same temperature change. In direct contrast, however, are the three quenched and tempered steels which show increases in total strain range at 400°F. The A-387,B steel is the least affected, while the A-212 and "T-1" steels are increased by 12.5% and 21% respectively at 400°F. This improvement in fatigue behavior is short lived, however, since at 600°F, the total strain range for all the steels and conditions drops to below 0.9%, lower than any steel at room temperature. The decline is continued to 800°F followed again by differing effects. At 900°F, the two normalized and stress relieved series seem to level off in their fatigue resistance. The quenched and tempered A-212 suffers a further reduction in allowable strain from 0.8% at 800°F to 0.69% at 900°F. However, the quenched and tempered A-387,B and "T-1" steels appear to undergo a slight recovery at 900°F, similar to that observed in the 12,000 cph tests. One important point to make here is the fact that all allowable strain values at 900°F in the 110 cph tests are substantially lower than their respective room temperature values, in contrast to that noted in the 12,000 cph tests.

The curves of Figure 24 can be compared with those of Figures 12 and 21 for a general indication of the cycling rate effect upon the 5,000 cycle lifetime region. In such a comparison, probably the most evident feature of the three plots is the trend toward closer grouping of all the steels in the 110 cph curves, particularly at 600°F, 800°F, and 900°F. Thus, it seems that as the cycling rate is decreased from 12,000 cph to 1100 cph to 110 cph, the overall effect is to show quite similar fatigue behavior by all the steels at temperatures above 600°F.

Combined Temperature and Cycle Rate Effects

Figures 25 through 29 show the 5,000 cycle lifetime allowable strain data in such a fashion as to evaluate the effects of cycle rate and temperature from the same plot. The first impression from these figures is that the normalized and stress relieved steels appear to be more sensitive to changes in cycling rate than do the quenched and tempered materials. The fatigue behavior of the normalized and stress relieved A-387,B series, shown in Figure 25, is markedly altered by the reduction in cycle rate from 12,000 cph to 1100 cph to 110 cph. Figure 26, showing the reaction of the normalized and stress relieved A-212 steel, very clearly indicates a decreasing fatigue resistance with the application of a decreasing cycling rate at temperatures in excess of 400°F. However, this relationship does not apply at room temperature, as shown in Figure 26, and is not as clearly evident in any of the other steels, since the indication of such an effect is distorted by the curve maxima shown in the figures. Figures 27, 28, and 29, showing the reactions of the quenched and tempered steels to the elevated temperatures and cycle rate variations, show similar effects between the three steels.

Viewing the five figures as a group reveals the following observations: a) at 12,000 cph the normalized and stress relieved A-212 and both conditions of the A-387,B steel show peaks at 600°F, the A-387,B peaks being the most pronounced; and b) all steels and conditions, except the normalized and stress relieved A-212, show severe dips in fatigue resistance at 800°F followed by an apparent recovery at 900°F; c) at 1100 cph the normalized and stress relieved A-387,B shows a strong peak at 600°F, while the quenched and tempered condition exhibits an elevated plateau in fatigue resistance over the 400°F to 800°F range; the "T-1" retains its room temperature behavior to beyond 400°F at which point a gradual deterioration begins; and d) at 110 cph all steels but the normalized and stress relieved A-212 show a peak or plateau in the 400°F region followed by a decline in fatigue resistance. Overall, the A-387,B steel, in both conditions of heat treatment, appears to show the most pronounced effects of the increasing temperature and decreasing cycling rate as applied in this study. The "T-1", in its mill quenched and tempered condition, closely parallels the behavior of the quenched and tempered A-387,B, as does the quenched and tempered A-212 steel.

The recovery behavior noted in the 12,000 cph tests at 900°F can be explained by the following. The plastic strain distribution discussed by Grover[16] can result in an increase in the deformation as measured in the strain determining step of the fatigue test. Since the state of strain (and stress) applied to a specimen is determined by a relative displacement between two fixed points on the specimen, the displacement (or strain in inches/inch) measured will be higher for those specimens which undergo considerable plastic deformation. Such deformation as

creep will have the effect of relieving the stress system within the specimen to a point somewhat lower than one might expect from the measured displacement. Thus while the measured displacement (or strain) is high, the actual stresses supported by the specimen in the presence of creep will be low. This would explain the apparent increase in fatigue resistance (as mentioned in the Introduction with Grover's analysis). That is, it would appear that the specimen is maintaining a higher stress state, due to the method of determining strain, than is actually the case for a given fatigue life. Kennedy[39] has shown that the application of a fatigue stress increases the creep rate and could conceivably lower the temperature at which creep is noticed. It is proposed that the recovery at 900°F for the 12,000 cph tests is not truly a recovery in fatigue resistance, but rather the result of the combined effects of fatigue and creep brought on by the applied cyclic load as described above. Further, it is proposed, that a similar improvement is absent in the 1100 cph tests as a result of the lower frequency of stressing which does not enhance the creep phenomenon sufficiently to lower its threshold temperature to 900°F.

The order and distribution of the peaks and plateaus in fatigue resistance present in Figures 25 through 29 indicate a strain-rate sensitivity for the steels tested. If one accepts the concept of dislocations and a common theory of strain aging, that of dislocation locking by solute atoms present in the steel, than the following can be proposed. The atomic mobility of such solute constituents is dependent upon, among other things, temperature. Since the solute atoms must be able to pursue and overtake dislocations in order to effectively 'lock' them, the

speed of the dislocation movement becomes important. The slower the dislocation movement, the less mobile the solute atom must be. Thus at high cycle rates, the speed of the dislocation motions is high, and the temperature must be high to provide sufficient atom mobility for dislocation locking. With a decrease in cycling frequency, the speed of the dislocation is also decreased, and the locking phenomenon is possible at lower temperatures. Thus peaks in fatigue resistance versus temperature plots would occur at lower temperatures for lower cycling rates. In effect, this is what is observed in Figures 25 through 29. The A-387,B steel seems to be much more sensitive to the temperature and frequency variables than do the other steels. Also, the strain hardening exponents (from Figure 6) for the two conditions of the A-387,B steels show an increase in excess of 40% in the 600°F to 700°F region. This increase in strain hardening rate could explain the more pronounced influence of the strain aging upon the A-387,B steel as found in this study. While the strain hardening exponents of the A-212 steel also increase quite sharply in this region, the respective tensile strengths have fallen off to a point where their expected high-strain fatigue resistance is quite low. Thus one would expect a lesser response in these steels.

The Anomalous "T-1"

The second phase of the study described in the experimental procedure involves the strange behavior of the "T-1" steel when tested at 800°F and 900°F at 12,000 cycles per hour. As mentioned previously, a subjective approach leads one to the irregular behavior shown on Figure 15. However, an objective approach, using a linear least-square

fit results in the following: the slopes of the curves generated from the room temperature, 600°F, 800°F, and 900°F tests were -0.243; -0.238; -0.238; and -0.237 respectively. It is obvious that these four slopes are identical when considering the type of test used in the study. It should not be considered unusual to note the absence of any apparent temperature effect upon the slope of the curve in the "T-1" while it was observed in the plain carbon A-212. Similar differences were noted in the temperature effects upon the tensile properties. It is felt that the remarkable agreement in the four slope values is more than merely coincidental, but rather a strong indication that the single straight line is more realistic.

A second factor in favor of the latter belief is the absence of any such anomalous knee in the 1100 cph tests. However, the claim that the irregular behavior may be strain rate sensitive is a valid one and must be evaluated.

In order to gain more information about this phenomenon, room temperature tensile tests and Charpy V-notch impact tests were performed on the "T-1" material. Samples were cut from the short piece of the broken fatigue specimen. This is the end which was firmly clamped and did not undergo any elastic or plastic deformation during testing. Also, the short piece was within the furnace and therefore at the same temperature as the fracture section of the fatigue specimen. Tests were run on as-received material for control purposes, on specimens which failed in fatigue before the "knee" in the curve, and on specimens which failed after the "knee". The results of these tests are listed in Table V. It is obvious that, except for a drop in

yield and tensile strengths experienced by all the specimens following fatigue testing at 800°F and 900°F, there is no apparent effect of increasing time at temperature during any given fatigue test. The 15ft.-lb. transition temperature values for the 800°F tests are identical when consideration is given to experimental error. The impact values for the 900°F tests are also in close agreement. Therefore, it should be concluded that increasing time at temperature for the duration of the reported fatigue tests apparently had no effect upon the room temperature tensile properties or the relative Charpy V-notch impact properties. The slight embrittlement noted in the 900°F tests, as compared with the room temperature and 800°F values is in relative agreement with that observed by Pense [40], and is indicative of the complex alloy make-up of the "T-1" steel.

Further evidence supporting the theory of a straight-line representation for the 800°F and 900°F data is given by a companion study presently in progress at Lehigh. Chivinsky [41] has performed fatigue tests upon similar specimens of the same heat of "T-1" material. The major difference between his specimen and that discussed herein is the application of a single weld pass on the top and bottom surfaces of Chivinsky's specimen prior to fatigue testing. His data involving the "T-1" steel do not suggest the type of break-down in fatigue properties illustrated in Figure 15. Rather, a straight line seems to fit his data quite well. Both 1100 cph and 12,000 cph cycle rates were applied in his work. It should also be mentioned that his welded and unwelded data seem to agree quite well for "T-1" and A-387,B, indicating the lack of an influence by the single pass longitudinal weld

upon fatigue resistance.

It was decided to try to ascertain the appropriate fatigue behavior of specimens taken from a new heat of "T-1" steel. This was necessitated by the exhaustion of the supply of the original heat material. The data and the least square-fit line combining both new and old material will be found on Figure 30. This curve represents the room temperature behavior of both heats combined. It should be pointed out that the two heats are very similar in their room temperature fatigue behavior. The slope of a straight line fit to the new material data points only is slightly shallower than that shown for the room temperature curve in Figure 15.

Figure 31 shows the 800°F least-suqare fit line for the new material and that for the original heat as well. It must be stated that there is considerably greater difference between the 800°F curves for the two heats than there was for the room temperature curves. However, this should be expected for several reasons. First, the elevated temperature tests inherently involve more scatter. Secondly, the complex make-up of the "T-1" material is such that one must expect somewhat differing reactions to similar conditions from heat to heat. This is evidenced by the markedly different transition temperatures between the two as-received materials as listed on Table V. And finally, since the heat treatment of the "T-1" steel is variable and dependent upon the resultant properties, there is a finite possibility that the thermal histories of the two heats were sufficiently different to cause such a differing response when tested at 800°F. The only compositional

difference to speak of is a 25% increase in chromium content from heat #1 to heat #2.

Further investigation into the possibility of an aging phenomena occurring within the "T-1" material involved pre-aging a group of specimens at 800°F for times ranging from 5 hours to 100 hours. These specimens were then fatigue tested in the normal way at 800°F at a strain which should cause failure at more than 50,000 cycles. These results are listed in Table VI. The last column in Table VI lists the cycle lifetimes for the various aging times with the data normalized to a total strain value of 0.6%. It is quite clear that the results differ markedly. In fact, there seems to be a deterioration in fatigue life with increasing aging time to 20 hours. The subsequent 50 and 100 hour treatments appear to indicate a mild recovery in fatigue resistance. The limited data seem to represent an aging phenomenon occuring, but further tests were in order. Charpy V-notch specimens were cut from these pre-aged specimens and the 15 ft-lb. transition temperatures for the respective conditions are listed on Table V. The order of merit noted in the normalized cycles to failure column of Table VI was maintained in the transition temperature values of Table V for these pre-aged specimens. The as-received value of -156°F is considerably lower than the comparable value for the original "T-1" heat. Five hours at 800°F prior to fatigue testing raised the transition temperature 16°F. An additional 15 hours aging time raised the transition temperature 8°F more and resulted in the poorest projected fatigue life for a total strain of 0.6%. (This embrittlement tendency is also in agreement with Pense's findings.) Further aging at 800°F for 100 hours preceding

fatigue testing restored the brittle fracture parameter, the 15-ft-lb. transition temperature, to its original as-received value, while the fatigue resistance was only slightly improved (over the 20-hour aged specimen) by this additional aging.

To further complicate matters, no apparent differences were observed in the resulting microstructures under either light or electron microscopy following the aging treatments. Also, no major change in crack morphology was noted throughout the study.

In general, one must admit that there does appear to be an aging phenomenon occuring within the "T-1" steel. This is evidenced by the impact and fatigue data of the aged specimens from heat #2 as well as the work of others. However, this aging effect appeared only after substantial aging treatments over-and-above those normally encountered in fatigue testing. The complete absence of any deterioration in fatigue resistance as noted by Chivinsky rules out the time at temperature during a standard fatigue test as sufficient to cause an embrittlement. The embrittlement which occurred, did so only in the specimens having considerably more time at temperature than that encountered in fatigue testing alone. A definite difference does exist between the two heats of steel (that of the brittle fracture tendencies), but this does not account for the absence of any deterioration in properties by the same material in the hands of another investigator.

All things considered, it is the writer's firm opinion that the irregular behavior of the "T-1" steel at 800°F and 12,000 cph indicated on Figure 15 is a spurious representation resulting from a subjective influence in viewing the data.

Mathematical Analysis

Utilizing the General Electric Computer-Library of programs, a Multiple Linear Regression Analysis was applied to the fatigue data. The testing conditions and static tensile properties of the respective steels and conditions were acted upon as independent variables, with the various fatigue curve parameters as the dependent variables. The results can be stated as follows: the correlation analysis revealed that the slope of the log-strain vs. log-cycles to failure curve was statistically related to the yield strength and yield to tensile ratio of the material with 90% to 95% confidence of significance and to the testing temperature with 95% to 99% confidence of significance; the total strain range for 5,000 cycle life was related only to the percent reduction in area with a 95% to 99% confidence of the variable being significant; the total strain range for 100,000 cycle life was correlated with the independent variables and found to depend upon the testing temperature with 90% to 95% confidence of significance and the percent reduction in area with 95% to 99% confidence that the area factor is significant; and finally, a fatigue constant factor (which will be explained later) was found to correlate with the yield to tensile ratio with 90% to 95% confidence of significance and the testing temperature with at least 99% confidence that the temperature is significant in determining this constant term.

A rather interesting point to note is the absence of any significant correlation between a fatigue parameter and the effective cycle rate. This is verified by the slight effect of cycle rate variation upon the 5,000 cycle allowable strain values shown in Table IV.

Combining the above information with an approach similar to Coffin's [19], but applying total strain values as opposed to plastic strain values, one comes upon the following relationship:

$$\epsilon N^m = c, \tag{3}$$

where ϵ is the total strain range, N is the number of cycles to failure, m is the absolute value of the slope of the fatigue curve, and c is a material constant which is dependent upon the composition class into which the material falls. This constant, c, is the fatigue constant factor discussed in the previous section on the regression analysis results.

Trial plots of the various correlations result in Figures 32 and 33 as the most reliable. Figure 32 indicates the reliability of predicting the total strain range allowable for 5,000 cycle life from the reduction in area obtained in a simple tension test. The resulting equation:

$$\epsilon_{5,000} = -0.01x(\%\text{Red.Area}) + 1.65 \tag{4}$$

will predict the 5,000 cycle strain value within the limits of probable error as shown on Figure 32. It must be pointed out that the percent reduction in area used in equation 4 must be measured in a tensile test made at the temperature for which the fatigue information is desired. This estimate of a strain value gives the ϵ factor in equation (3). A second factor is necessary for solving the equation and predicting fatigue behavior. This second factor is the fatigue constant term, c. Figure 33 reveals the relationship used in obtaining this constant term and, also its dependence upon composition as previously mentioned. In order to estimate c one must determine the composition class into which

his alloy falls. If the total alloy content is less than 1.75%, or reacts as a plain carbon steel, the line to use is that with the 0.85 slope. Should the total alloy content be greater than 1.75% and react as a low alloy engineering steel, then the less steep line (slope=0.12) should be used. It is difficult to say why there is no overlap between these two lines on the part of the data, but they are presented as they occurred. The resulting constant values are in general agreement with those reported by Pense and Stout [23], as is the composition break-down. However, the three groupings used in their paper do not appear in the computer analysis. The resulting two curves of Figure 33 more closely depict the relatively marked difference between mechanical properties of a plain carbon steel and a low alloy steel while the differentiation between low alloy steels is slight. The temperature referred to in Figure 33 is meant to be the temperature of interest for fatigue data, and the yield to tensile ratio is that ratio taken from a tension test performed at the temperature of interest.

The estimation of $\epsilon_{5,000}$ and c from Figures 32 and 33 permits one to calculate the slope of the log-strain versus log-cycles curve, and ultimately predict the entire fatigue curve to 100,000 cycle life-times. In an effort to reduce the possible error from such an approach, it would be to the investigator's advantage to evaluate the allowable strain at 5,000 cycles from several short-time fatigue tests if at all possible. This would eliminate the possibility of under- or over-estimating the 5,000 cycle strain by as much as 20% as indicated on Figure 32. It is felt that this is the weakest point in this empirical approach.

Care must be taken not to extend this mathematical approach too far. The cautions expressed in the Introduction certainly apply here as well as any other type of laboratory testing. The resulting equations for predicting fatigue life, as presented here, should be limited in their application to equivalent types of fatigue tests involving roughly the same size specimen and same types of steels. Further limitations as to temperature should involve room temperature up to 900°F with no reliability intended above or below this range. As previously stated, the cycle rate apparently has little effect upon the resulting fatigue values over the range of 110 to 12,000 cycles per hour. This also has its limitations as mentioned in the Introduction should one desire to expand the applicable range.

Metallographic Aspect

Basic Microstructure: Figures 34 through 38 are representative of the base microstructures for the three steels in the various conditions of heat treatment. Unless otherwise stated, all light photomicrographs are magnifications of 500 times. A 2% Nital etch was used in all cases.

The base structure of the A-212 steel depicted by Figures 34 and 35 show the normal differences one would expect between the normalized and stress relieved and the quenched and tempered conditions of a plain carbon steel possessing relatively poor hardenability. The normalized and stress relieved steel shows normal grain size (ASTM G.S. No. 7-8) and rather coarse, easily distinguishable pearlite lamella. On the other hand, the quenched and tempered A-212 steel, while still composed of a ferrite-pearlite aggregate, exhibits a finer grain size as a ramification of the more rapid cooling rate of the quenching treatment.

These basic structures remained essentially unaltered throughout the course of the fatigue study.

The fact that the two heats of A-387,B steel were obtained as 'made to coarse-grain practice' (ASTM G.S. No. 3-4) is clearly evidenced in Figures 36 and 37. The normalized and stress relieved A-387,B is a coarse ferrite-pearlite aggregate with the pearlite being of the "blotchy" type; that is, the pearlitic areas, rather than displaying the classical, fine ferrite-carbide lamella, appear as small islands of such unresolvable material in a sea of ferrite. This is the combined effect of a rapid cooling rate, moderate alloy composition, and low carbon content, all of which alter the pearlite formation. Since the alloy content of the A-387,B is higher than that of the A-212, similar cooling rates result in dissimilar structures. The pearlite formed in the normalized and stress relieved A-387,B is very fine and discontinuous when compared with that of the normalized and stress relieved A-212. The quenched and tempered A-387,B structure is markedly different from that of the A-212. Extremely fine but acicular ferrite and carbide particles compose the A-387,B quenched and tempered material. The rather coarse prior austenite grain size is clearly indicated in Figure 37.

Figure 38 shows the base structure of the "T-1" material as-received in its mill quenched and tempered condition. This "T-1" structure is very similar to the quenched and tempered A-387,B as might be expected. The most significant difference between the two structures is the slightly finer grain size exhibited by the "T-1" steel. There are also more numerous and larger regions of 'free-ferrite' present in the "T-1".

This is probably the result of the higher tempering temperature of 1200°F used on the "T-1" steel. It is doubtful that such areas are proeutectoid ferrite since the alloy content of "T-1" and the water spray quench on a 3/4-inch plate should guarantee 'through hardening', and therefore, no proeutectoid ferrite should be present in the structure assuming proper austenization. The A-387 and "T-1" structures also showed no marked change during the various fatigue tests. This is not surprising when one considers the time and temperature relationships in tempering or stress relieving. Applying the Holloman and Jaffe tempering parameter [42] to the temperatures of 1150°F and 900°F, one finds that for equivalent resulting hardnesses, it would be necessary to temper at 900°F for 8,000 hours to reproduce a one-hour treatment at 1150°F. This is verified by the negligible changes in Brinell hardness numbers as seen in the data in the Appendix. Thus, it is expected that one would notice no change in microstructure resulting from elevated temperature fatigue tests at 900°F for times of 100 hours or less. This, in fact, is the observation of the investigator.

Figures 39 through 42 are electron micrographs of the A-212,B and A-387,B steels, both in the normalized and stress relieved conditions. The plastic replicas represented in these figures were obtained from broken fatigue specimens which had been tested at 800°F and 900°F respectively. One can clearly note the grain boundary areas between adjacent ferrite grains and those separating ferrite from pearlite. The 10,000 magnifications show no evidence of segregate particles or precipitates at the grain boundaries or within the grains themselves. This further substantiates the contention that no general microstructural

change occurred within the fatigue specimen during elevated temperature testing.

Crack Morphology: Previous room temperature fatigue tests performed by the writer [12] revealed a general tendency for transcrystalline failure. In cases where the microstructures were acicular, the crack tended to follow aligned carbide particles when coincident with its direction of growth. This was determined by tracing secondary crack propagation paths. These secondary cracks developed adjacent to the fracture plane and grew to a size which proved to be less than the critical size required for failure. It was assumed that the morphologies of the primary and secondary cracks are identical.

The same technique was used in the present study to determine the effect of elevated temperature and cycle rate variations upon the cracking tendencies of the steels. Typical cracks are shown in Figures 43 through 60. All but one of the cracks represented in this group of figures grew in from the upper or lower surface of the fatigue specimen in a plane parallel to the final fracture surface. The one exception to this statement is that of Figure 43 which shows a crack growing into an A-212, normalized and stress relieved fatigue specimen from the fracture surface, perpendicular to the plane of failure, in a plane parallel to the rolling plane. This specimen was tested at room temperature. An interesting point to note is the convenient ferrite path supplied in the steel. This nominally straight ferrite path is a result of the banding tendency of the hot-rolling technique. The crack is observed to follow the ferrite while avoiding the pearlite by a slight bend as seen in the left half of the figure. This tendency to follow

the ferrite when convenient is to be expected since the ferrite, having the lowest yield strength of the constituents present, undergoes the most plastic deformation, therefore failing before the pearlite. The crack shown in Figure 43 is oriented parallel to the direction of loading and in a plane parallel to the rolling plane. The cracks shown in the remainder of the figures are all oriented at right angles to the direction of loading and transverse to the rolling direction as well.

Figures 44 and 45 show typical secondary cracks in both the normalized and stress relieved and the quenched and tempered A-212 steel tested at 600°F and 800°F respectively. Both figures show the transcrystalline nature of the crack path through both ferrite or pearlite. Figure 44 shows a common observance, that of the crack splitting at the tips in tests of 600°F or higher. This has been observed by other investigators (18) as well.

Figures 46 through 51 show secondary cracks found in the A-387,B steel as tested in the normalized and stress relieved condition. Both Figures 46 and 47 show rather fine cracks splitting a pearlite area in two, continuing through a ferrite region, and finally coming to rest in pearlite. Figure 47 shows the upper edge of the fatigue specimen and how the crack traversed the structure. Both these specimens were tested at room temperature but at different cycle rates. Figure 48 shows a fine crack which has been halted in a ferrite grain. This specimen was tested at 600°F at 1100 cph. Figure 49 shows a crack which has branched off to form two cracks which in turn have rejoined to continue as one. The specimen from which this structure came was tested at 800°F at 12,000 cph. Figures 50 and 51 show rather large cracks, both from

the same 900°F fatigue specimen but from different areas. The crack in Figure 50 also shows this branching and rejoining as noted on a finer scale in Figure 49. Figure 51 shows the abrupt halting of a crack in a ferritic area.

Figures 52 and 53 are typical of the cracks observed in the quenched and tempered A-387,B specimens. There does not appear to be any strong relationship between the character of the microstructure and that of the crack travelling through the structure. Note the splitting tendencies of the cracks in Figures 52 and 53.

Figure 54, however, shows a strong influence of the coarser acicular structure of the "T-1" steel. The crack, while propagating in essentially a straight line, is encouraged to branch out at right angles to its intended direction by the sharp spike-like ferrite and carbide particles, or possibly by the presence of weak but brittle sulfide inclusions which could cause the same splitting tendency. This branching, however, did not extend much beyond that shown in Figure 54.

Figures 55, a and b, are two halves of the same continuous set of cracks which had to be separated to fit the page. Figure 55a shows an interesting point in that the upper surface edge is shown at the top of the picture. Note the discontinuity presented by the material between the two cracks. From the size of the cracks and the voids below the surface, one deduces that the block of material was displaced upward during the crack's propagation. In propagating, several unusual occurrences can be noted concerning the parallel cracks. Again one sees the branching and rejoining tendency as noted previously. Also note the fact that both ferrite and pearlite regions are split in two by the crack

with no attempt made to avoid the stronger pearlitic areas. Figure 55b shows the two cracks bridging over to one another, but still maintaining their individuality in further propagation. Following the two cracks to their ends one notes that one comes to rest in ferrite while the other is arrested in a fine pearlite area. There is also an indication by the crack on the right to branch along the aligned pearlite areas near its end by sending out two small "fingers".

An unexpected observation is noted in Figures 56 and 57 which show a crack in the normalized and stress relieved A-387,B steel. Figure 56 is a low magnification (150X) picture of the crack from the surface of the specimen to its end within the specimen to give one an idea of the total length involved. Figure 57 shows the same crack at 500X and the manner which it traversed the specimen. Again note the splitting of the ferrite and pearlite areas and the branching near the crack tip. Note that both the main crack and the small "finger" are arrested in ferrite. Specific attention should be given to the ferrite grains in Figure 57. The randomly oriented, parallel bands within the ferrite are of particular interest. These deformation bands are the first indication of massive plastic deformation occurring within the fatigue specimens in the area of failure. These bands will be discussed in more detail in a later section.

Figures 58, 59, and 60 are electron micrographs of cracks found in normalized and stress relieved specimens tested in fatigue at 800°F and 900°F. The crack in Figure 58 seems to be stopping at a grain boundary shown in the lower left corner of the plate. This is contrasted with the crack in Figure 59 which is halted at an inclusion and that of

Figure 60 which comes to rest in the center of a ferrite grain, however, this is not evident from the photograph.

The following conclusions can be made in summary of the basic microstructural study. No evidence for any favored crack path or medium was found in any of the structures observed. It appears that neither testing temperature nor cycling rate, within the respective limits of 80°F to 900°F and 110 cph to 12,000 cph, had any effect upon the tendency of the crack to propagate in a transcrystalline fashion. Neither did there appear to be a favored arresting constituent for the cracks with about half of those observed coming to rest in ferrite and the others halting in pearlite.

Deformation Bands: The deformation bands were observed only in the A-387,B normalized and stress relieved steel specimens under certain testing conditions. Samples taken from specimens tested at 800°F and 900°F exhibited this band phenomenon while room temperature and 600°F specimens did not. When they were present they occurred only in the upper and lower corners of the fracture plane in the area of maximum deformation during testing. Figure 56 shows the higher density of bands near the surface of the specimen, while below the tip of the crack there are very few to be seen. Further displays of these deformation bands are found in the light photomicrographs of Figures 61 and 62. Close scrutiny of these two figures will show that the striations are typical of deformation bands in that they are relatively straight and parallel within any given ferrite grain. Some bands appear to extend their influence across the grain boundary into adjacent grains. Figure 62 shows evidence of such bands starting or stopping within a grain as opposed to-

traversing the grain's entire width.

Figures 63 through 68 are electron micrographs showing more detail of these bands. Figure 63 shows a series of finer bands which appear to start at the grain boundary and fade out as they traverse the grain. Figure 64 shows four much coarser bands halting at a grain boundary. Figure 65 and 66 show similar bands being interrupted by pearlite obstructions with little effect in deviating their direction. Figure 65 shows two orientations of the bands. The 900°F specimens of Figures 67 and 68 also showed this banding effect. Note the very uniform etching characteristics displayed by the deformation bands in Figure 68.

The observation of these slip bands is not new. Thompson[43] reported the presence of 'persistent slip bands' in copper fatigue specimens after electro-polishing[44]. It is proposed that the presence of such persistent bands tend to support the theory that the work hardening process within the slip band, which would normally force slip to occur on other slip systems within the crystal, is suppressed under cyclic loading. As a result, deformation is limited to several active slip bands which become very intense upon further cycling. Such movements, though referred to as slip, differ from the conventional slip concept. Such a non-conventional slip was described as a viscous motion by Bullen and Wood[45] due to the absence of local strain hardening. (The absence of any local increase in hardness in the region of the bands was substantiated by the writer in that Tukon hardness tests using a 100 gram load indicated no change in hardness occurred in the deformed region when compared with the undeformed base material). While wavy slip bands are normally found in alpha-iron, Gough[46] has shown that

straight slip bands are observed in iron upon the application of cyclic load.

While these bands, as viewed by the electron microscope, are suggestive of the intrusion-extrusion phenomenon noted in past fatigue studies, one must be aware of the fact that the bands are observed internally within the specimen. Any discussion of the occurrence of such intrusions and extrusions involves a free surface, which is not present in this case. Therefore, it is the writer's contention that these bands are regions of numerous repeated dislocation motions caused by the cyclic loading at elevated temperatures which create a localized disruption of the crystal structure resulting in the increased tendency to etch heavily during the normal preparation of the metallographic sample.

CONCLUSIONS

1. The influence of increasing temperature upon the fatigue resistance of the various steels and conditions studied varies with the strain level considered and the applied cycle rate. In general, the 5,000 and 100,000 cycle life fatigue resistance of steels such as A-212,B; A-387,B and "T-1" is not markedly changed over the temperature range of room temperature to 800°F, except for intervening strain aging influences in specific temperature intervals.

2. A general decline in fatigue resistance at 800°F and subsequent recovery at 900°F was noted for the 12,000 cph cycling rate. This apparent recovery is attributed to the stress reduction influence of massive plastic deformation resulting from the onset of creep, initiated by the cyclic loading.

3. A mild decrease is noted at 400°F for certain of the steels at a cycling rate of 1100 cph, followed by a recovery of 600°F to 800°F. A similar fatigue resistance peak occurs at about 400°F for the 110 cph cycling rate. This shift in maxima temperature is attributed to a strain rate sensitive-aging phenomenon.

4. Generally, the influence of temperature and cycling rate is less pronounced for the elastically strained 100,000 cycle lifetime specimens than for the highly plastically strained 5,000 cycle specimens. That is, the separation between allowable strain values for all steels and conditions is less pronounced at any given temperature for the 100,000 cycle values as compared with the 5,000 cycle data.

5. The A-387,B steel seems to be more sensitive to the effects of cycling rate and temperature than do the other steels. This could

be a result of its increased rate of strain hardening with increasing temperature, while maintaining a respectable tensile strength.

6. The A-212 normalized and stress relieved steel shows a decrease in fatigue resistance with a decrease in cycling rate from 12,000 cph to 110 cph at temperatures over 600°F. The other steels and conditions do not indicate as clear-cut an effect of decreasing cycling frequency. That is, there is no consistent cycling rate effect noted upon the moderate-strength, low-alloy steels when tested in reversed bending as in this study. However, this observation could be distorted by the effects of the strain-rate sensitive influences noted in (3) and (4).

7. Fatigue behavior for alloys similar to the range of compositions covered by the A-212,B; A-387,B; and "T-1" steels can be predicted for temperatures between 80°F and 900°F at cycling rates between 110 cph to 12,000 cph. The generalized Coffin expression, $\epsilon N^m = c$, is used where ϵ is a total strain value ($\epsilon_{5,000}$ can be estimated from the steel's reduction in area), N is the lifetime in cycles, m is the absolute value of the slope of the log-strain versus log-cycles curve, and c is a material constant which can be estimated from the temperature of interest, the yield to tensile ratio at the temperature of interest, and the total alloy content of the steel.

8. No microstructural changes were noted in any of the steels throughout the 80°F to 900°F temperature range.

9. Neither cycling rate nor testing temperature had any effect upon the noted crack morphology. The tendency for transcrystalline

failure was maintained throughout the entire testing range of 80°F to 900°F.

10. Deformation bands were noted in the ferrite regions of the normalized and stress relieved A-387 specimens after testing at 800°F and 900°F. The bands appeared in the areas of maximum deformation and are attributed to regions of lattice disruption resulting from localized disorientation through cross-slip operation.

REFERENCES

(1) Cazaud, R., Fatigue of Metals, Chapman and Hall Ltd., London, 1953.

(2) Timoshenko, S. P., History of Strength of Materials, McGraw-Hill Book Company, New York, 1953.

(3) Cleeman, T. M., Railroad Engineer's Practice, D. Van Nostrand Co., New York, 1892.

(4) Cooper, T., Discussion on "Kentucky and Indiana Bridge", Transactions ASCE, Vol. XVII, 1887, pp. 181ff.

(5) Prichard, H. S., The Effects of Straining Structural Steel and Wrought Iron, Transactions ASCE, Vol. LXXX, 1916, p. 1429.

(6) Hammond, R., Engineering Structural Failures, Oldhams Press Ltd., London, 1956.

(7) References on Fatigue, ASTM Special Technical Publications No. 9-A to 9-0, 1950 to 1963 inclusive.

(8) Tor, S. S., Ruzek, J. M., and Stout, R. D., "Repeated Load Tests on Welded and Prestrained Steels", Welding Journal, Vol. 31, #5, 1952, pp. 238sff.

(9) Gross, J. H., Tsang, S., and Stout, R. D., "Factors Affecting Resistance of Pressure Vessel Steels to Repeated Overloading", Welding Journal, Vol. 32, #1, 1953, pp. 23sff.

(10) Gross, J. H., Gucer, D. E., and Stout, R. D., "The Plastic Fatigue Strength of Pressure Vessel Steels", Welding Journal, Vol. 33, #1, January 1954.

(11) Gross, J. H., and Stout, R. D., "Plastic Fatigue Properties of High-Strength Pressure-Vessel Steels", Welding Journal, Vol. 34, April 1955, pp. 161sff.

(12) DePaul, R. A., "Some Microstructural and Alloying Effects Upon Low-Cycle Fatigue Life of Pressure-Vessel Steels", unpublished Master's Thesis, Lehigh University, 1963.

(13) McClintock, F. A., "The Statistical Planning and Interpretation of Fatigue Tests", Metal Fatigue, Ed. by George Sines and J. L. Waisman, McGraw-Hill Book Co., Inc., New York, 1959, pp. 112ff.

(14) Savitsky, E. M., The Influence of Temperature on the Mechanical Properties of Metals and Alloys, Stanford University Press, 1961.

(15) Cazaud, R., Fatigue of Metals, ibid.

(16) Grover, H. J., "Fatigue of Materials at High Temperatures", Metal Fatigue, ibid, pp. 232ff.

(17) Low, A. C., "Short Endurance Fatigue", Proceedings of International Conference on Fatigue of Metals, Institution of Mechanical Engineers, London, 1956, pp. 206ff.

(18) Johanson, A., "Fatigue of Steels at Constant Strain Amplitude and Elevated Temperature", Colloquim on Fatigue, Proceedings, Stockholm, May, 1955, Ed. by W. Weibull and K. G. Folke, Odquist-Springer-Verlag, Berlin, 1956, pp. 112ff.

(19) Gross, J. H., "PVRC Interpretive Report of Pressure Vessel Research", Welding Research Council, Bulletin, No. 101, Section 2-Material Considerations, 1964, p. 10.

(20) Tavernelli, J. F. and Coffin, L. F., Jr., "A Compilation and Interpretation of Cyclic Strain Fatigue Tests on Metals", Transactions, ASM, Vol. 51, 1959, pp. 438ff.

(21) Tavernelli, J. F. and Coffin, L. F., Jr., "Experimental Support For Generalized Equation Predicting Low Cycle Fatigue", Journal of Basic Engineering, ASME, Vol. 84, Series D, No. 4, December 1962, pp. 533ff.

(22) Morrow, J. D. and Johnson, T. A., "Correlation Between Cyclic Strain Range and Low-Cycle Fatigue Life of Metals", A Technical Note, Materials Research and Standards, ASTM, Vol. 5, No. 1, January 1965, pp. 30-32.

(23) Weiss, V., Sessler, J., and Packman, P., "Low-Cycle Fatigue of Pressure Vessel Materials", Syracuse University Research Institute Report No. Met. E. 575-662-F, 1962.

(24) Stout, R. D. and Pense, A. W., "Effect of Composition and Microstructure on the Low-Cycle Fatigue Strength of Structural Steels", Journal of Basic Engineering, ASME, Vol. 87, Series D, No. 2, June 1965, pp. 269ff.

(25) Canonico, D. A. and DePaul, R. A., Unpublished Fatigue Data Correlation Study, Lehigh University, 1962.

(26) Waisman, J. L., "Factors Affecting Fatigue Strength", Metal Fatigue, ibid, pp. 7-35.

(27) Benham, P. P., "Fatigue of Metals Caused by a Relatively Few Cycles of High Load or Strain Amplitude", Metallurgical Reviews, 1958, Vol. 3, #11, pp. 203-234.

(28) Allen, N. P. and Forrest, P. G., "The Influence of Temperature on the Fatigue of Metals", Proceedings of the International Conference on Fatigue of Metals, ibid, pp. 327-340.

(29) Coffin, L. F., Jr., "The Effect of Quench Aging and Cyclic Strain Aging on Low Carbon Steel", Metals Engineering Division, The American Society of Mechanical Engineers, Paper No. 64-Met. 8.

(30) Coffin, L. F., Jr., "Cyclic Strain and Fatigue Study of a 0.1 pct. C-2.0 pct. Mo Steel at Elevated Temperatures", Transactions of AIME, Vol. 230, December 1964, pp. 1690-1699.

(31) Forrest, P. G., "Speed Effect in Fatigue", Proceedings of the Royal Society, Vol. A242, 1957, pp. 223ff.

(32) Baird, J. D., "Strain Aging of Steel - A Critical Review - Part III: Dynamic Strain Aging", Iron and Steel, Vol. 36, #10, (1963), pp. 450ff.

(33) Rally, F. C. and Sinclair, G. M., Rep. No. 87 (1955) University of Illinois, Dept. of Theoretical and Applied Mechanics.

(34) Canonico, D. A., Kottcamp, E. H., Jr., and Stout, R. D., "Accelerated Cooling of Carbon Steels for Pressure Vessels", Welding Journal, Vol. 40, #9, (1961), pp. 400sff.

(35) Gross, J. H., Gucer, D. E., Stout, R. D., "The Plastic Fatigue Strength of Pressure Vessel Steels", The Welding Journal, Vol. 33, No. 1, January 1954, Research Supplement.

(36) Laxar, F. H., "The Relationship of Plastic Fatigue Resistance to Mechanical Properties and Microstructure of Steels", Unpublished Ph.D. Dissertation, Lehigh University, 1956.

(37) Quenched and Tempered Alloy-Steel Plates, Technical Booklet published by Climax Molybdenum, 1964.

(38) Forrest, P. G. and Tapsell, H. J., Proceedings of Institute of Mechanical Engineers, Vol. 168, p. 763.

(39) Kennedy, A. J., "Problems of Combined Creep and Fatigue Design", The Engineer, Sept. 27, 1957, pp. 444ff.

(40) Pense, A. W., "A Study of Subcritical Embrittlement in Pressure Vessel Steels", unpublished Ph.D. dissertation, Lehigh University, 1962.

(41) Chivinsky, J., Private communication involving data currently being gathered for Master's Thesis, Lehigh University, 1965.

(42) Alloying Elements in Steel, E. C. Bain and H. W. Paxton, ASM Book, Metals Park, Ohio, 2nd Ed., 1961, p. 188.

(43) Thompson, N., Wadsworth, N., and Louat, N., "The Origin of Fatigue Fracture in Copper", Philosophical Magazine, Ser. 8, Vol. 1, 1956, pp. 113ff.

(44) Low, J. R., "Microstructural Aspects of Fracture", Fracture of Solids, AIME, Vol. 20, Ed. D. C. Drucker and J. J. Gilman, 1963, pp. 213-215.

(45) Bullen, F. P., Head, A. K., and Wood, W. A., "Structural Changes During the Fatigue of Metals", Proc. Roy. Soc. (London) A, Vol. 216, 1953, pp. 332ff.

(46) Gough, H. J., and Hanson, D., "Behavior of Metals Subjected to Repeated Stresses", Proc. Roy. Soc. (London) A, Vol. 104, 1923, pp. 539ff.

(47) DePaul, R. A., Pense, A. W., and Stout, R. D., "The Elevated Temperature Fatigue Properties of Pressure Vessel Steels", Presented at AWS Annual Meeting, Chicago, 1965.

Table I
Chemical Compositions and Heat Treatment Temperatures of the Pressure Vessel Steels

Steel	Grade	C	Mn	P	S	Si	Ni	Cr	Mo	V	Ti	Cu	B
1-"T-1"	-	0.18	0.85	0.008	0.017	0.25	0.85	0.48	0.50	0.04	0.003	0.27	0.004
2-"T-1"	-	0.17	0.87	0.008	0.018	0.22	0.84	0.57	0.48	0.04	-	0.26	0.002
1-A-387	B	0.17	0.59	0.012	0.024	0.21	-	0.91	0.51	-	-	-	-
2-A-387	B	0.11	0.63	0.022	0.023	0.20	-	0.98	0.54	-	-	-	-
1-A-212	B	0.26	0.70	0.010	0.024	0.23	-	-	-	-	-	-	-
2-A-212	B	0.25	0.67	0.008	0.019	0.23	-	-	-	-	-	-	-

Steel	Austenitizing Temp.-°F	Tempering Temp.-°F	Stress Relieving Temp.-°F
"T-1"	1700	1200	-
A-387,B	1675	1150	1150
A-212,B	1650	1150	1150

Table II
Tensile Property Data

Steel	Temp.-°F	Y.S.Ksi	T.S.Ksi	YS/TS %	% Elong.	%R.A.	Strain Hard. Exp.
"T-1"	R.T.	119.0	131.0	90.8	19.5	63.2	.096
Mill Q-T*	600	91.2	102.5	89.0	20.0	57.1	.107
	800	85.2	101.5	83.9	21.0	61.8	.081
	900	81.4	92.5	88.0	19.0	67.0	.056
A-387,B	R.T.	129.5	140.6	92.1	16.0	63.8	.071
Q-T	600	101.2	116.2	87.1	22.0	62.4	.101
	800	97.0	108.0	89.8	22.0	67.8	.068
	900	89.8	101.0	88.9	18.5	68.2	.097
A-387,B	R.T.	68.9	95.8	71.9	26.5	60.8	.134
N-SR**	600	64.4	88.6	72.7	21.0	55.9	.126
	800	58.5	83.6	70.0	23.0	62.5	.155
	900	60.4	81.0	74.6	25.0	68.9	.159
A-212,B	R.T.	49.4	79.5	62.1	30.0	67.1	.194
Q-T	600	28.1	73.3	38.3	24.8	74.5	.332
	800	29.2	58.4	50.0	42.0	82.6	.216
	900	24.4	45.2	54.0	48.5	86.8	.169
A-212,B	R.T.	44.3	72.8	60.9	37.5	60.8	.203
N-SR	600	29.5	67.7	43.6	28.0	65.3	.336
	800	26.5	56.0	47.3	41.5	77.2	.364
	900	20.0	43.3	46.2	44.0	82.8	.232

* Q-T: Spray Quenched and Tempered
** N-SR: Normalized and Stress Relieved

Table III
Fatigue Property Data

Steel	Temp.-°F	Percent Total Strain				
		12,000cyc./hr.		1100cyc./hr.		110cyc./hr.
		5,000cyc.	100,000cyc.	5,000cyc.	100,000cyc.	5,000cyc.
"T-1"	R.T.	1.00	0.51	1.01	0.48	0.95[a]
Mill Q-T	400	-	-	1.01[a]	0.46[a]	1.15[a]
	600	0.97	0.47	0.98	0.42	0.88[a]
	800	0.84	0.42	0.90	0.48	0.84[a]
	900	0.96	0.48	0.84	0.31	0.97[a]
A-387,B	R.T.	0.92	0.48	0.92	0.47	0.97[b]
Q-T	400	-	-	1.05[b]	0.47	1.01[b]
	600	1.18	0.48	1.02	0.39	0.90[b]
	800	0.92	0.43	1.04[b]	0.49[b]	0.78[b]
	900	1.09	0.57	0.96[b]	0.44[b]	0.88[b]
A-387,B	R.T.	0.94	0.43	0.99	0.38	0.96[b]
N-SR	400	-	-	0.90[b]	0.37[b]	0.96[b]
	600	1.45	0.46	1.23	0.59	0.87[b]
	800	0.74	0.24	1.00[b]	0.61[b]	0.76[b]
	900	1.00	0.46	0.96[b]	0.49[b]	0.76[b]
A-212,B	R.T.	1.13	0.31	1.09	0.31	1.11[c]
Q-T	400	-	-	1.00[c]	0.40[c]	1.25[c]
	600	0.96	0.37	0.87	0.35	0.90[c]
	800	0.63	0.40	0.74[c]	0.31[c]	0.80[c]
	900	0.90	0.35	0.65[c]	0.21[c]	0.69[c]
A-212,B	R.T.	1.12	0.32	1.20	0.29	1.18[c]
N-SR	400	-	-	1.00[c]	0.345[c]	1.00[c]
	600	1.17	0.45	0.98	0.29	0.82[c]
	800	0.92	0.34	0.84[c]	0.31[c]	0.76
	900	0.78	0.42	0.74[c]	0.25[c]	0.74

a: 2-"T-1", All Other Tests 1-"T-1"

b: 2-A387, All Other Tests 1-A387

c: 2-A212, All Other Tests 1-A212

Table IV
The Influence of Cycle Rate Upon
the 5,000 Cycle Allowable Strain Values (%)

Cycle Rate	"T-1" Q-T	A-387,B Q-T	A-387,B N-SR	A-212,B Q-T	A-212,B N-SR
Room Temperature					
110 cph	0.95[a]	0.97[b]	0.96[b]	1.11[c]	1.18[c]
1100 cph	1.01	0.92	0.99	1.09	1.20
12,000 cph	1.05	0.94	0.94	1.13	1.12
400°F					
110 cph	1.15[a]	1.01[b]	0.96[b]	1.25[c]	1.00[c]
1100 cph	1.01[a]	1.05[b]	0.90[b]	1.00[c]	1.00[c]
12,000 cph	-	-	-	-	-
600°F					
110 cph	0.88[a]	0.90[b]	0.87[b]	0.90[c]	0.82[c]
1100 cph	0.98	1.02	1.23	0.87	0.98
12,000 cph	0.97	1.18	1.45	0.96	1.17
800°F					
110 cph	0.84[a]	0.78[b]	0.76[b]	0.80[c]	0.76
1100 cph	0.90	1.04[b]	1.00[b]	0.74[c]	0.84[c]
12,000 cph	0.84	0.92	0.74	0.63	0.92
900°F					
110 cph	0.97[a]	0.88[b]	0.76[b]	0.69[c]	0.74
1100 cph	0.84	0.96[b]	0.96[b]	0.65[c]	0.74[c]
12,000 cph	0.96	1.09	1.00	0.90	0.78

a: 2-"T-1", All Other Tests 1-"T-1"

b: 2-A-387,B, All Other Tests 1-A-387,B

c: 2-A-212,B, All Other Tests 1-A-212,B

Table V
Tensile and Impact Properties of
As-Tested "T-1" Fatigue Specimens

Condition	Y.S. (Kips)	T.S. (Kips)	YS/TS (%)	Elong. (%)	R.A. (%)	n*	15 ft.lb. Trans.Temp.
Heat 1							
As-Received	119.0	131.0	90.9	19.5	63.3	0.096	-104°F
Fatigue Tested at 800°F-5,280 cyc.	106.9	117.8	90.8	11.0	63.0	0.114	-102°F
Fatigue Tested at 800°F-50,000 cyc.	107.3	118.6	90.5	10.5	64.5	0.112	-98°F
Fatigue Tested at 800°F-57,000 cyc.	107.4	118.8	90.4	10.5	62.4	0.114	-
Fatigue Tested at 800°F-111,000 cyc.	-	-	-	-	-	-	-102°F
Fatigue Tested at 900°F-10,200 cyc.	107.4	119.4	90.2	12.5	64.4	0.124	-92°F
Fatigue Tested at 900°F-24,000 cyc.	109.2	120.4	90.7	13.5	65.4	0.118	-
Fatigue Tested at 900°F-45,600 cyc.	-	-	-	-	-	-	-80°F
Fatigue Tested at 900°F-156,000 cyc.	-	-	-	-	-	-	-90°F
Heat 2							
As-Received	122.0	132.8	91.8	-	53.9	0.101	-156°F
Aged 800°F-5 hrs. Fatigue Tested at 800°F-77,000 cyc.	-	-	-	-	-	-	-140°F
Aged 800°F-20 hrs. Fatigue Tested at 800°F-35,000 cyc.	-	-	-	-	-	-	-132°F
Aged 800°F-100 hrs. Fatigue Tested at 800°F-73,000 cyc.	-	-	-	-	-	-	-160°F

* Strain hardening exponent

Table VI
Results of Pretest Aging Study on "T-1" Steel

Heat No. 2

800°F Aging Temperature and Testing Temperature

Aging Time Prior to Testing	% Total Strain	Cycles to Failure	Cycles to Failure Normalized to 0.6% Total Strain
5 hours	0.58	77,000	60,000
10 hours	0.595	35,000	33,000
20 hours	0.555	35,000	20,000
50 hours	0.625	29,600	40,000
100 hours	0.53	73,000	30,000

(a) Elastic Stress

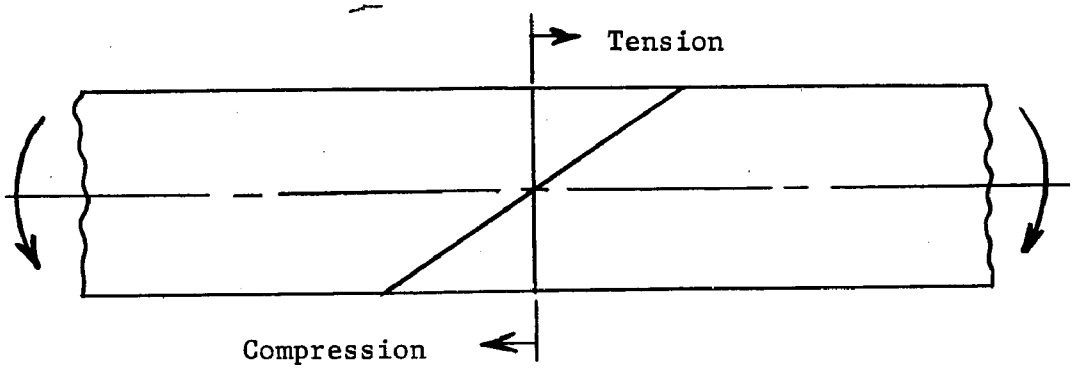

(b) Elastic + Plastic Stress

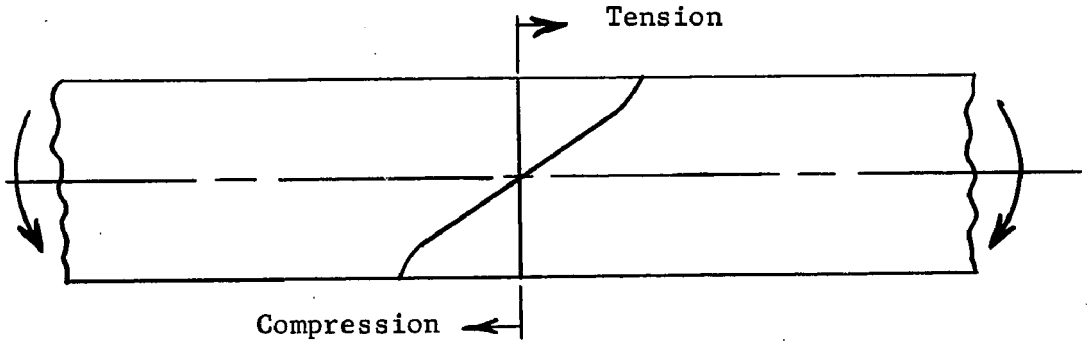

(c) Plastic Stress (Limiting Case)

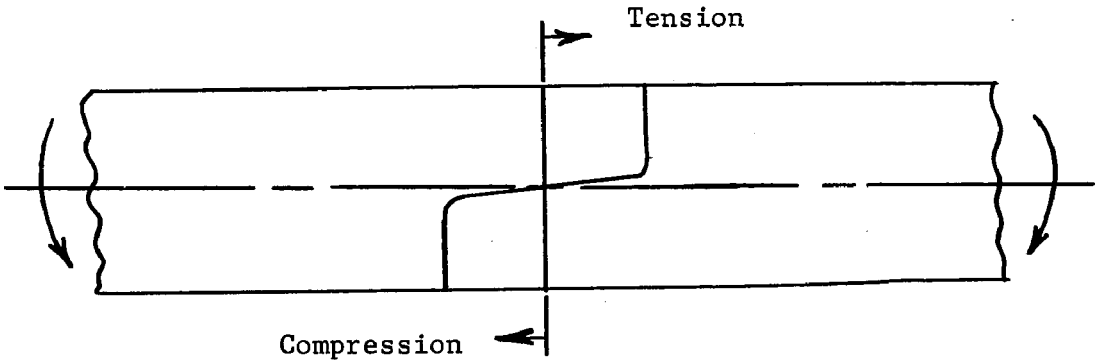

Figure 1 - Stress Distribution in Simple Beam Under Bending Moment[16]

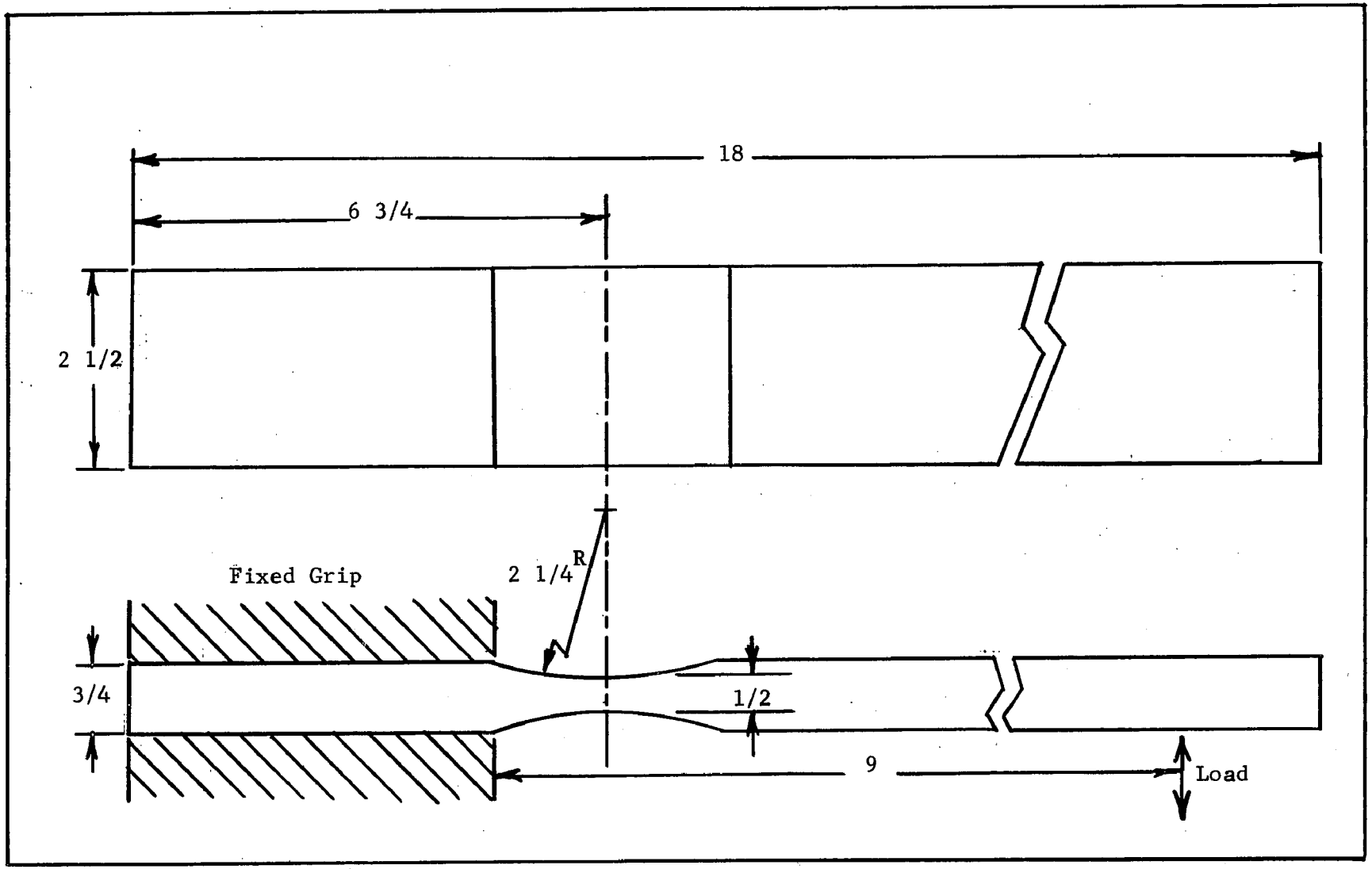

Figure 2 - Standard Lehigh Cantilever Specimen Geometry

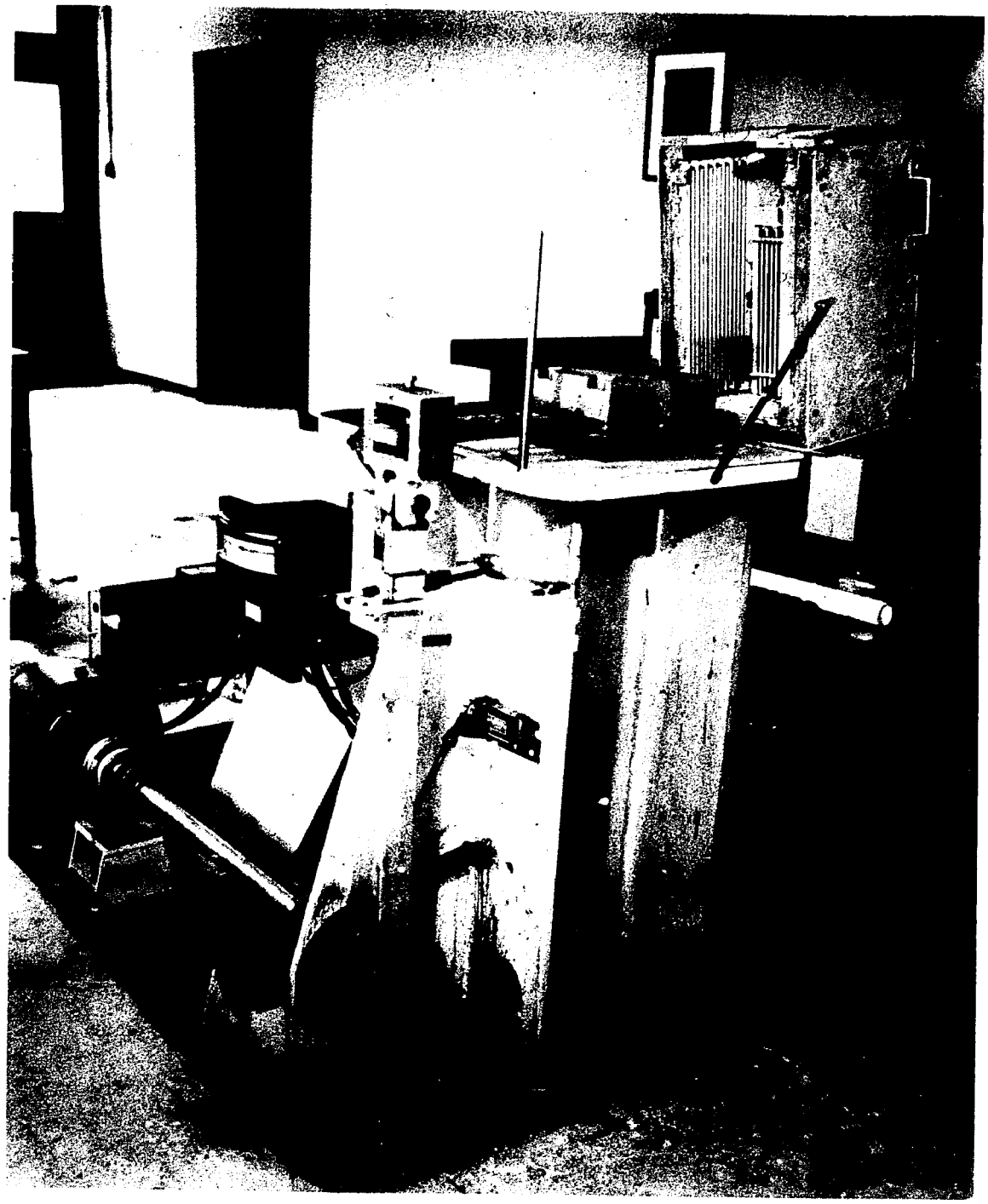

Figure 3 - The Elevated Temperature Fatigue Testing Equipment

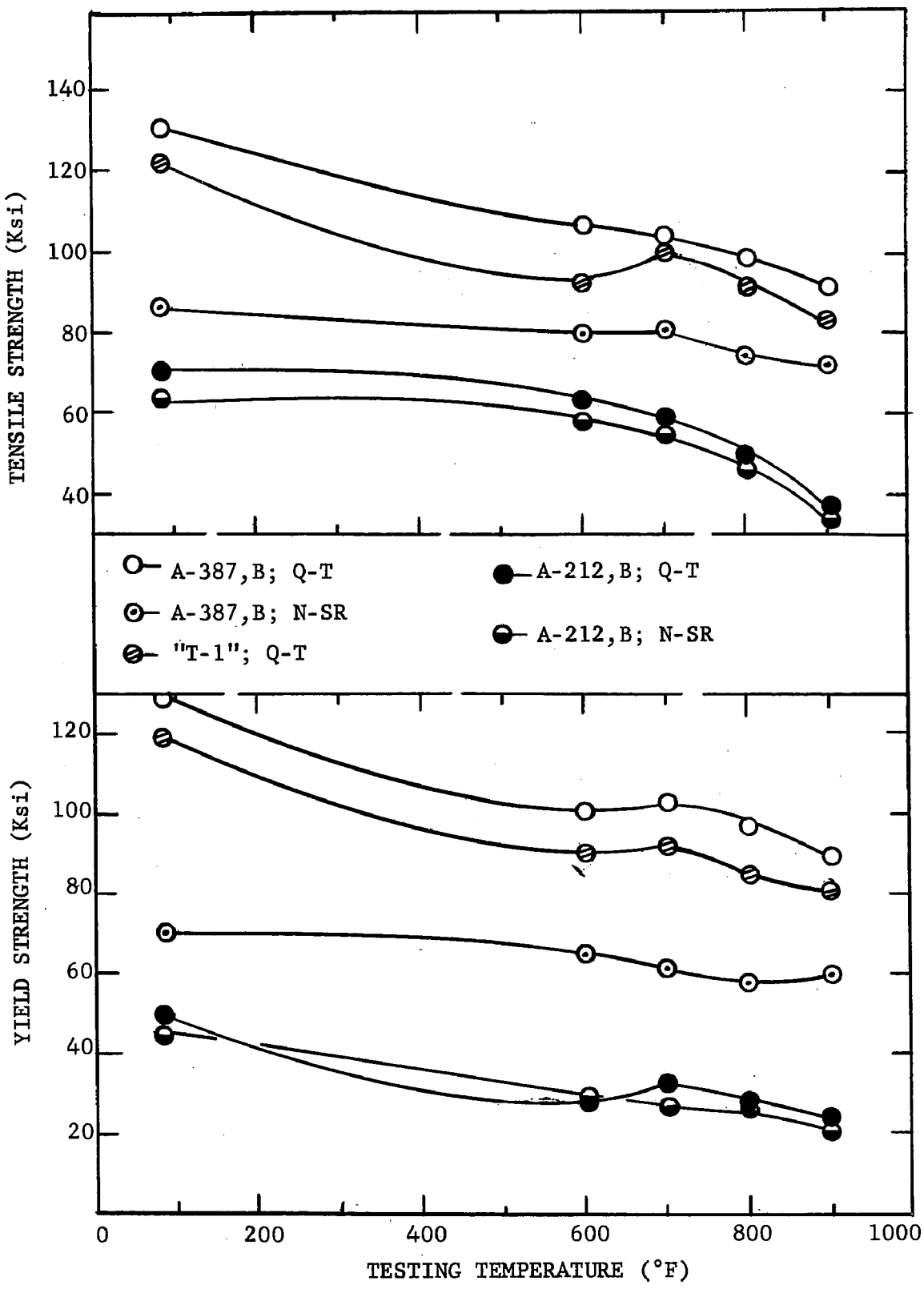

Figure 4 - Elevated Temperature Strength Properties

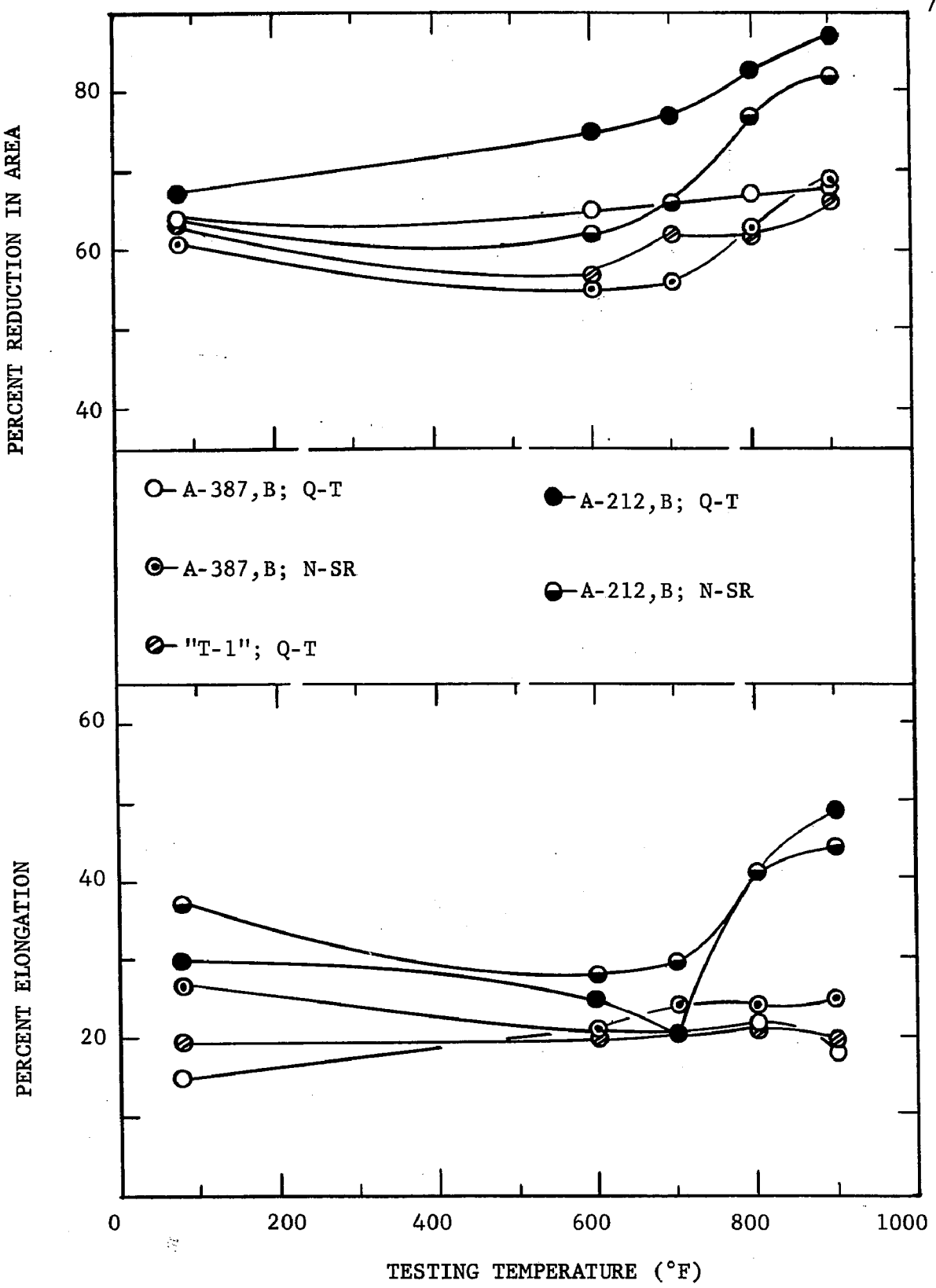

Figure 5 - Elevated Temperature Ductility Properties

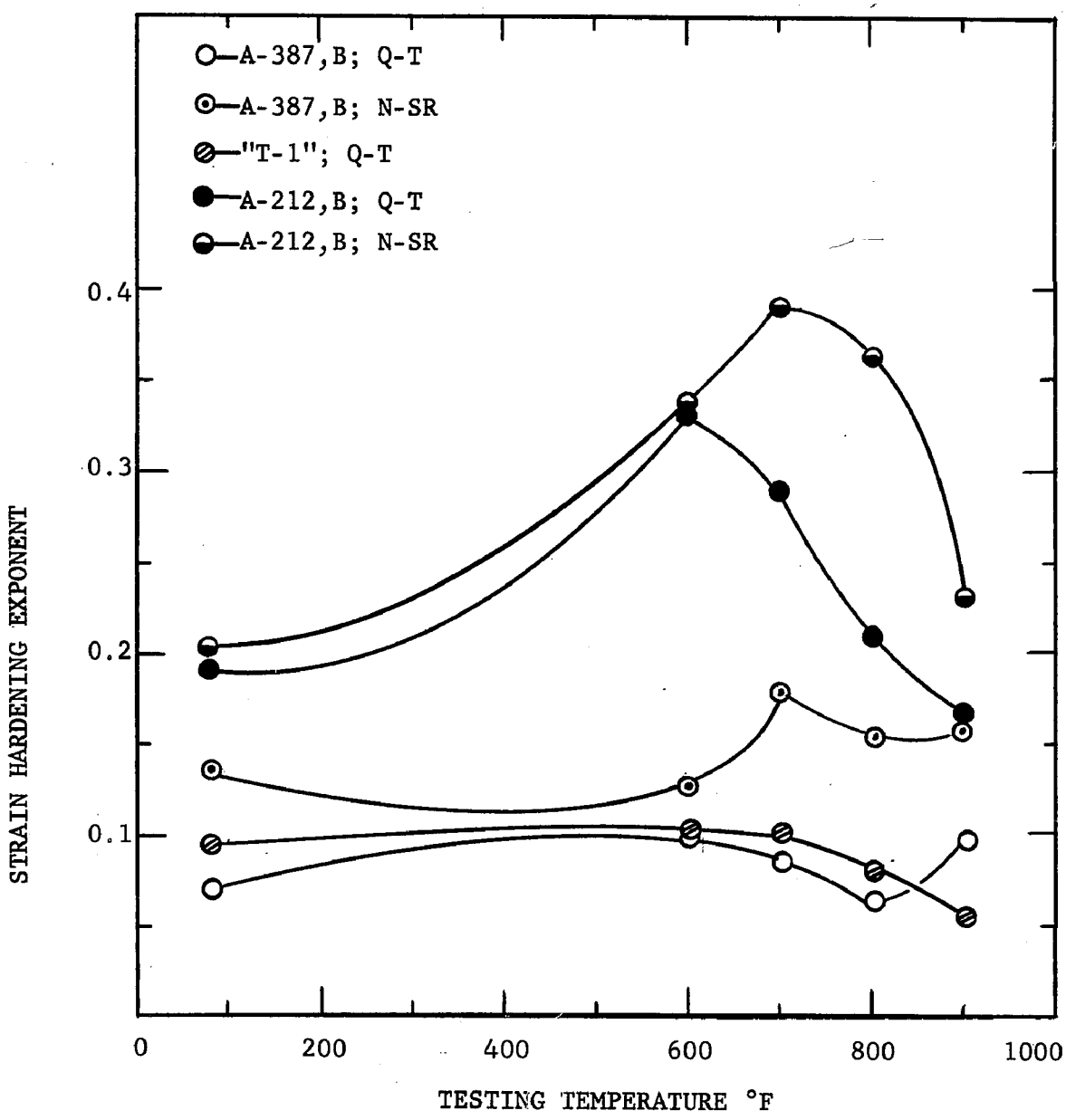

Figure 6 - Elevated Temperature Strain Hardening Exponents

Figure 7 - Total Strain Versus Cycle Lifetime, "T-1" Steel, Mill Q-T, 12,000 cph

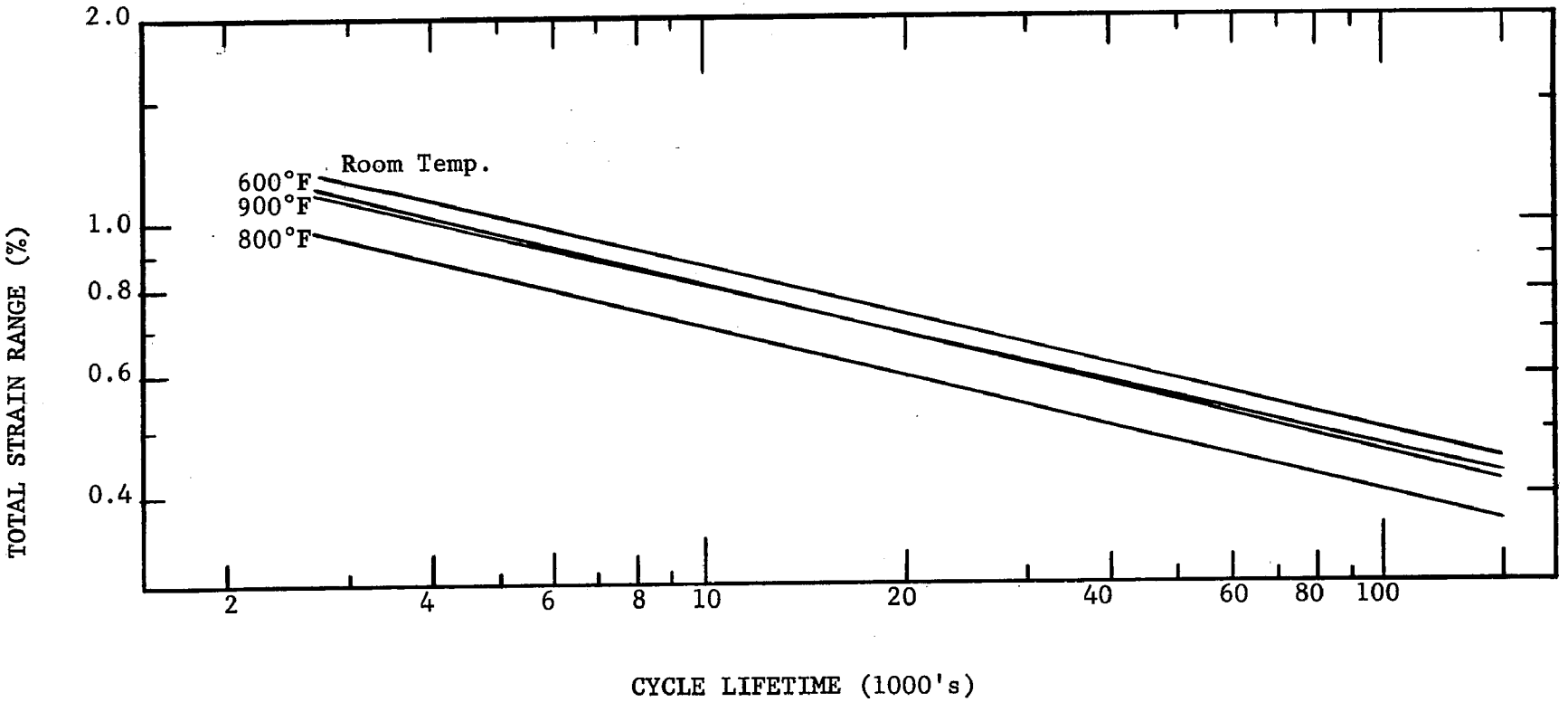

Figure 8 - Total Strain Versus Cycle Lifetime, A-387,B Steel, Q-T, 12,000 cph

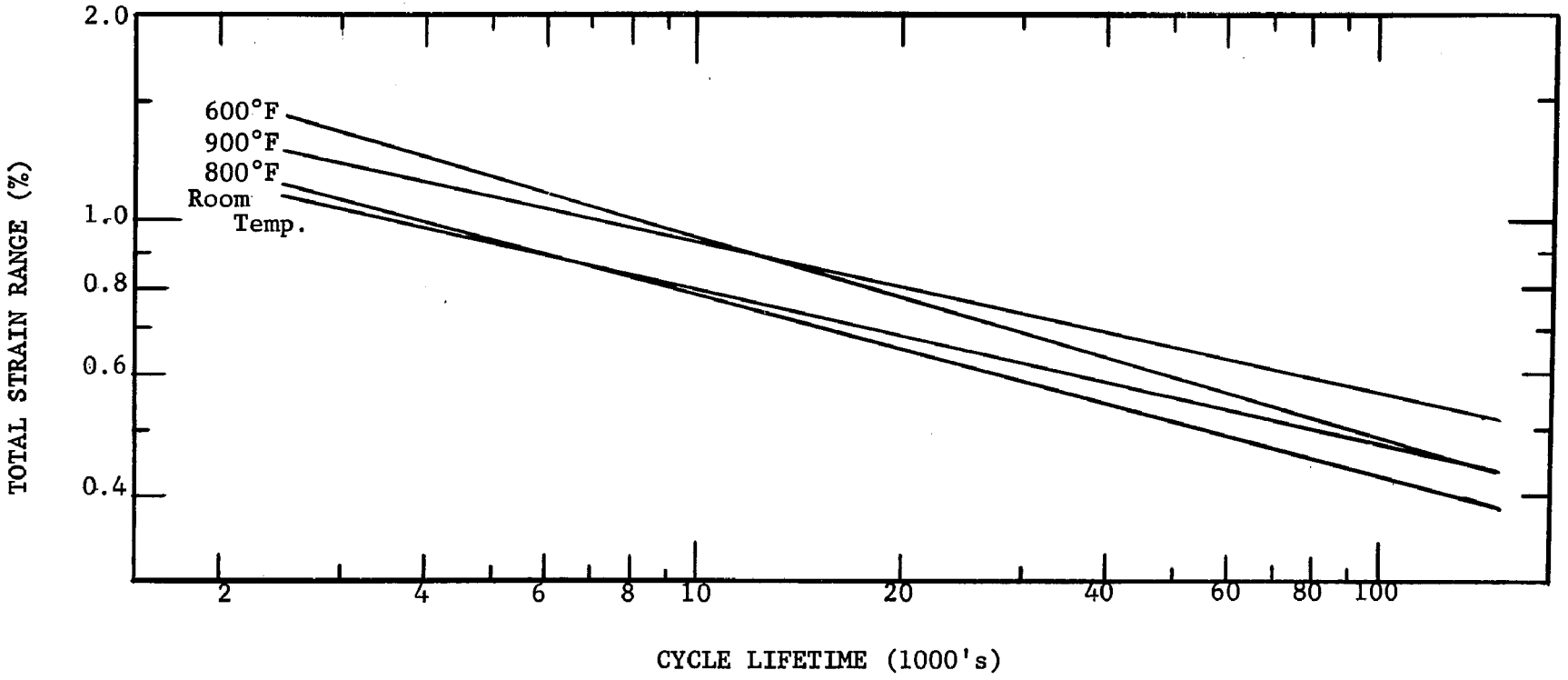

Figure 9 - Total Strain Versus Cycle Lifetime, A-387,B Steel, N-SR, 12,000 cph

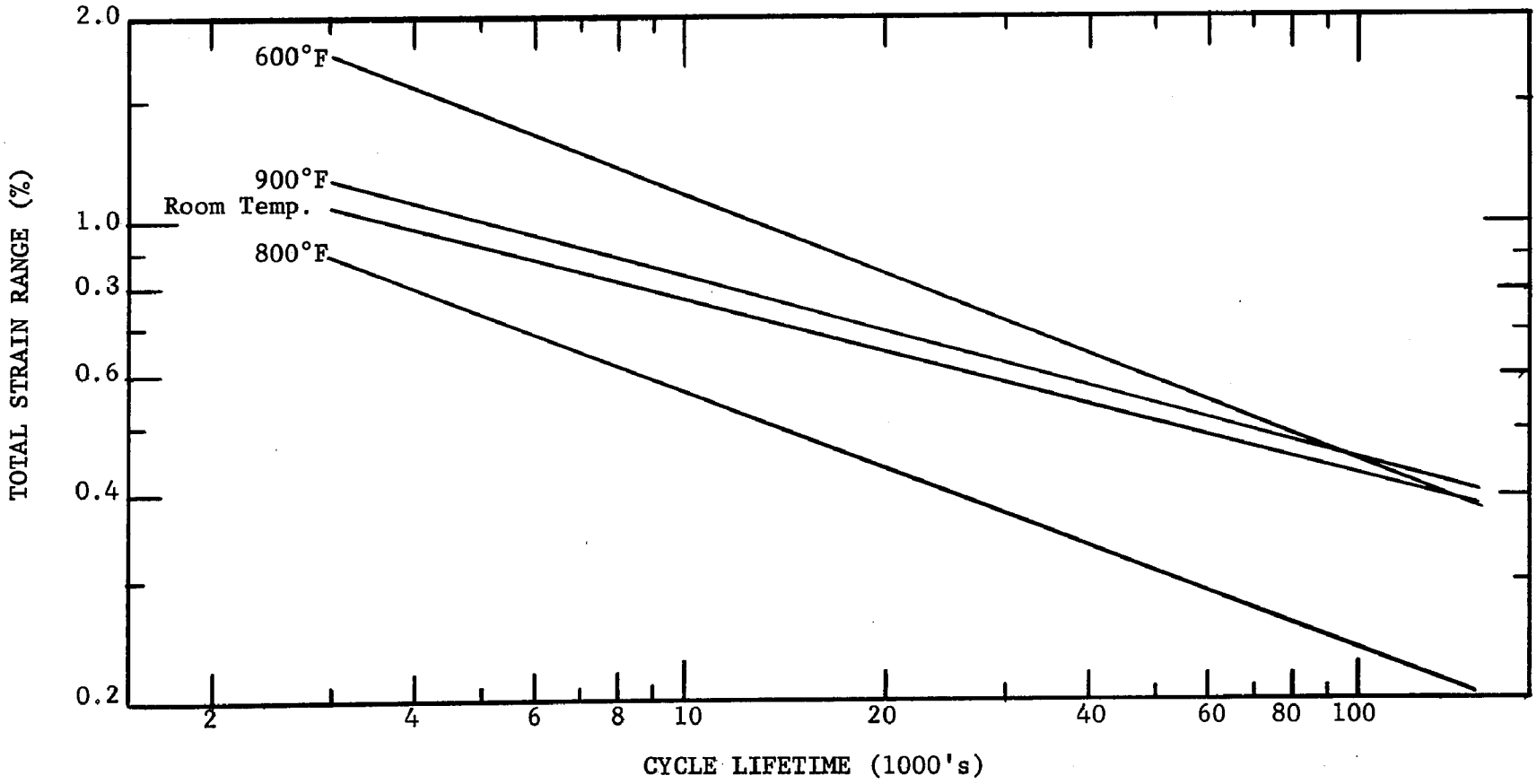

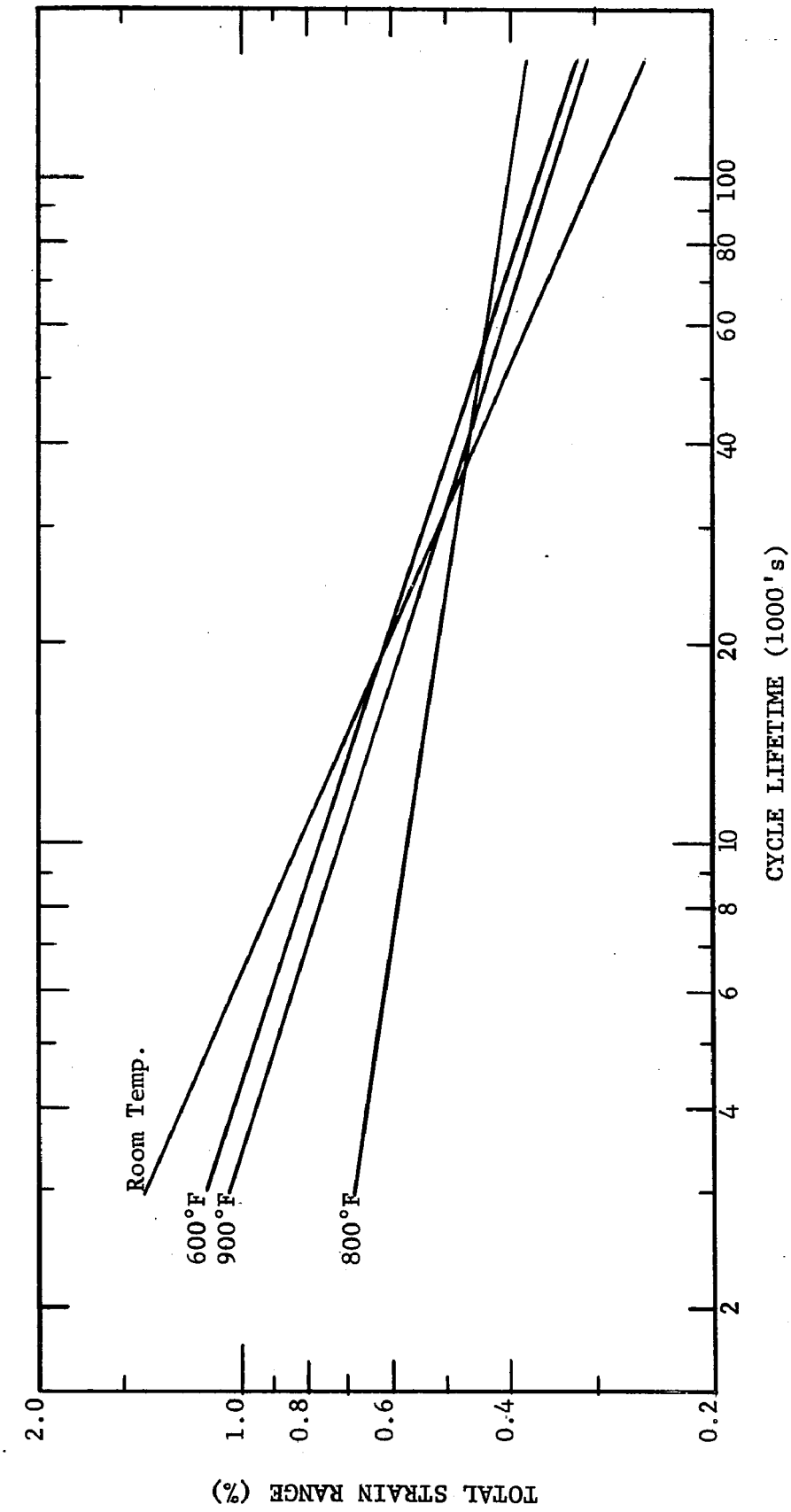

Figure 10 - Total Strain Versus Cycle Lifetime, A-212, B Steel, Q-T, 12,000 cph

Figure 11 - Total Strain Versus Cycle Lifetime, A-212,B Steel, N-SR, 12,000 cph

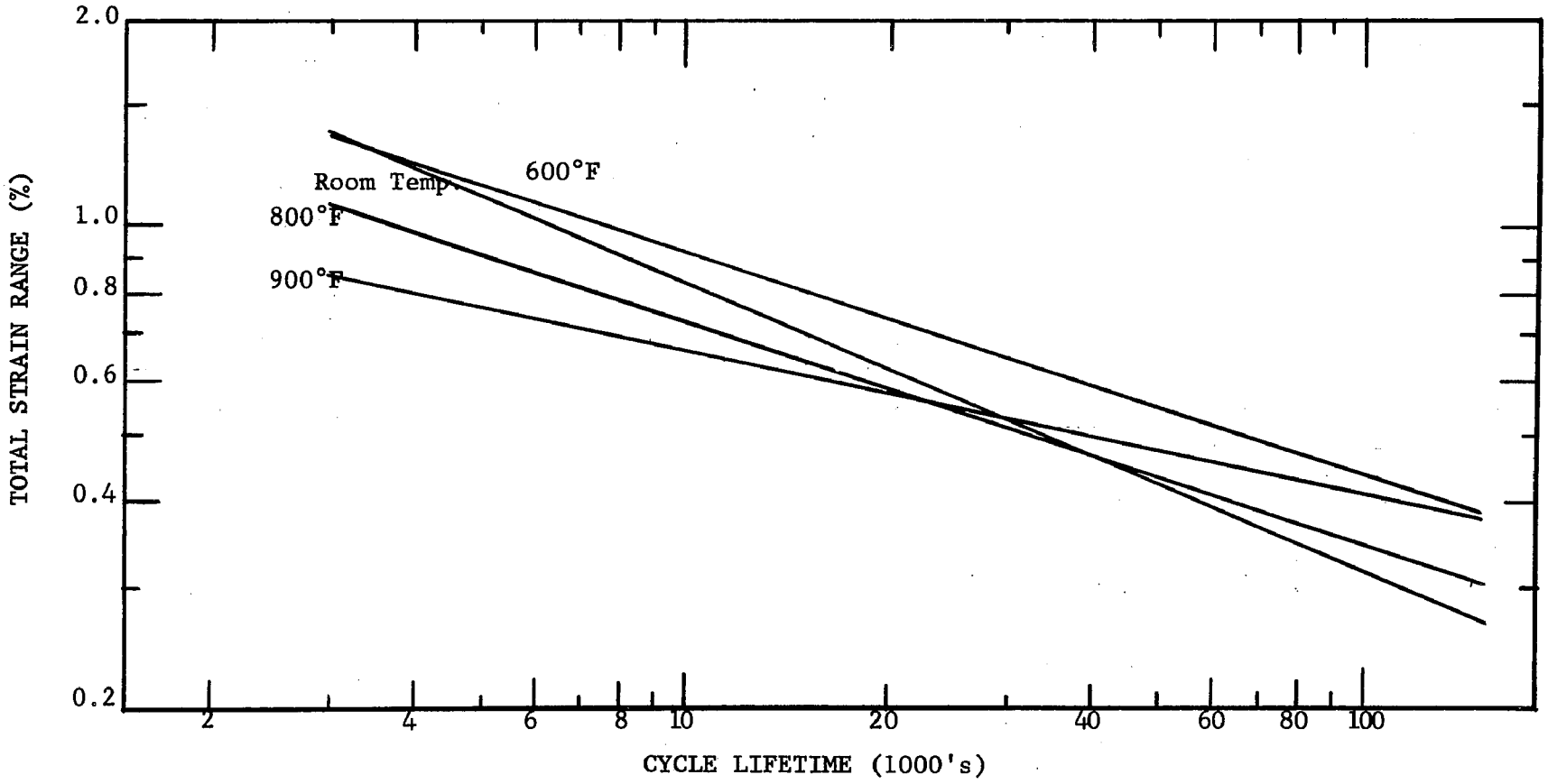

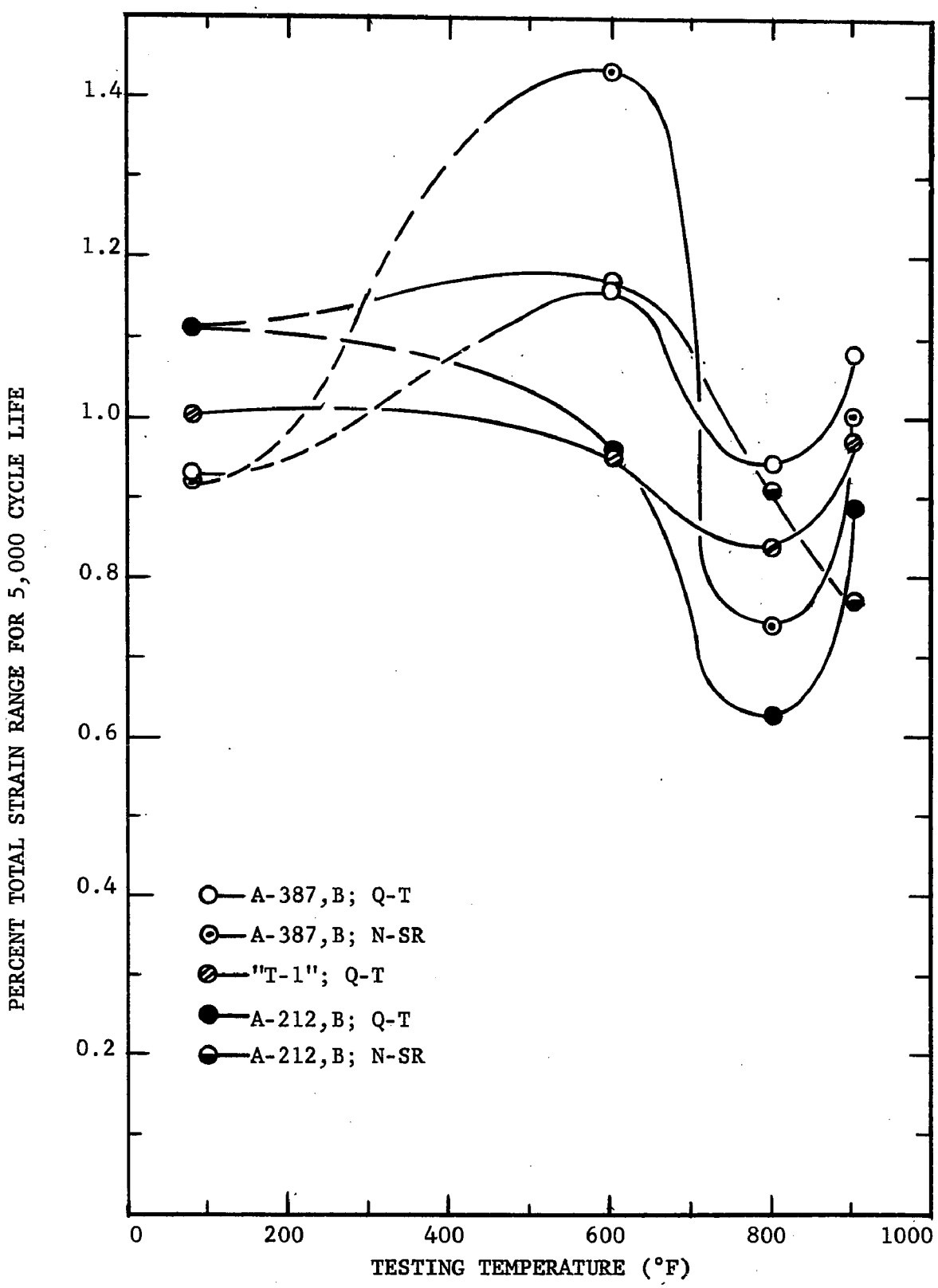

Figure 12 - 5,000 Cycle Life Allowable Strain Ranges-12,000cph

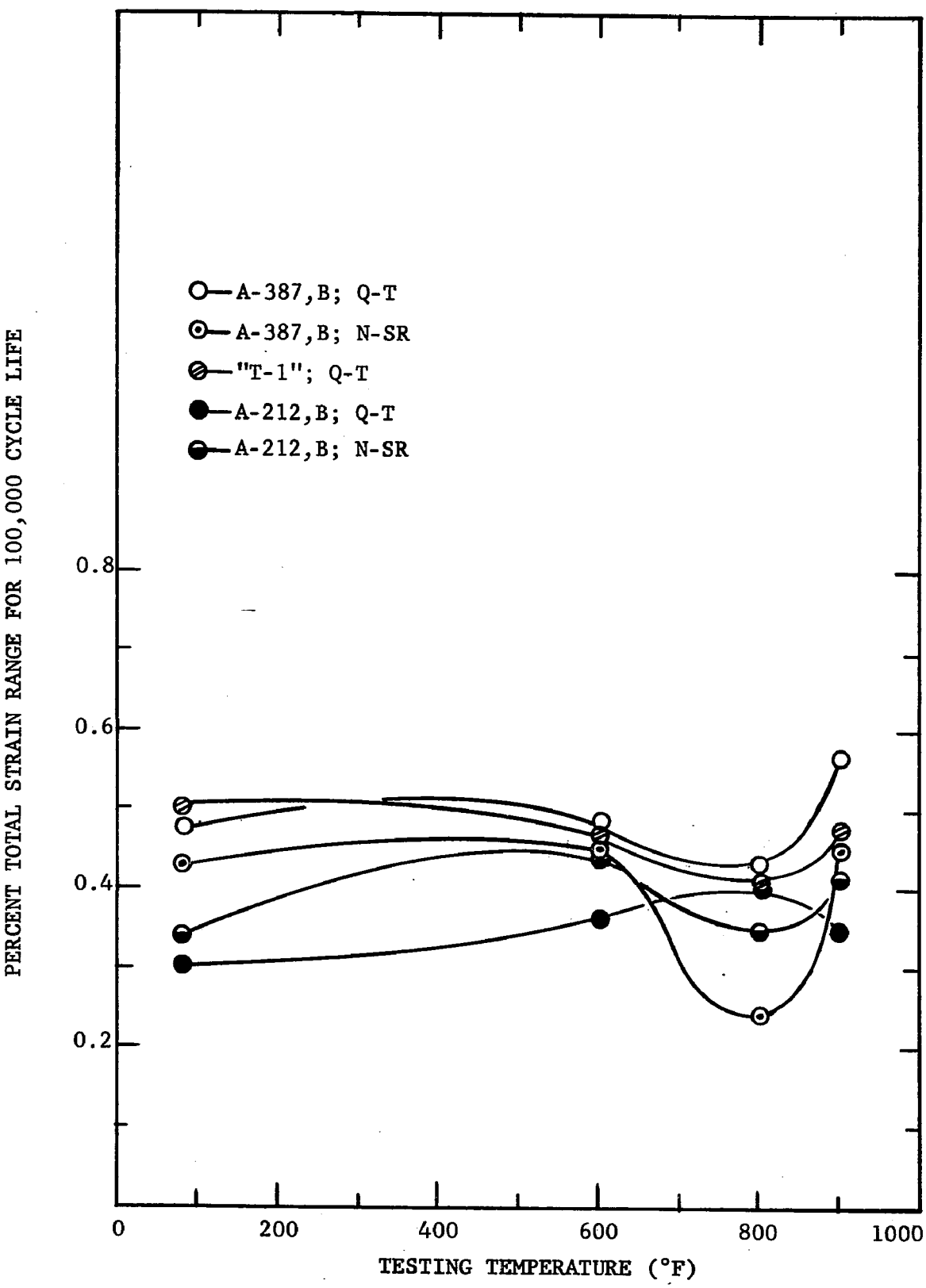

Figure 13 - 100,000 Cycle Life Allowable Strain Ranges
12,000cph

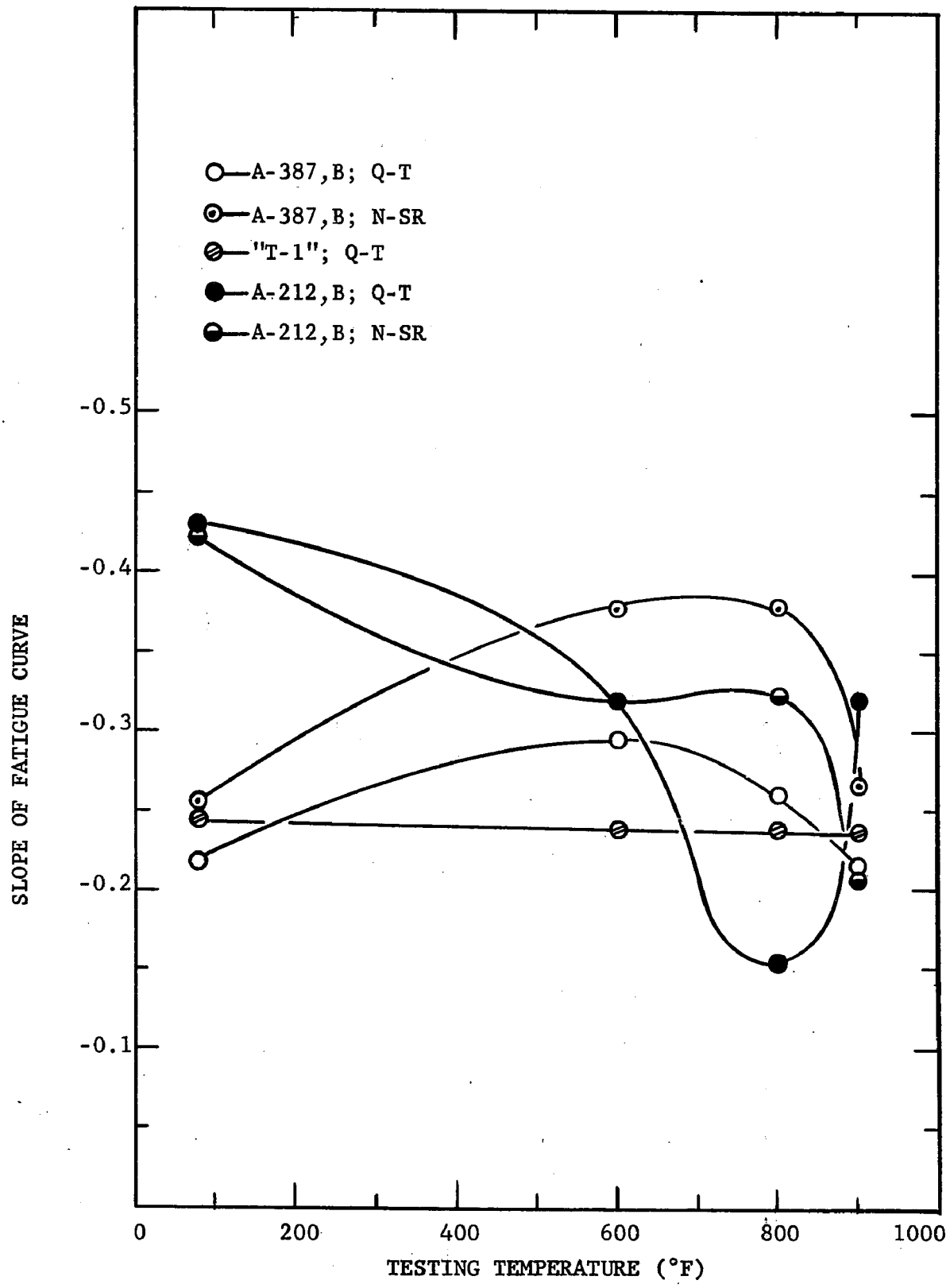

Figure 14 - 12,000cph Slope Values

Figure 15 - Anomalous "T-1" Fatigue Behavior - 12,000cph

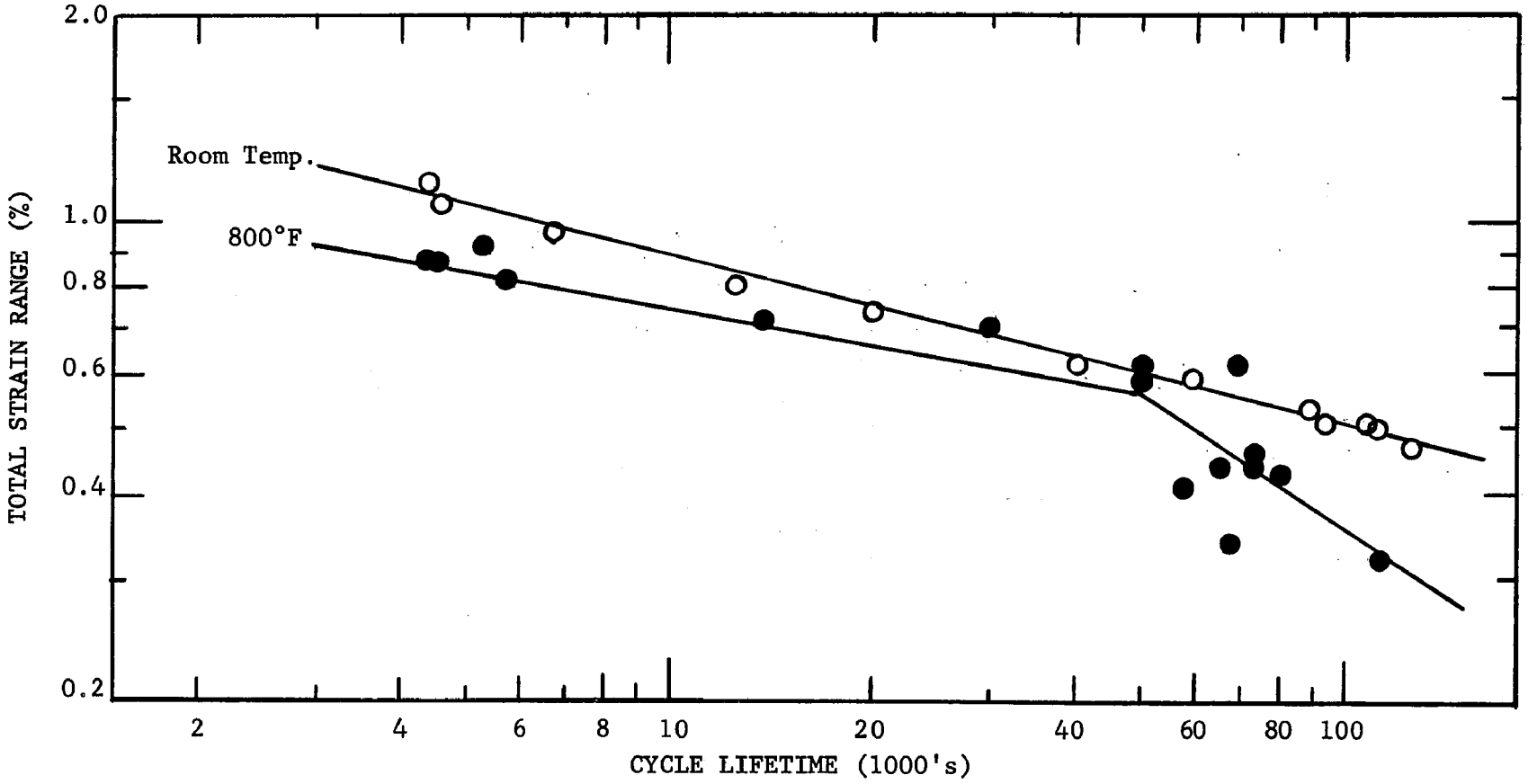

Figure 16 - Total Strain Versus Cycle Lifetime, "T-1" Steel, Mill Q-T
1100cph

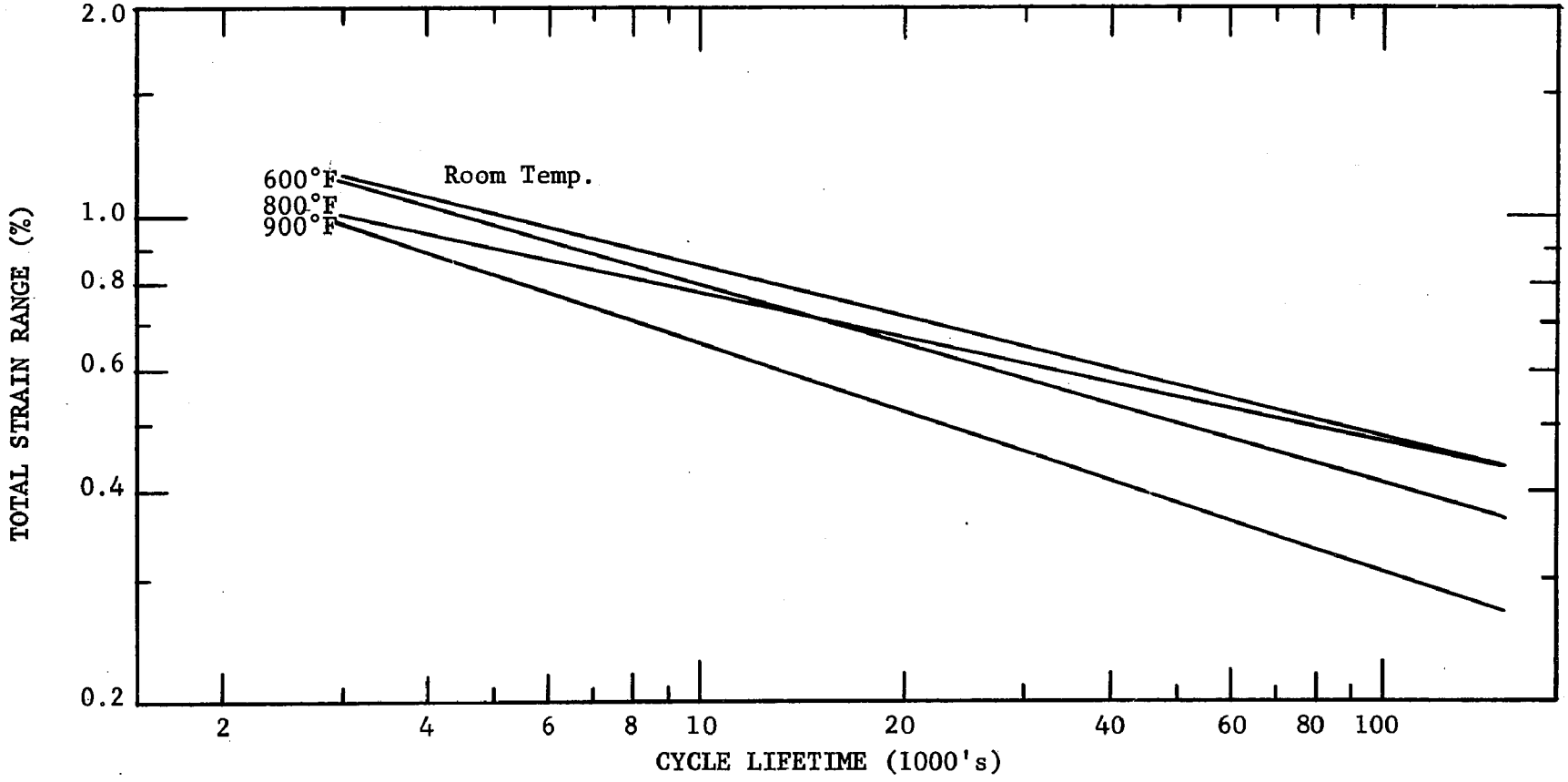

Figure 17 - Total Strain Versus Cycle Lifetime, A-387,B Steel, Q-T, 1100cph

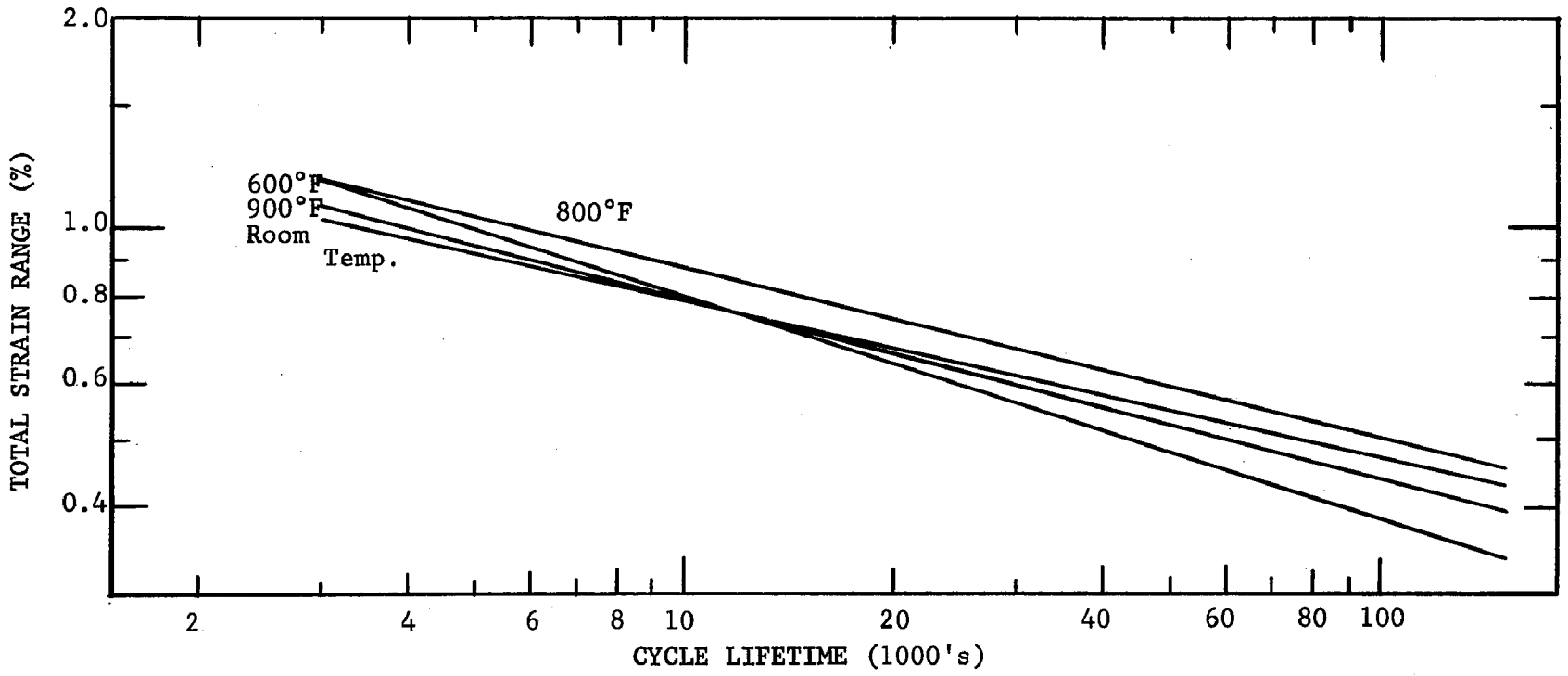

Figure 18 - Total Strain Versus Cycle Lifetime, A-387,B Steel, N-SR, 1100cph

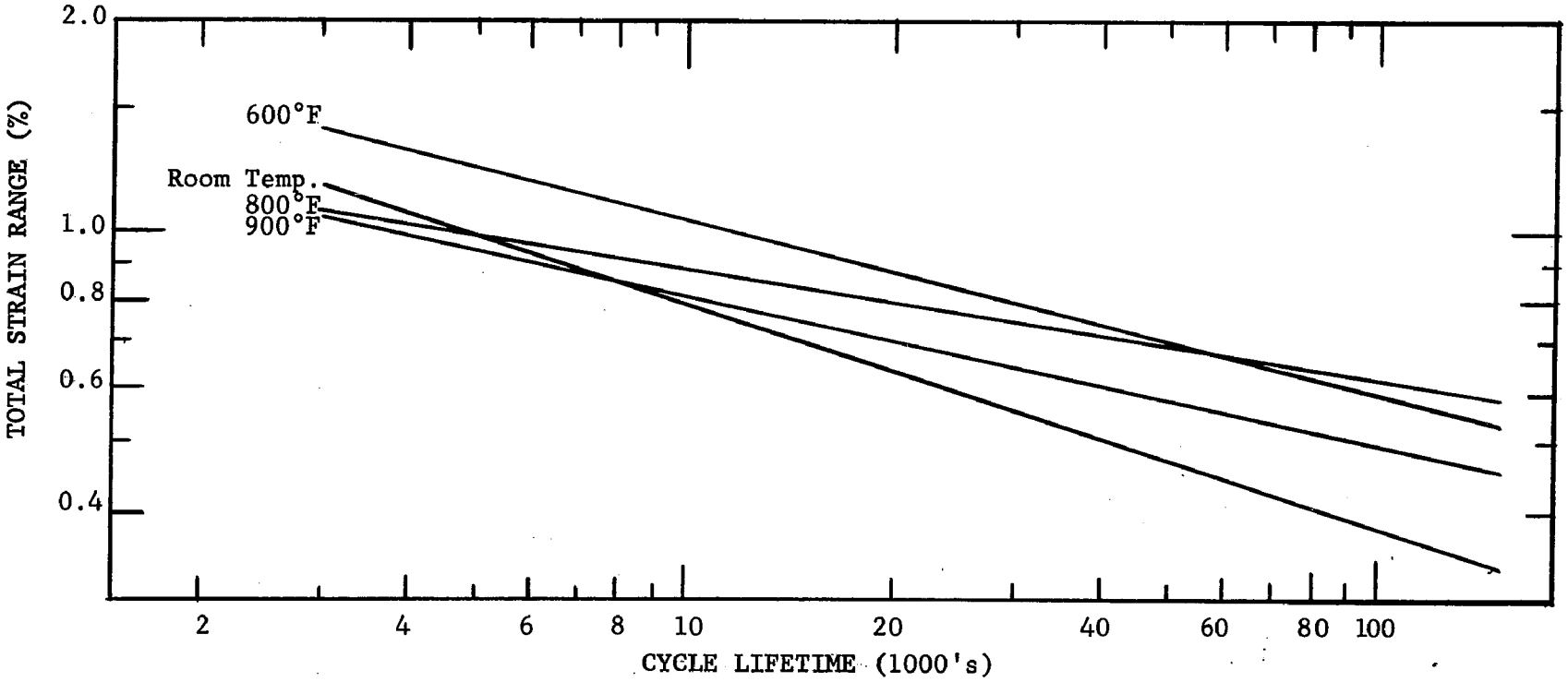

Figure 19 - Total Strain Versus Cycle Lifetime, A-212,B Steel, Q-T, 1100cph

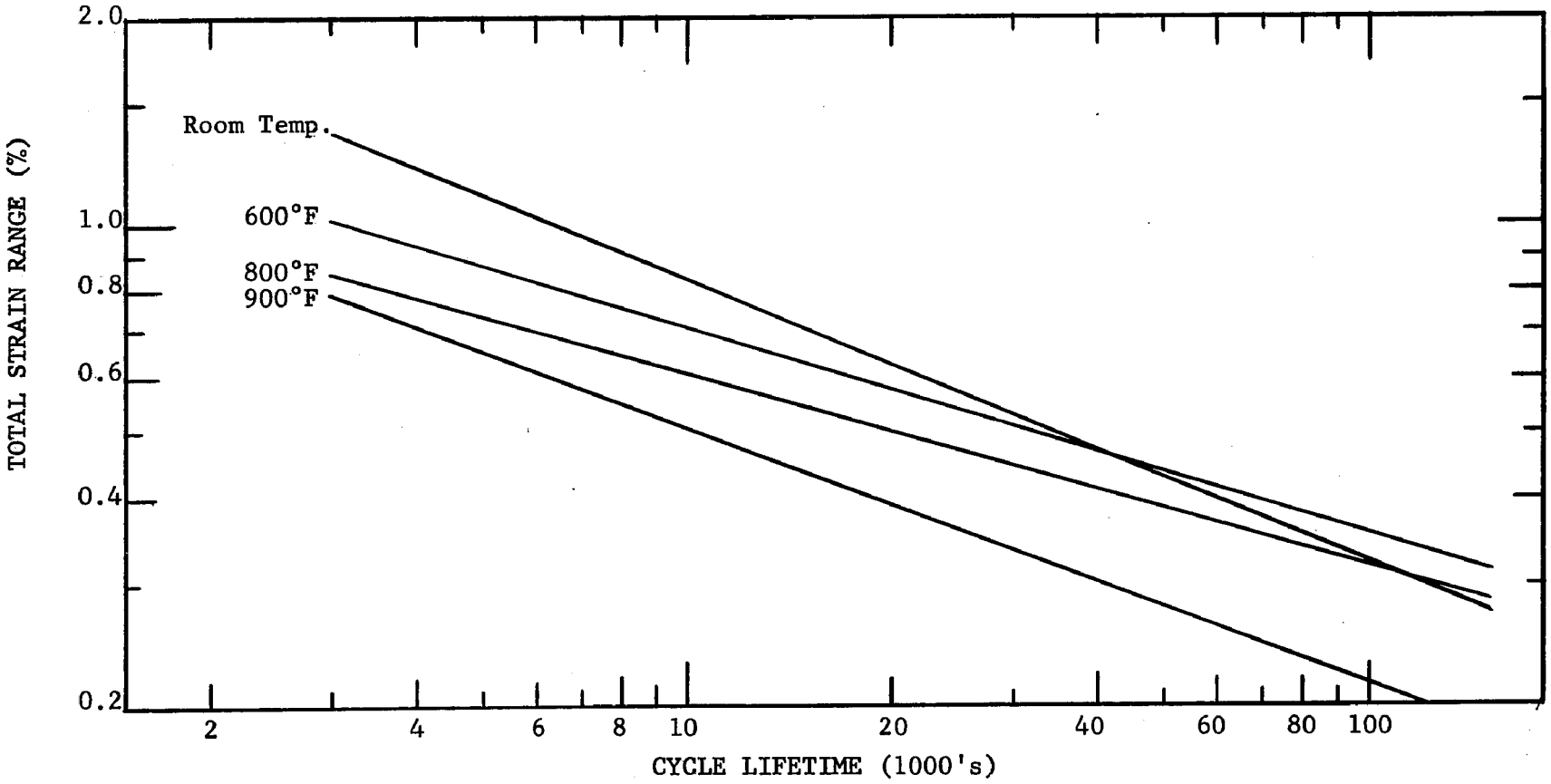

Figure 20 - Total Strain Versus Cycle Lifetime, A-212,B Steel, N-SR, 1100cph

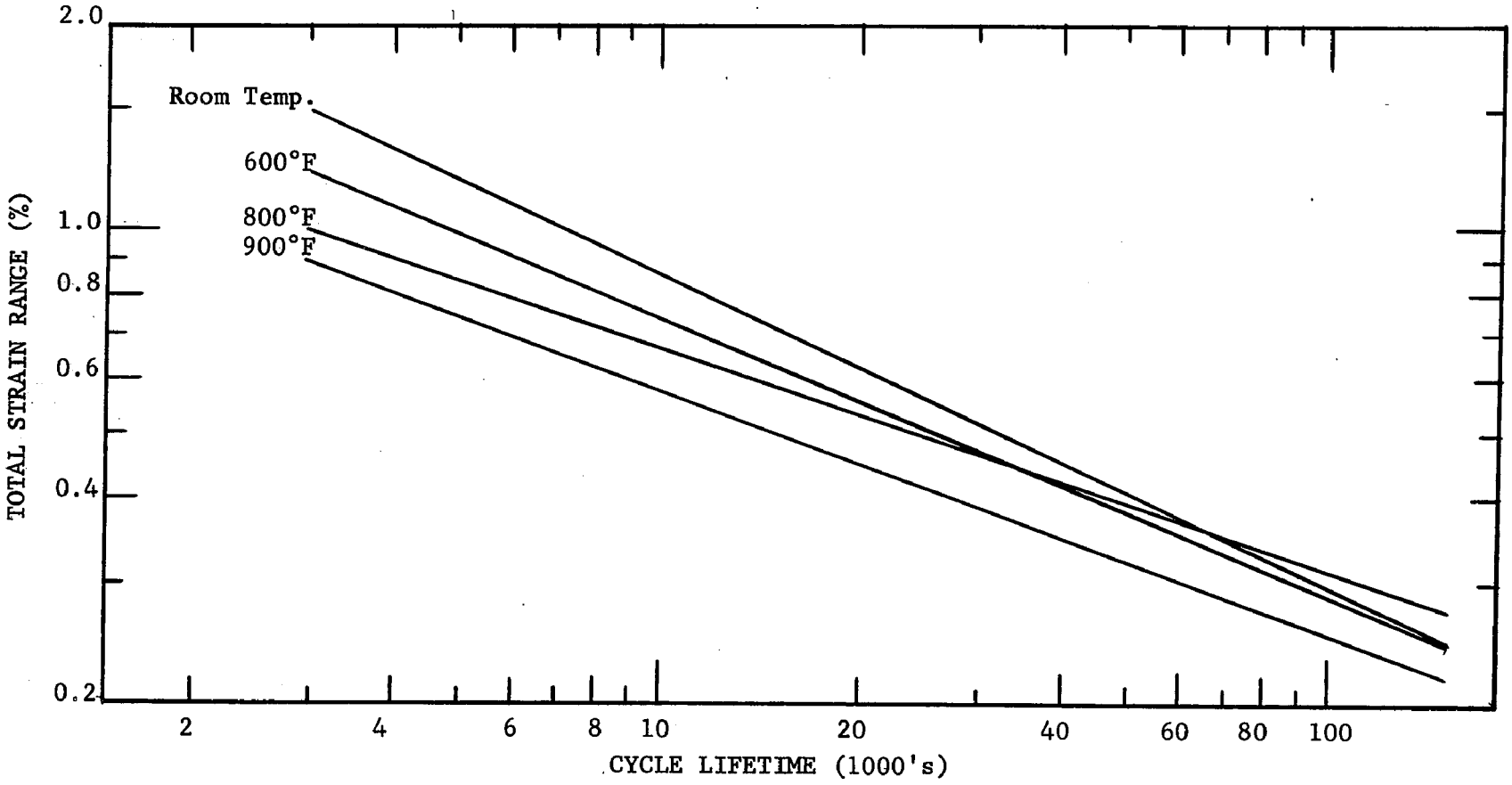

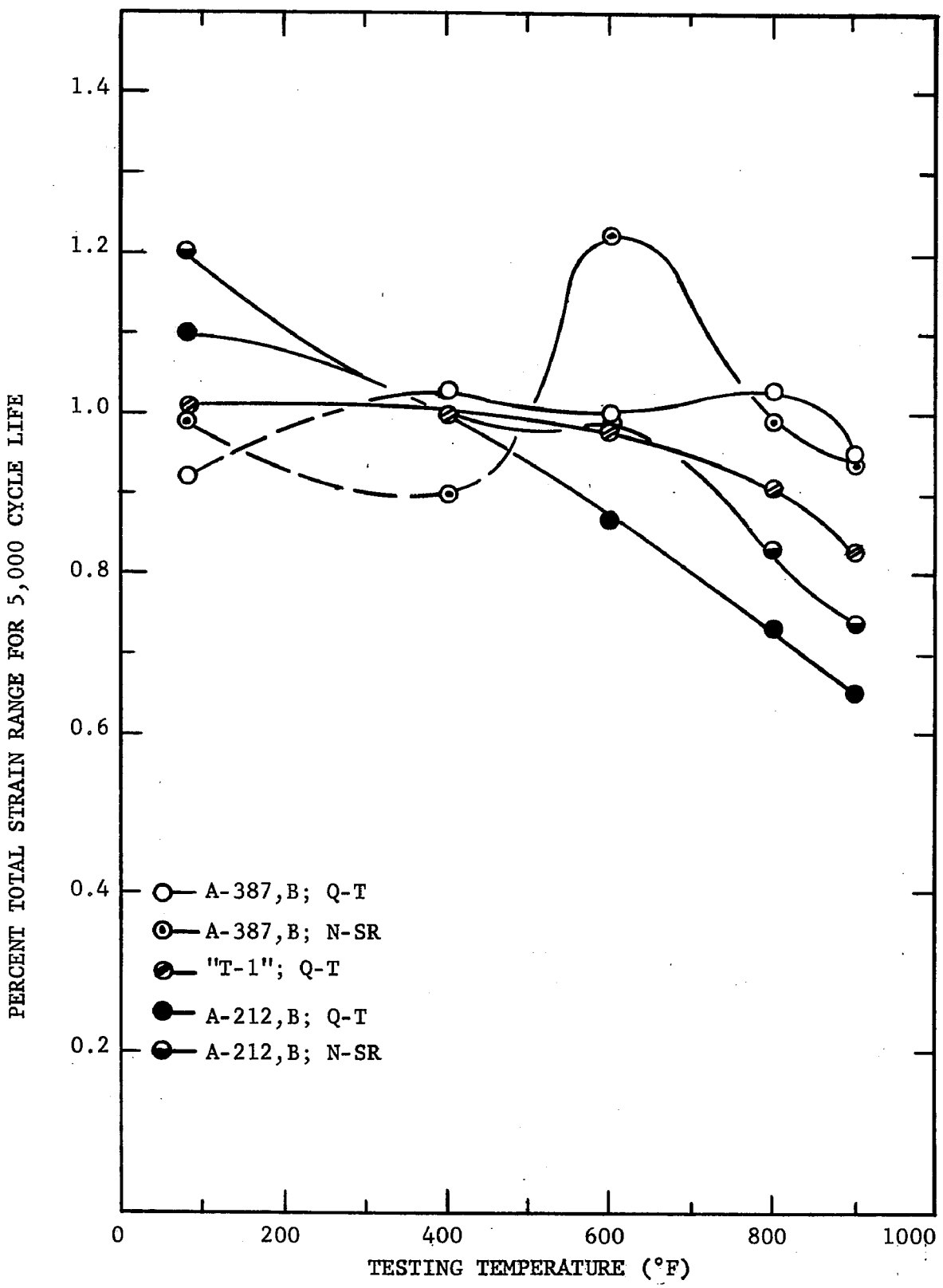

Figure 21 - 5,000 Cycle Life Allowable Strain Ranges - 1100cph

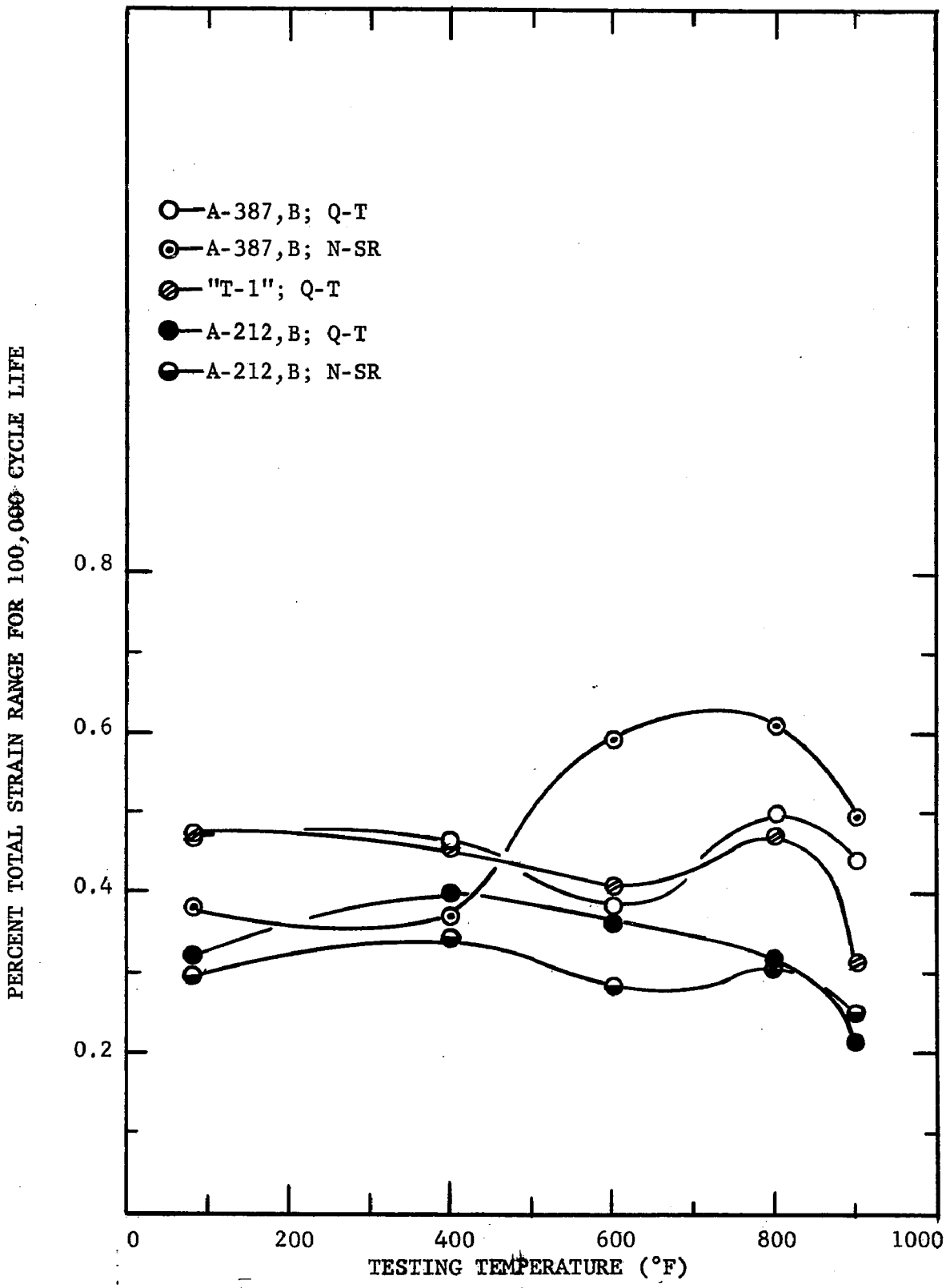

Figure 22 - 100,000 Cycle Life Allowable Strain Ranges - 1100cph

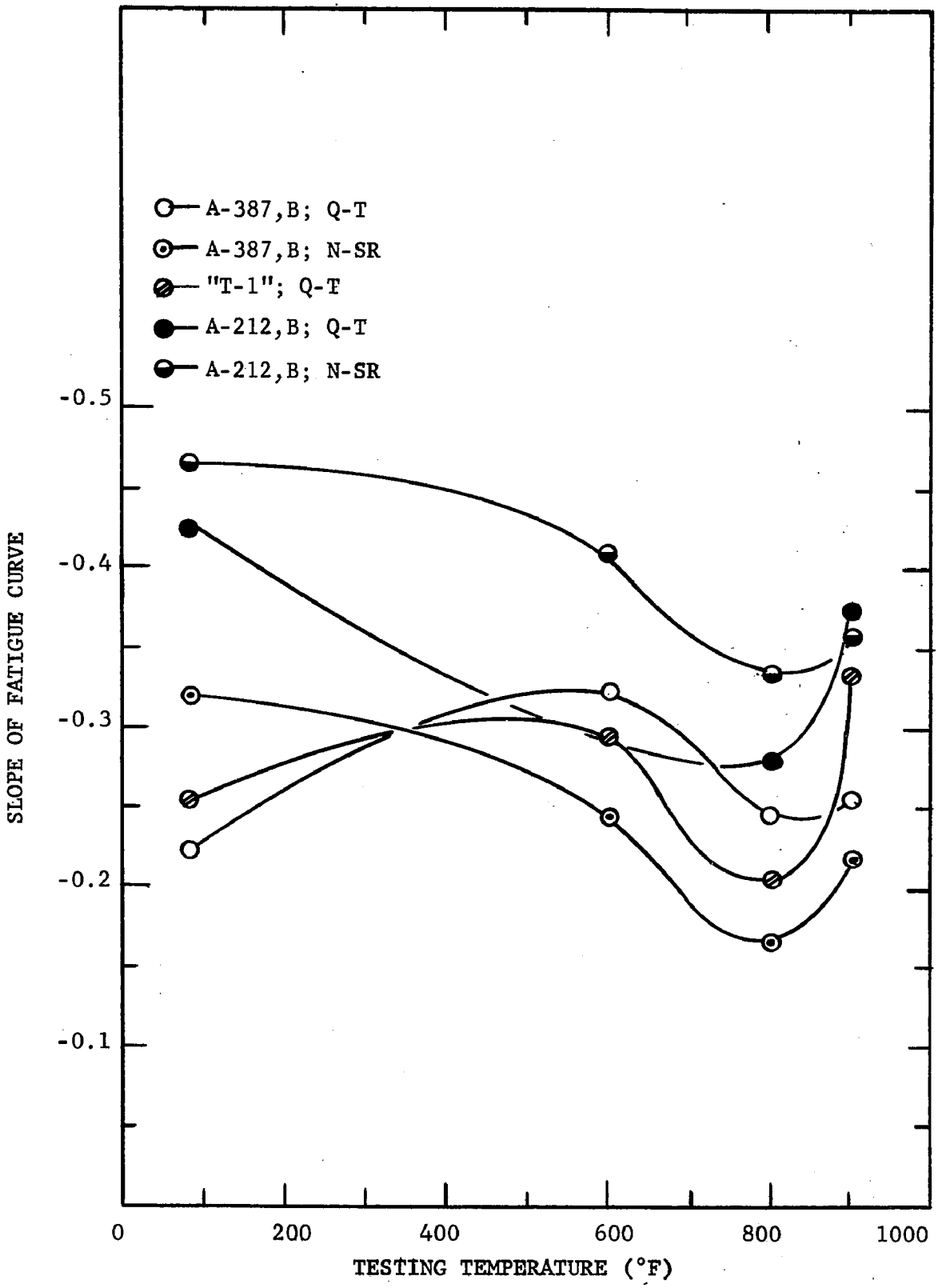

Figure 23 - 1100cph Slope Values

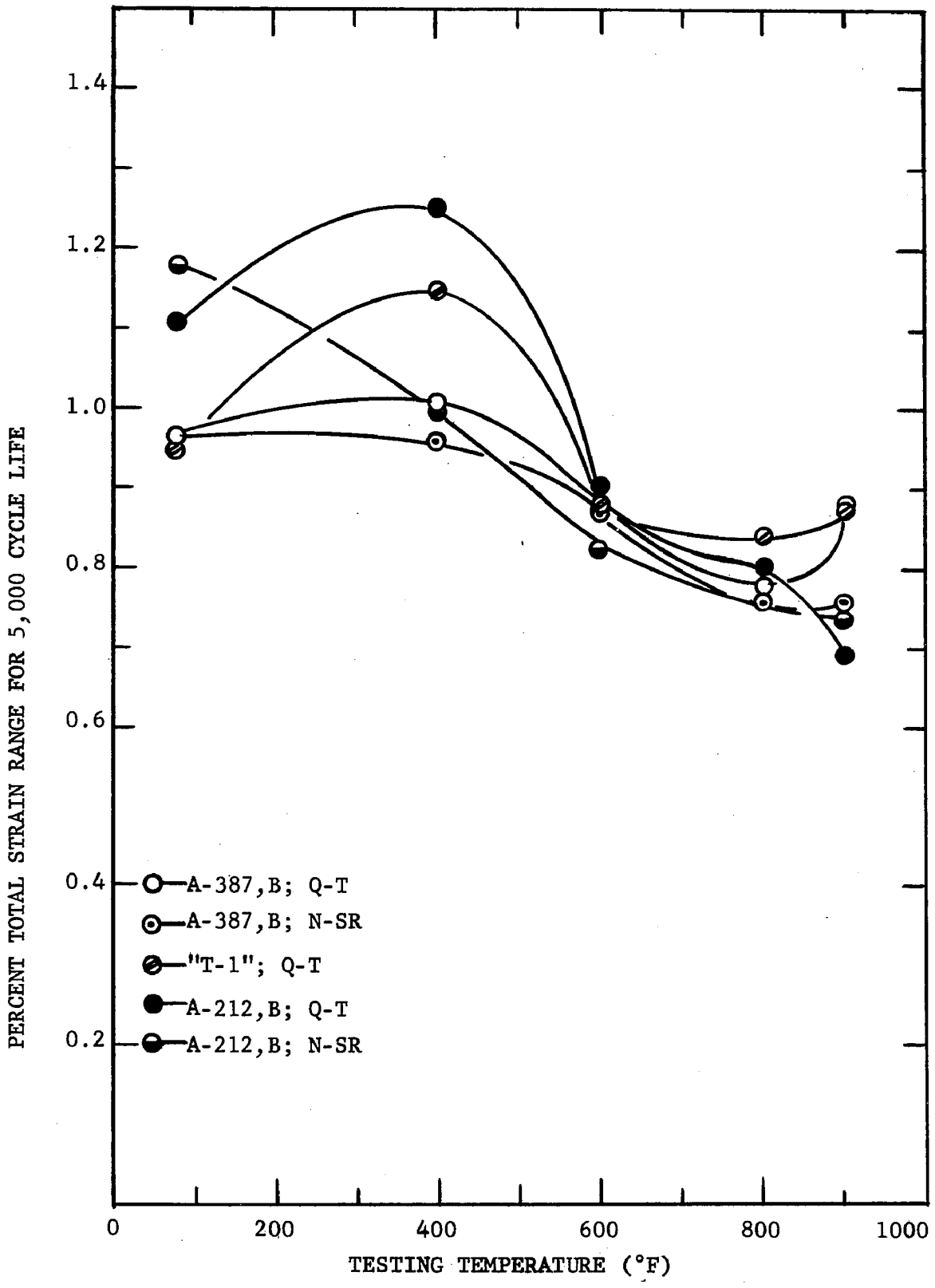

Figure 24 - 5,000 Cycle Life Allowable Strain Ranges - 110cph

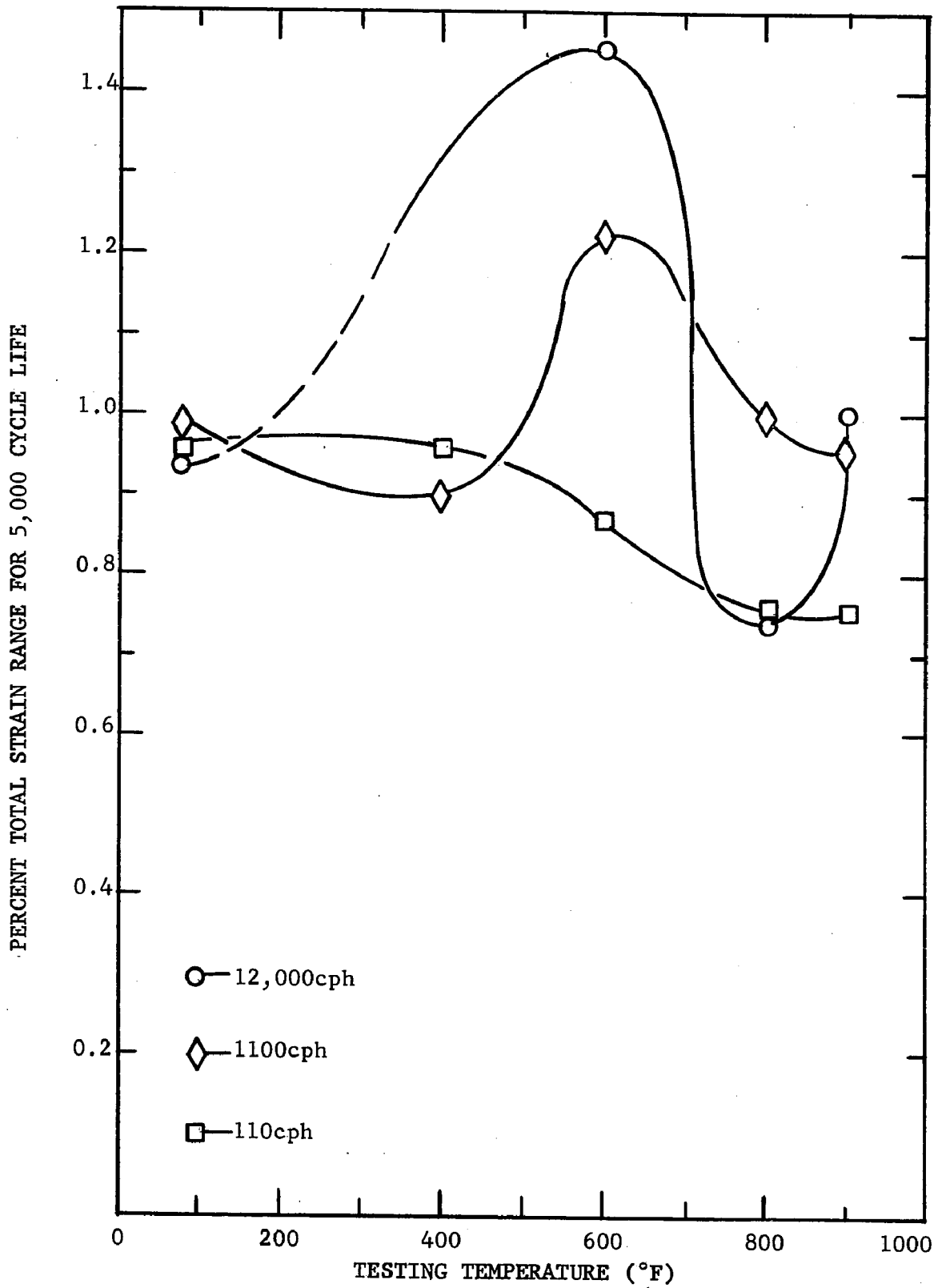

Figure 25 - Influence of Cycle Rate and Temperature Upon The 5,000 Cycle Strain Range - A-387,B Steel, N-SR

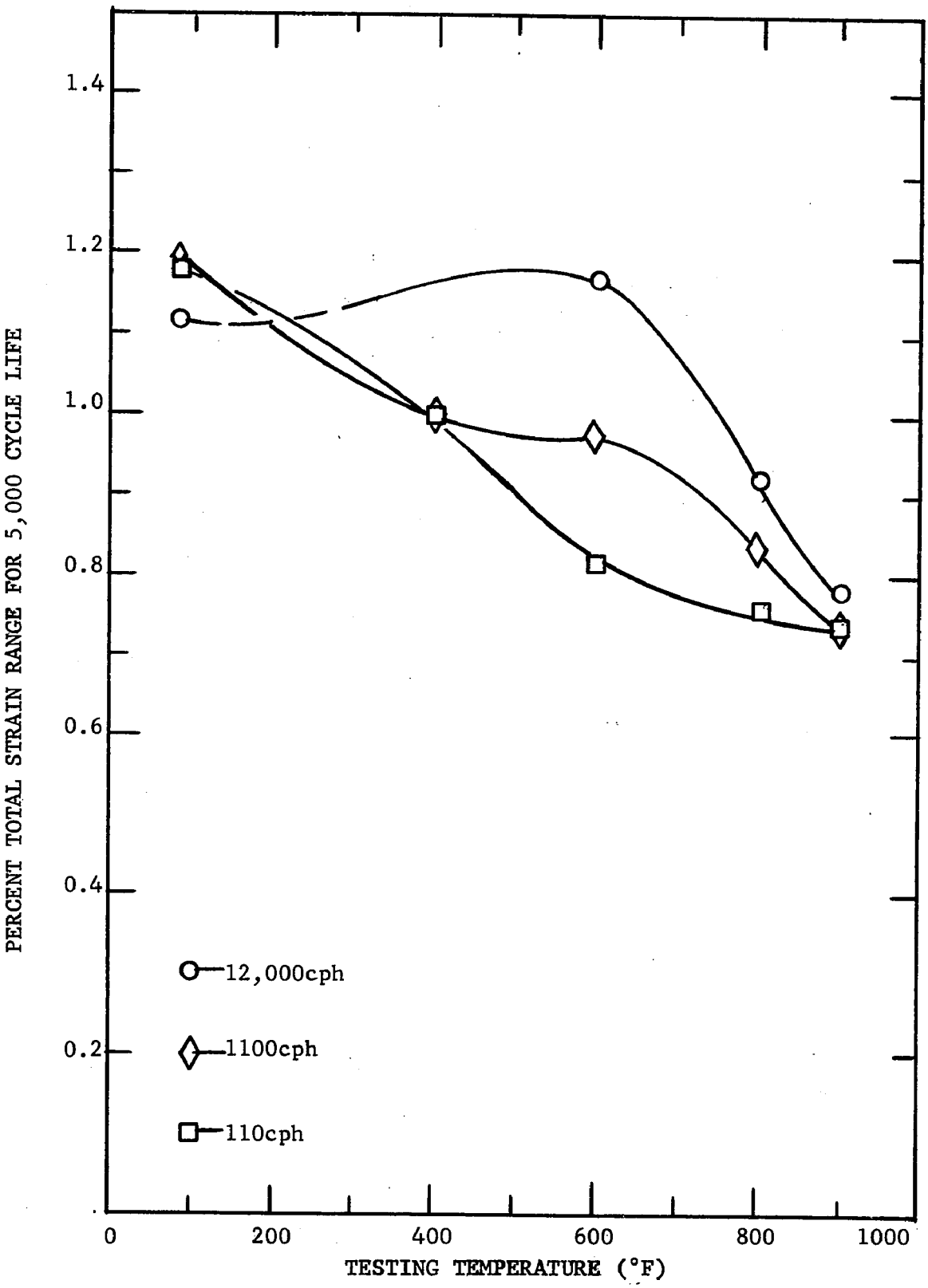

Figure 26 - Influence of Cycle Rate and Temperature Upon The 5,000 Cycle Strain Range - A-212,B Steel, N-SR

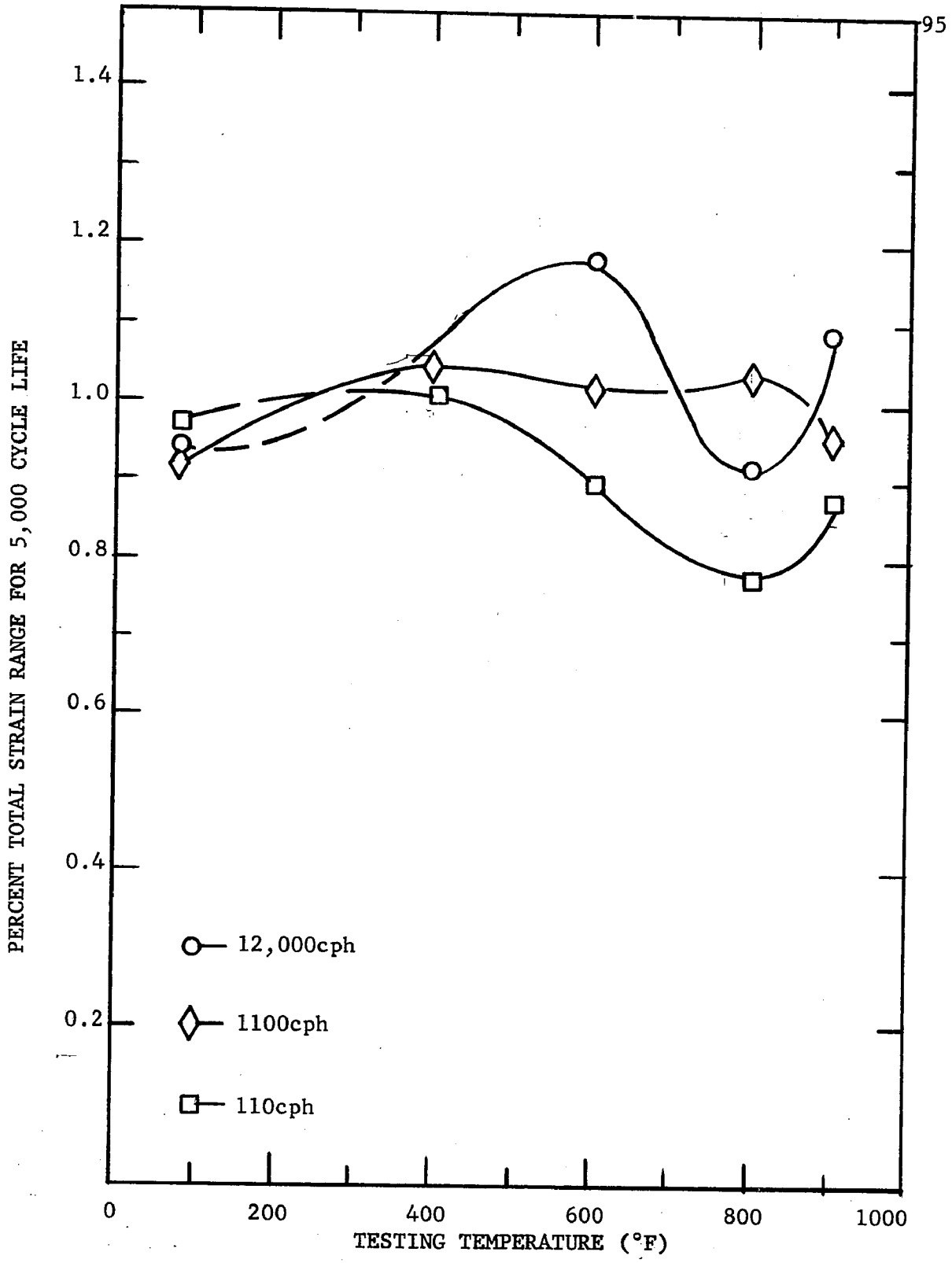

Figure 27 - Influence of Cycle Rate and Temperature Upon The 5,000 Cycle Strain Range - A-387,B Steel, Q-T

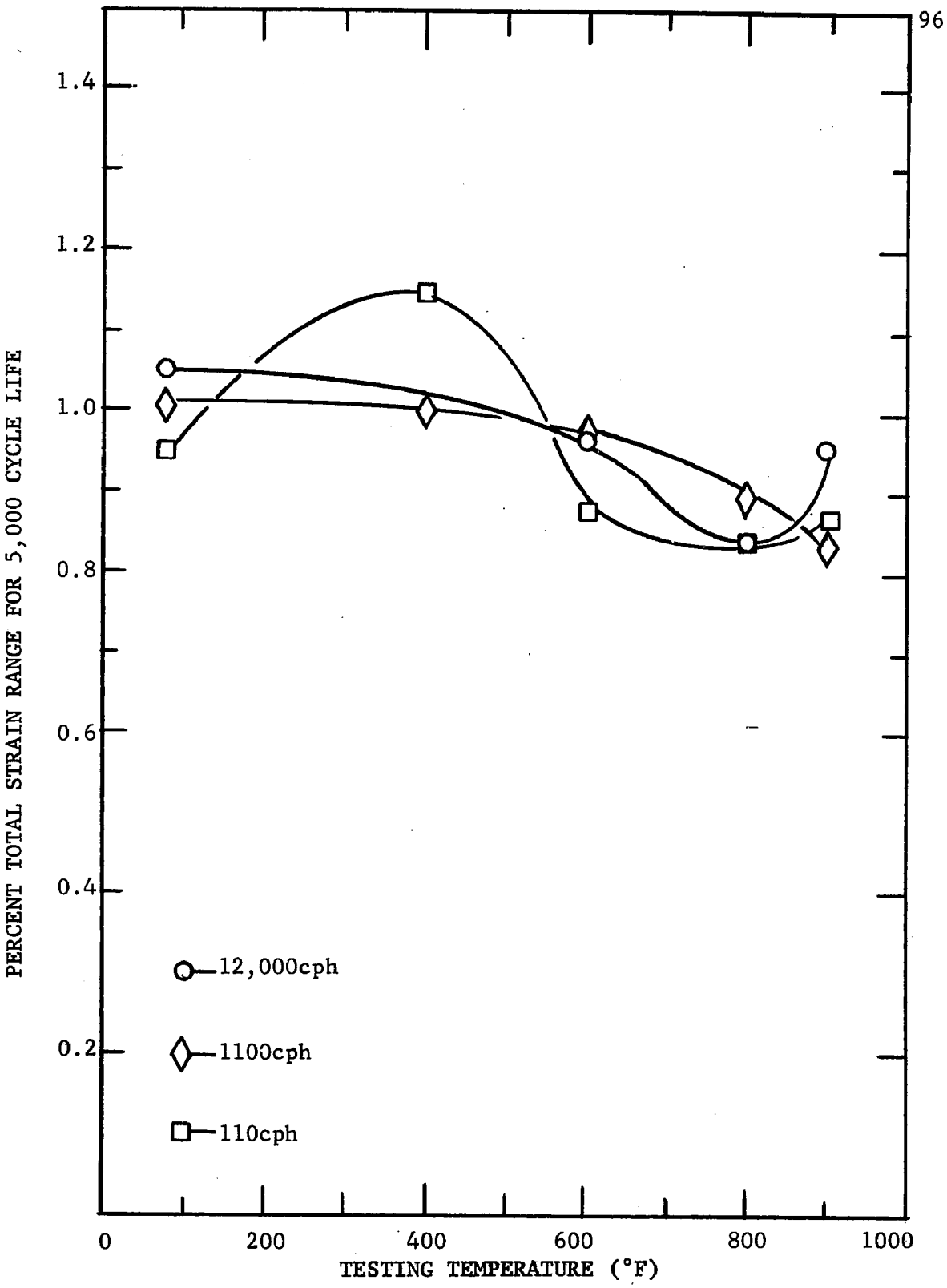

Figure 28 - Influence of Cycle Rate and Temperature Upon The 5,000 Cycle Strain Range - "T-1" Steel, Mill Q-T

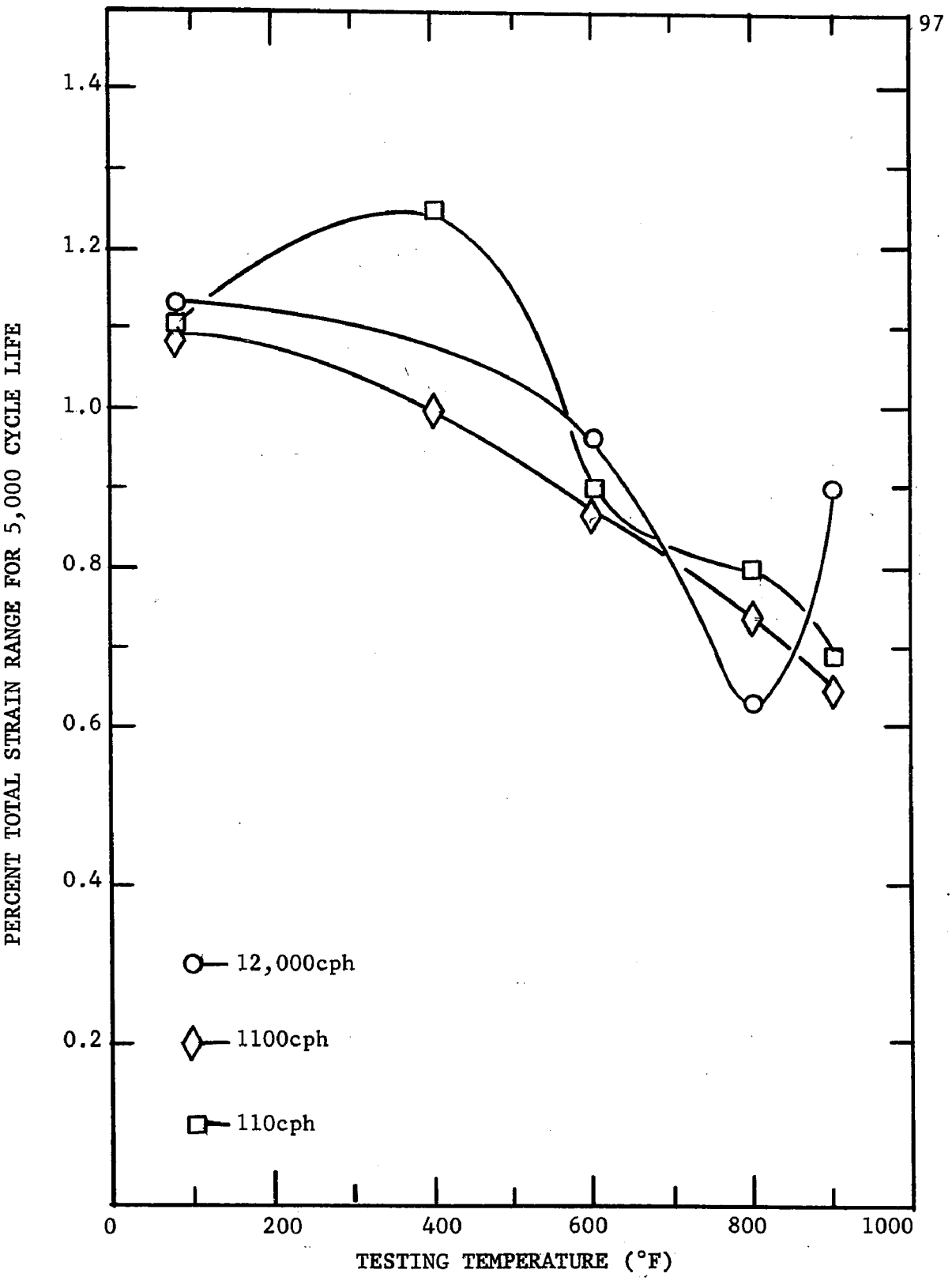

Figure 29 - Influence of Cycle Rate and Temperature Upon The 5,000 Cycle Strain Range - A-212,B Steel, Q-T

Figure 30 - Combined Room Temperature Fatigue Curve of "T-1" Steel, Mill Q-T, 12,000cph

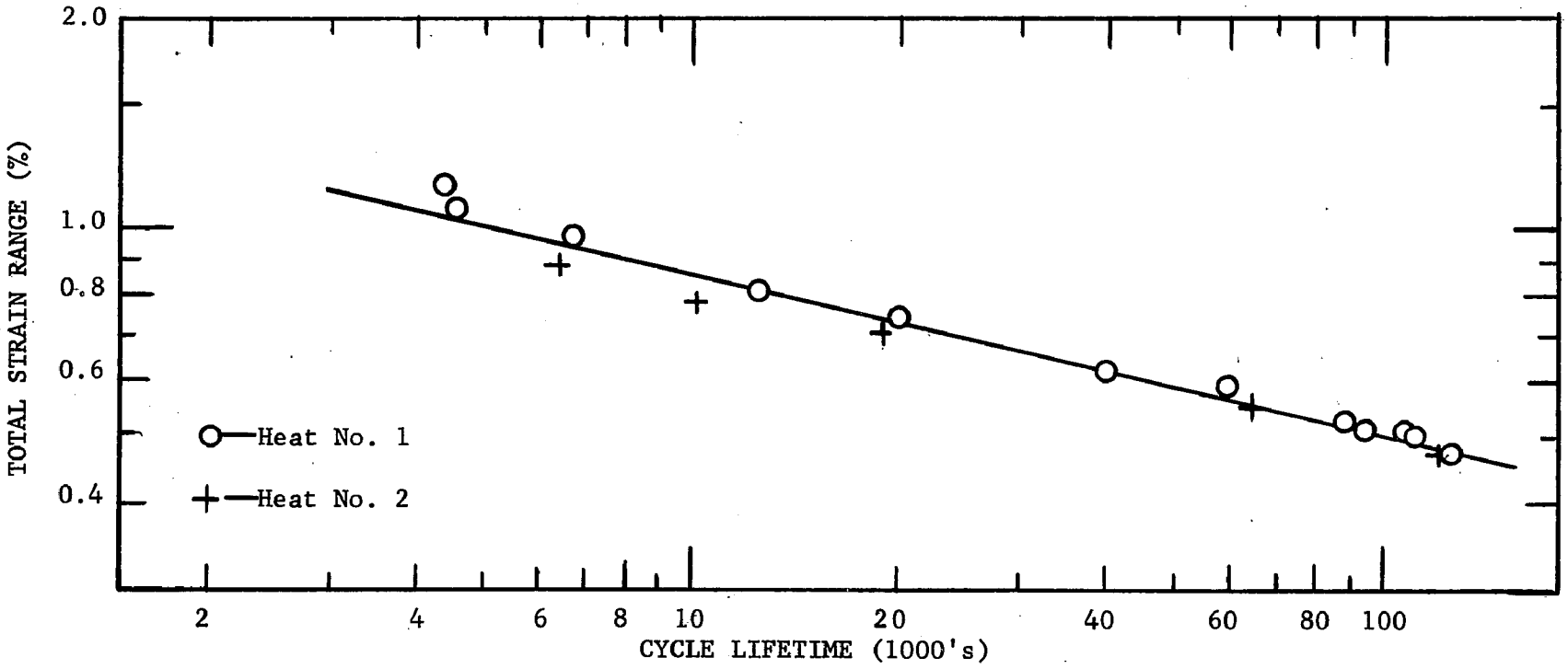

Figure 31 - 800°F Fatigue Curves of Old and New Heats of "T-1" Steel, 12,000cph

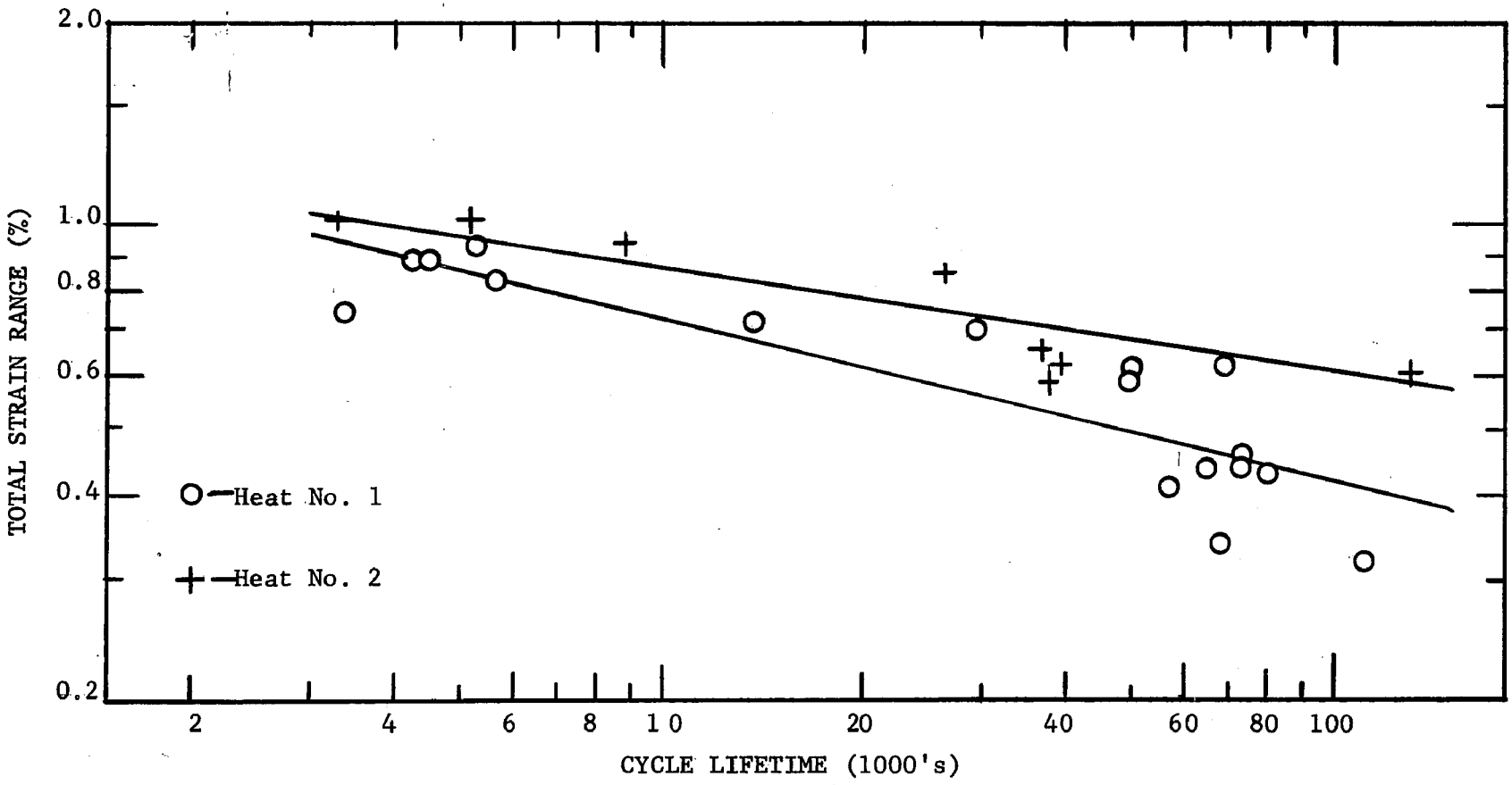

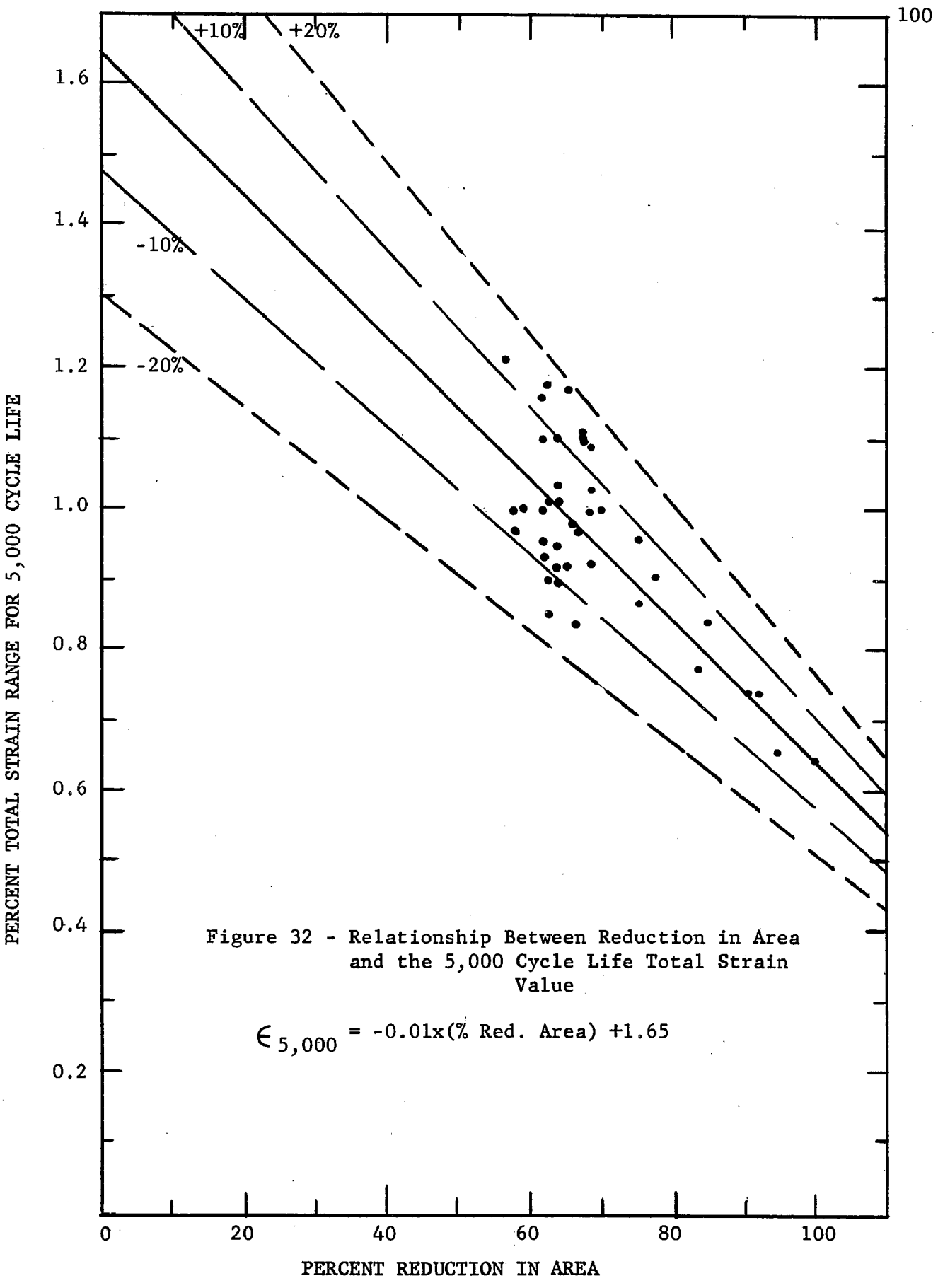

Figure 32 - Relationship Between Reduction in Area and the 5,000 Cycle Life Total Strain Value

$\epsilon_{5,000} = -0.01x(\%\ \text{Red. Area}) + 1.65$

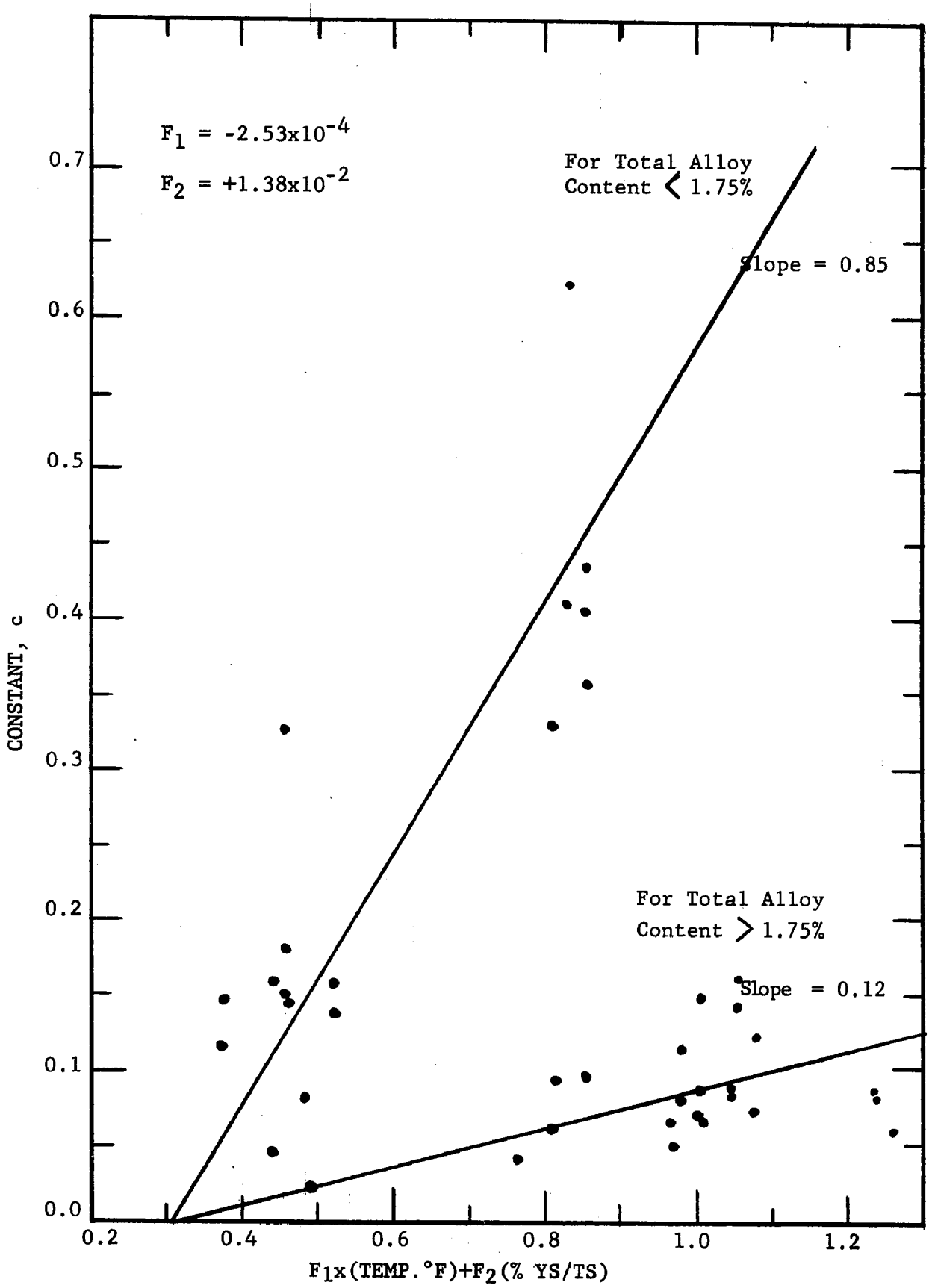

Figure 33 - Plot for Estimating the Material Parameter, c, in the Generalized Fatigue Equation

Figure 34
A-212,B Steel, N-SR

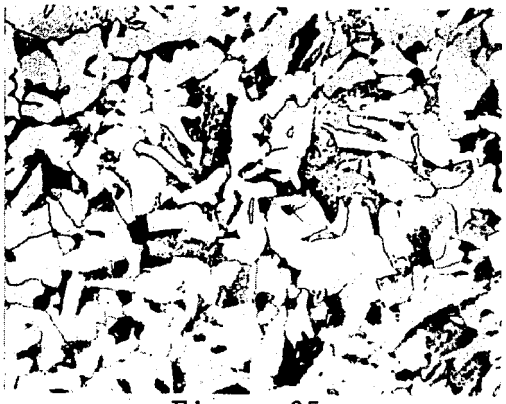

Figure 35
A-212,B Steel, Q-T

Figure 36
A-387,B Steel, N-SR

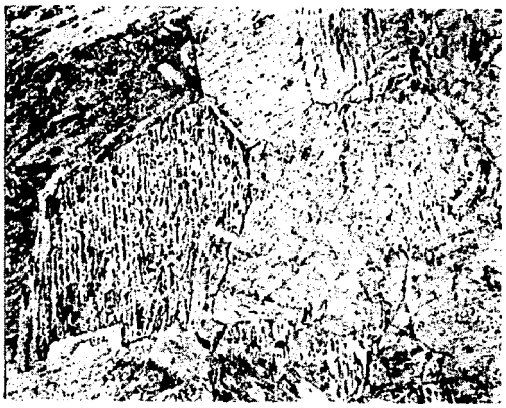

Figure 37
A-387,B Steel, Q-T

Nital Etch 500X

Figure 38
"T-1" Steel, Mill Q-T

Base Microstructures of Materials Used in Study

Figure 39
Fatigue Tested at 800°F

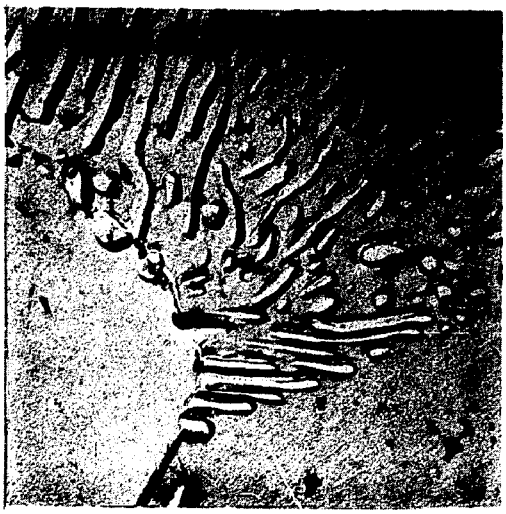

Figure 40
Fatigue Tested at 900°F

Electron Photomicrographs of A-212,B, N-SR Steel
Showing Adjacent Ferrite and Pearlite Areas

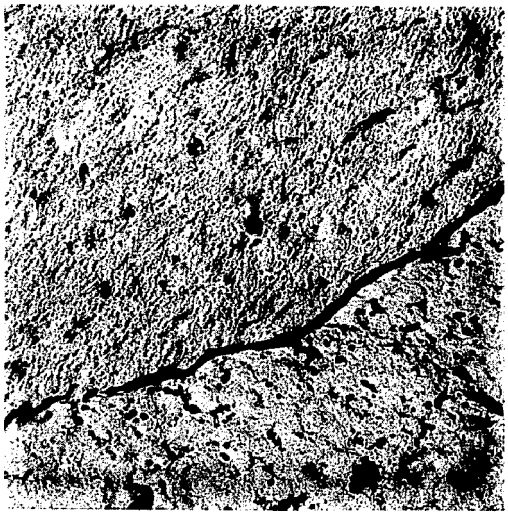

Figure 41
Fatigue Tested at 800°F

Figure 42
Fatigue Tested at 900°F

Electron Photomicrographs of A-387,B, N-SR Steel
Showing Typical Grain Boundary Areas

Plastic Replicas 10,000X As Shown

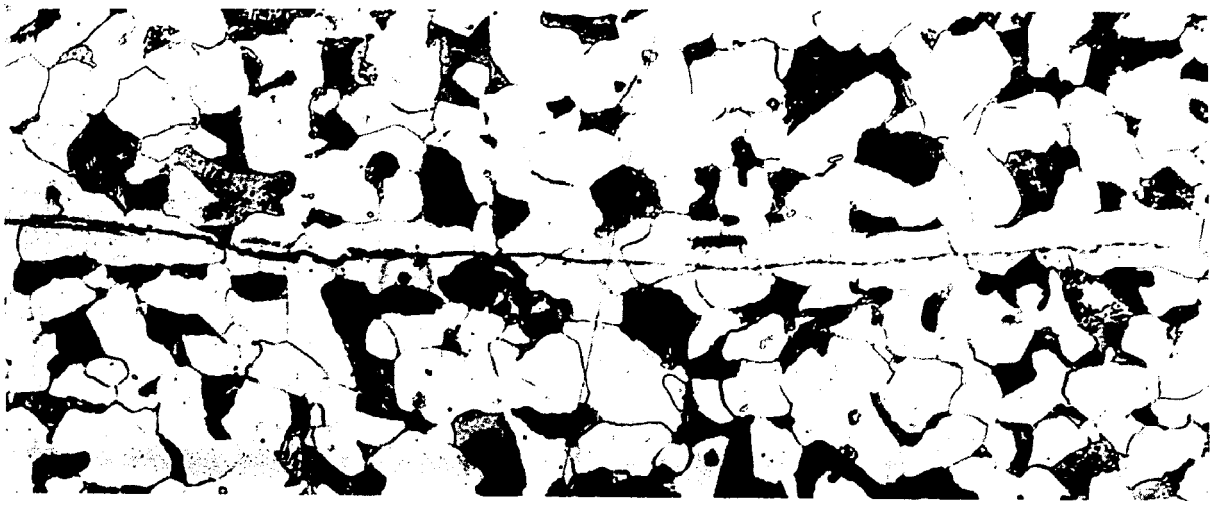

Figure 43

Crack Found in A-212,B, N-SR Steel, Tested at 80°F. Crack is Growing in from Fracture Surface in a Plane Parallel to the Rolling Plane and Loading Direction.

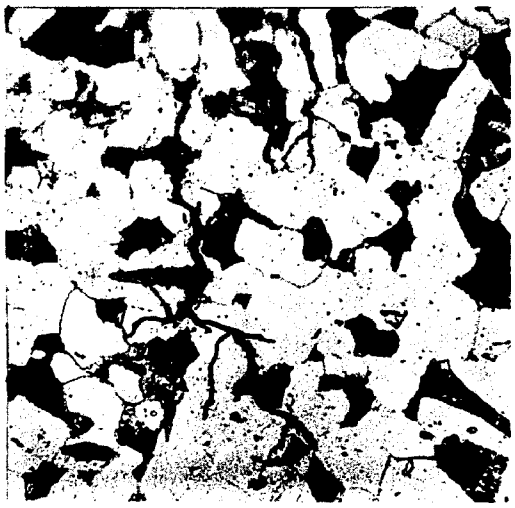

Figure 44
Crack in A-212, N-SR, Tested at 600°F; Growing Down from Surface, Perpendicular to Direction of Loading.

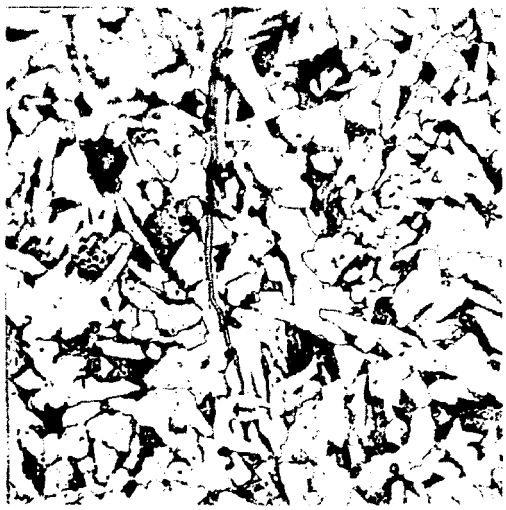

Figure 45
Crack in A-212, Q-T, Tested at 800°F; Growing Down from Surface, Perpendicular to Direction of Loading.

Nital Etch Secondary Cracks 500X

Figure 46
Tested at 80°F,
12,000 cph

Figure 47
Tested at 80°F,
110 cph

Figure 48
Tested at 600°F,
1100 cph

Figure 49
Tested at 800°F,
12,000 cph

Figure 50
Tested at 900°F
1100 cph

Figure 51
Tested at 900°F
1100 cph

Secondary Cracks in A-387,B Steel, N-SR

Nital Etch 500X

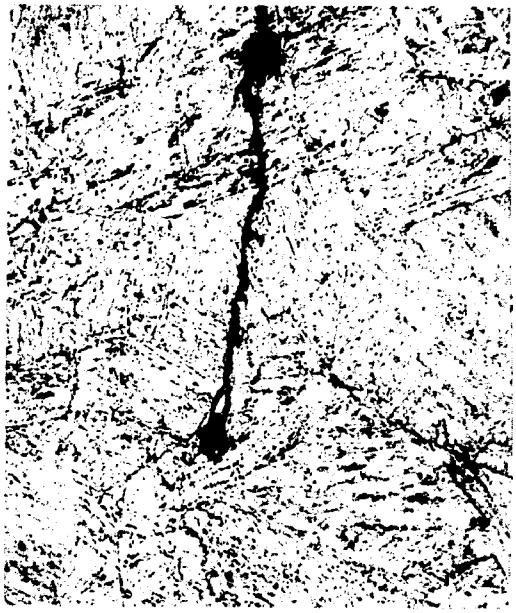

Figure 52
Tested at 600°F, 1100 cph

Figure 53
Tested at 800°F, 12,000 cph

Secondary Cracks in A-387,B Steel, Q-T

Figure 54

Secondary Crack in "T-1", Mill Q-T
Tested at 800°F, 110 cph

Nital Etch

500X

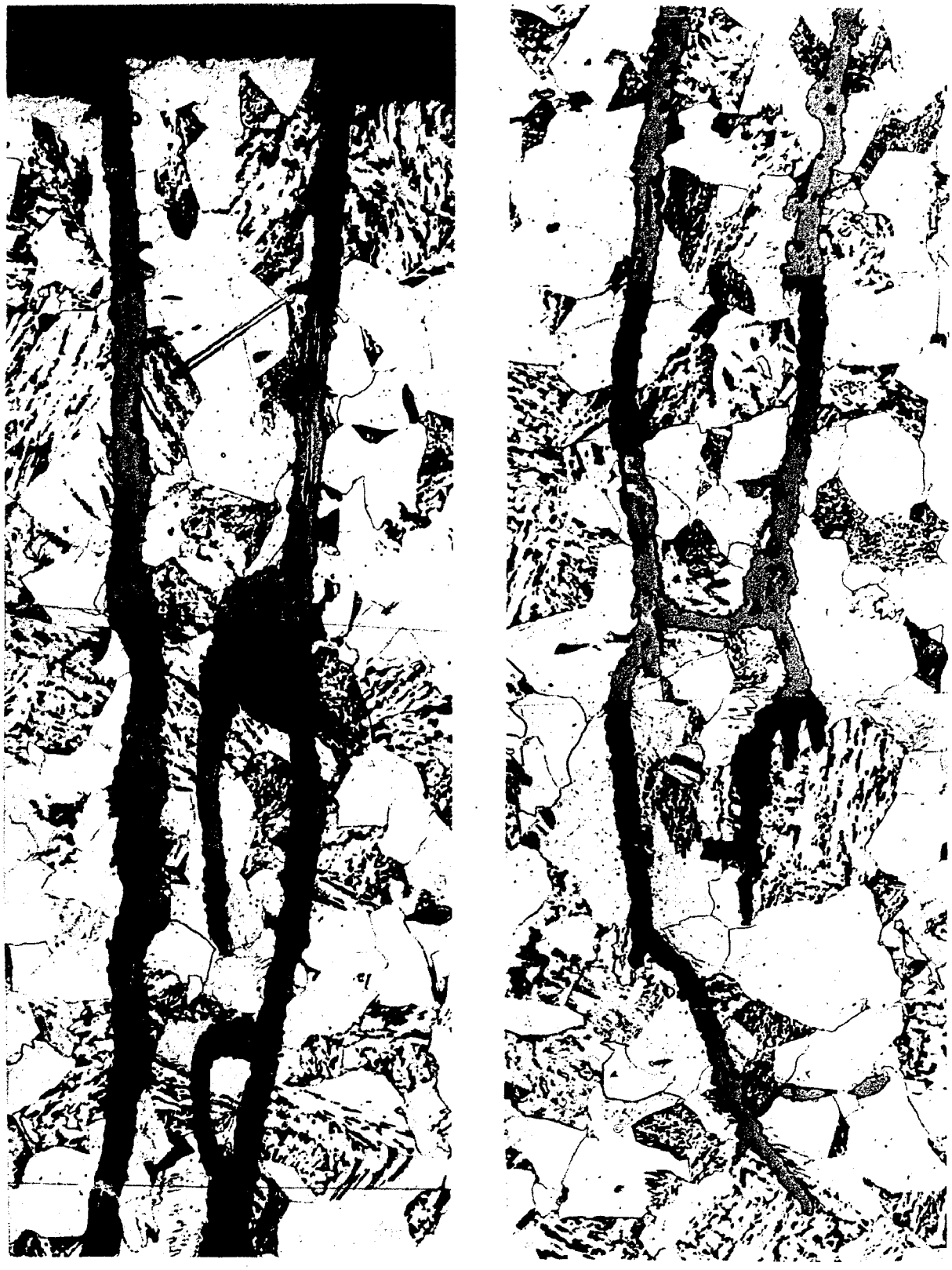

(a) (b)

Figure 55
Lengthy Cracks in A-387,B Steel, N-SR
Tested at 800°F, 110 cph

Nital Etch 500X

Figure 56
Low Magnification Picture
of Secondary Crack in
A-387,B Steel, N-SR
Tested at 900°F, 1100 cph
150X

Figure 57
Enlarged View of
Crack Shown in Fig.56
Showing Crack Morphology
and Deformation Bands.
500X

Nital Etch

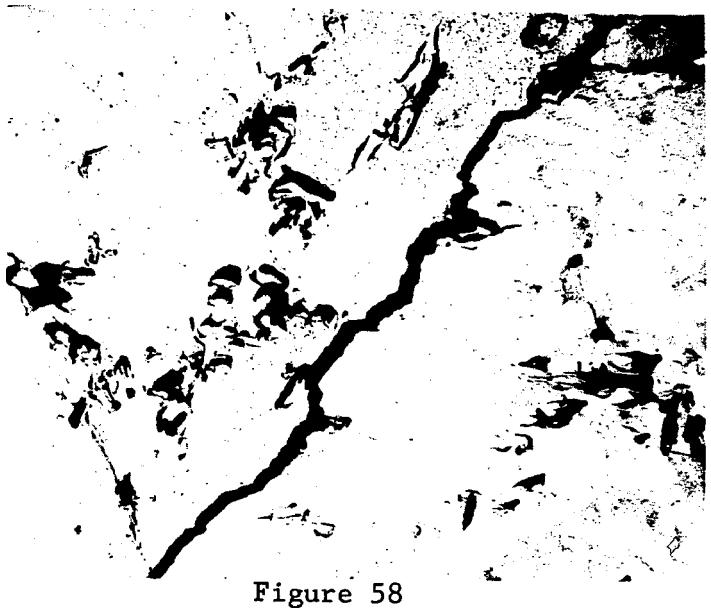

Figure 58
Tested at 800°F, 1100 cph

Figure 59
Tested at 800°F, 1100 cph

Figure 60
Tested at 900°F, 1100 cph

Electron Photomicrographs of Cracks in A-387,B, N-SR Steel

Plastic Replicas

5,000X

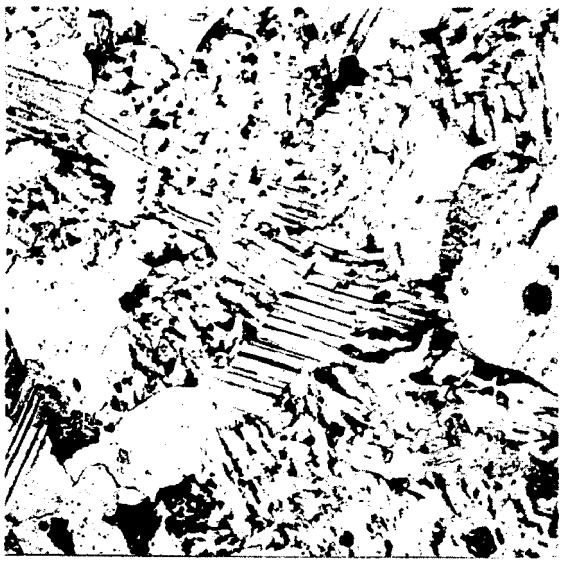

Figure 61
Tested at 800°F, 1100 cph
500X

Figure 62
Tested at 800°F, 1100 cph
1000X

Deformation Bands in A-387,B Steel
Nital Etch N-SR

Figure 63
Tested at 800°F, 1100 cph

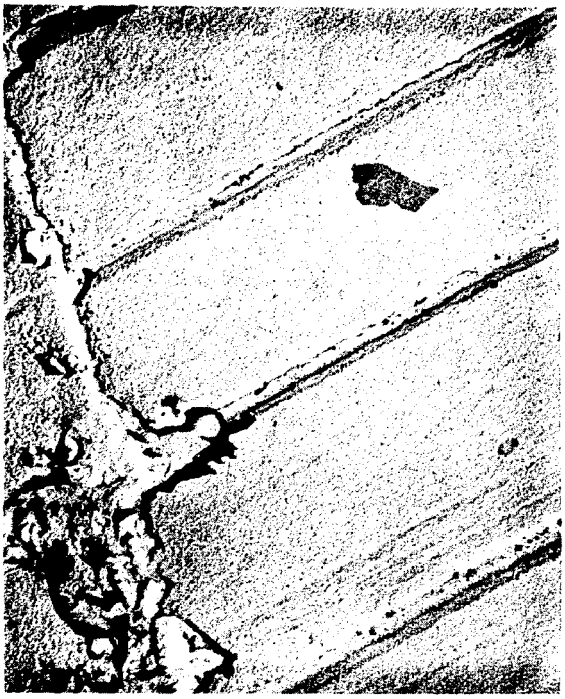

Figure 64
Tested at 800°F, 1100 cph

Figure 65
Tested at 800°F, 1100 cph

Figure 66
Tested at 800°F, 1100 cph

Electron Photomicrographs of Deformation Bands in A-387,B
Plastic Replicas N-SR Steel 5,000X

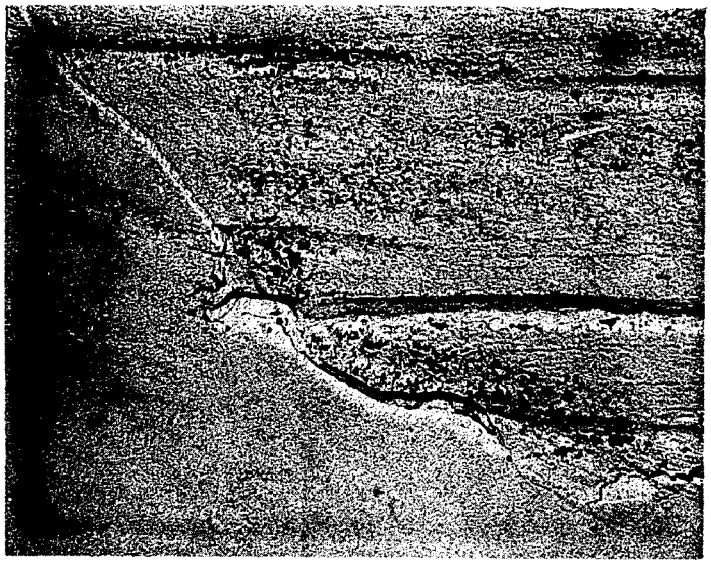

Figure 67
Tested at 900°F, 1100 cph

Figure 68
Tested at 900°F, 1100 cph

Electron Photomicrographs of Deformation Bands
in A-387,B Steel, N-SR

Plastic Replicas 5,000X

APPENDIX

Full-Scale Fatigue Tests

The prototype or full-scale approach to fatigue testing, alluded to in the Introduction, has been attempted in an effort to determine the reliability of the laboratory scale tests. Such a full-scale study was performed on pressure-vessels at the Southwest Research Institute. Since the fabrication of a pressure-vessel involves considerable forming and welding, it would be of interest to determine the general stress raising effects of such welding techniques, as well as those introduced by attaching the various nozzles and fittings normally applied to such vessels in practice. The results of such a study (19) are shown graphically in Figure A-1. Plotted here is the ratio of strain range for fatigue failure in laboratory cantilever beam specimens to membrane strain producing comparable lifetime fatigue failure in full size pressure-vessels. The plot indicates that the ratio, defined as the fatigue strength reduction factor, is sensitive to the cyclic lifetime but not to the composition of the steel. The A-201 steel is a plain carbon material of nominally 0.15%C; the A-302 steel is a 1.5% Mn-0.4% Mo steel; and the "T-1" steel is comparable to that used in the present study.

If one considers the 100,000 cycle life as satisfactory for a pressure-vessel, then a realistic fatigue strength reduction factor equal to about 4 can be obtained from the plot of Figure A-1. Thus, one could take laboratory data, alter it by a factor of four, and have a reasonable approximation of the effective fatigue strength of a full-

size pressure-vessel. However, the point must be made that Figure A-1 is based upon a very limited number of full-size fatigue tests, six to be exact, and care must be exercised in extending such a generalized statement.

Design Criteria

The results of combining the fatigue study data and those of the creep rupture study are presented in Figures A-2, A-3, and A-4 (47). As mentioned previously, the common design criterion for pressure-vessel construction today is the one-quarter tensile strength value at the temperature of service. There are two other possibilities which must be considered, that of the stress for rupture in 100,000 hours based upon creep rupture studies, and secondly, the stress for 100,000 cycle fatigue life divided by four. The factor four is obtained from the full-scale vessel tests just discussed. (It must be assumed that this factor is not sensitive to temperature changes since the data generating it are room temperature values.)

Figure A-2 reveals that the stress necessary for 100,000 cycle fatigue failure at 1100 cph or 12,000 cph is not critical in designing a pressure-vessel of A-212 steel. Over the room temperature to 850°F range, the one-quarter tensile strength factor is controlling, while above 850°F, the stress for rupture in 100,000 hours must be considered dominant. This is true for both heat treated conditions of A-212. Similar plots for the A-387,B and "T-1" steels, shown in Figures A-3 and A-4, indicate that the one-quarter tensile strength factor is critical up to about 700°F, at which point the 12,000 cph fatigue data show a dip below the tensile curve. This critical area

for the fatigue strength ranges from 700°F to about 900°F, where the 1100 cph values dip down at about the same point at which the 12,000 cph data show a recovery. This recovery is proposed to be the combined effect of fatigue and creep as opposed to the results of simple fatigue testing. At about 950°F the stress for rupture in 100,000 hours again becomes dominant. In all three plots of Figures A-3 and A-4, the fatigue data from the 1100 cph tests show superior fatigue strength up to about 900°F. Since the 110 cph tests were not extended to 100,000 cycle lifetimes, it is not possible to say what effect the slower rates will have on these plots.

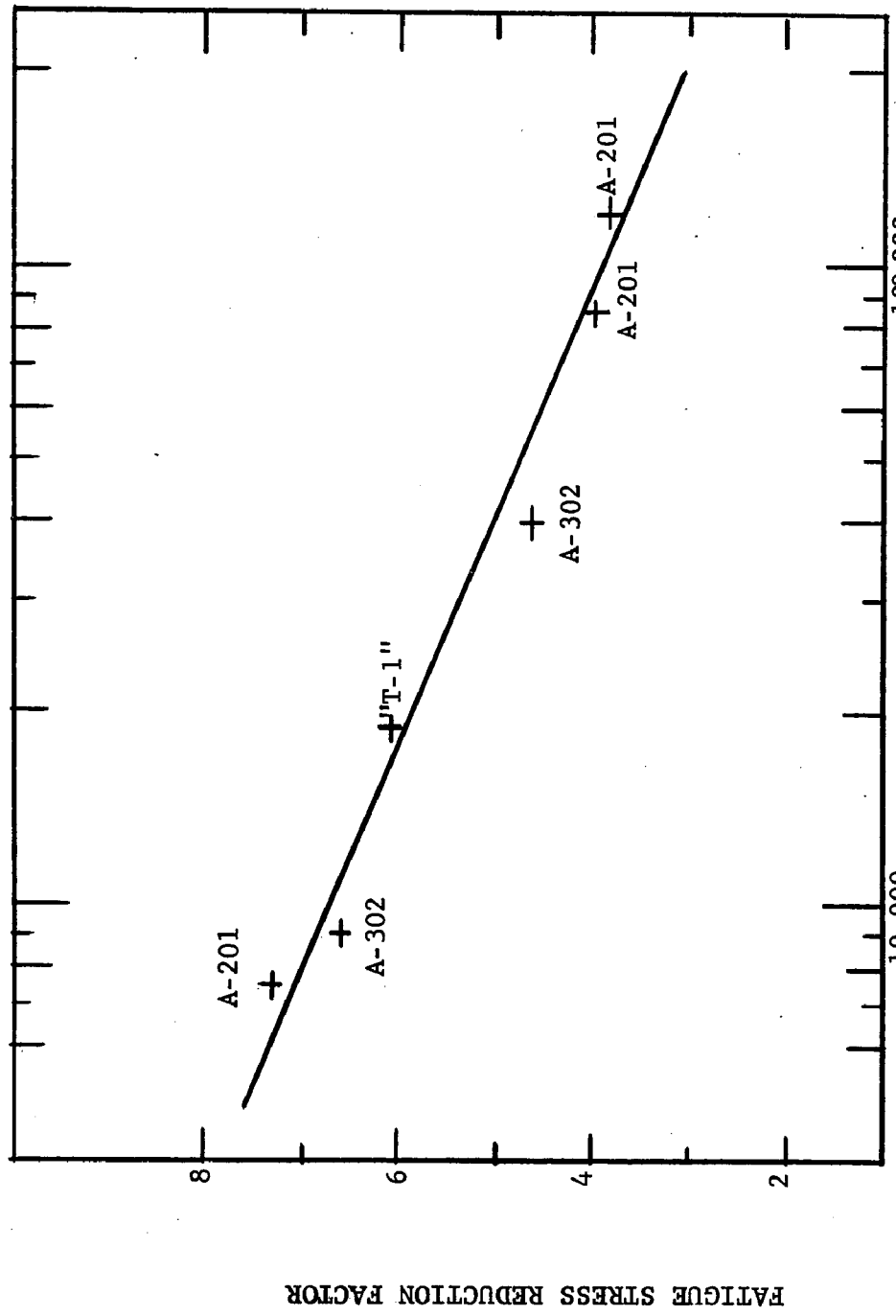

Figure A-1 - Relationship Between Full-Size and Laboratory-Scale Tests

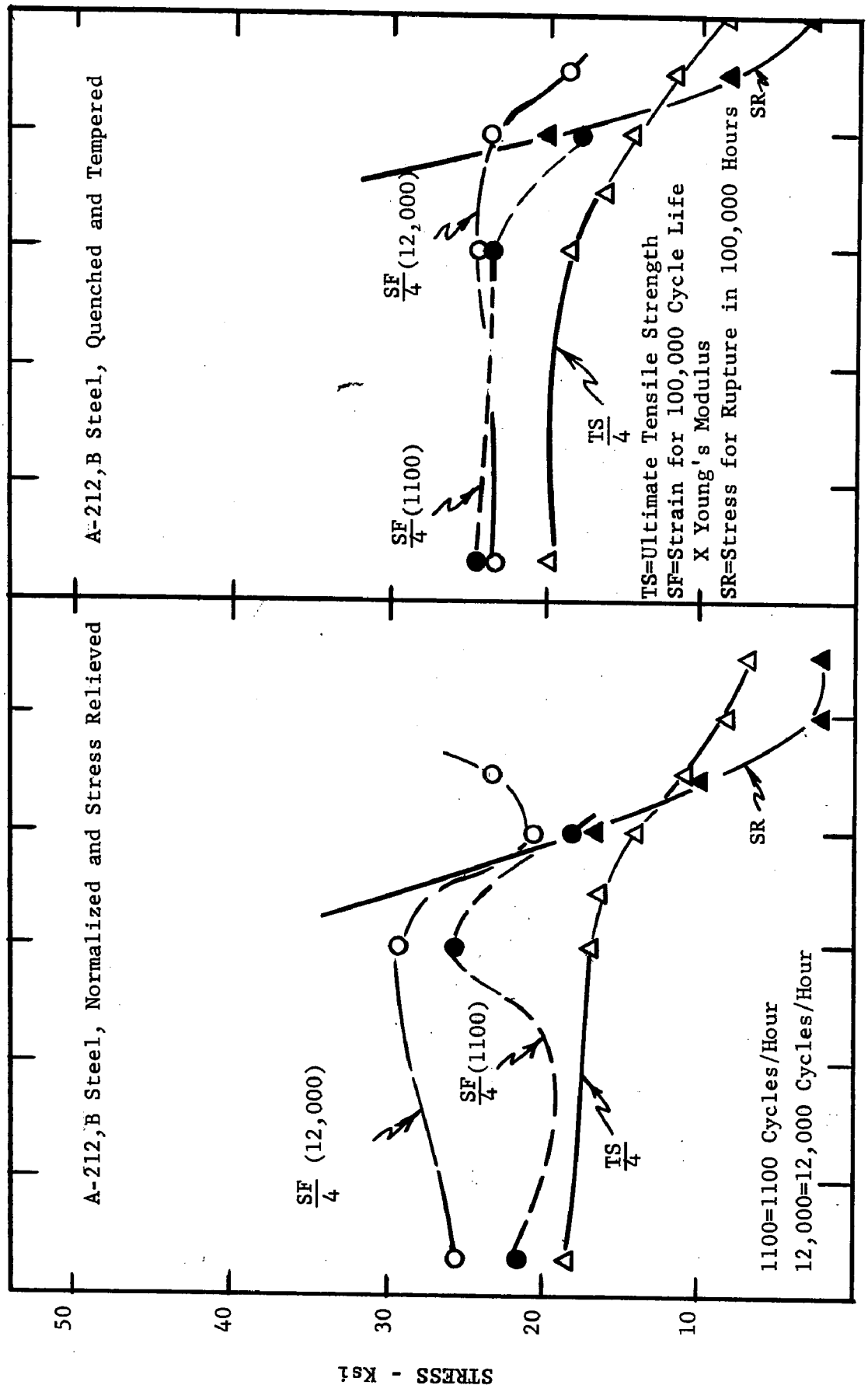

Figure A-2 - Relationship Between Various Design Criteria for A-212,B Steel

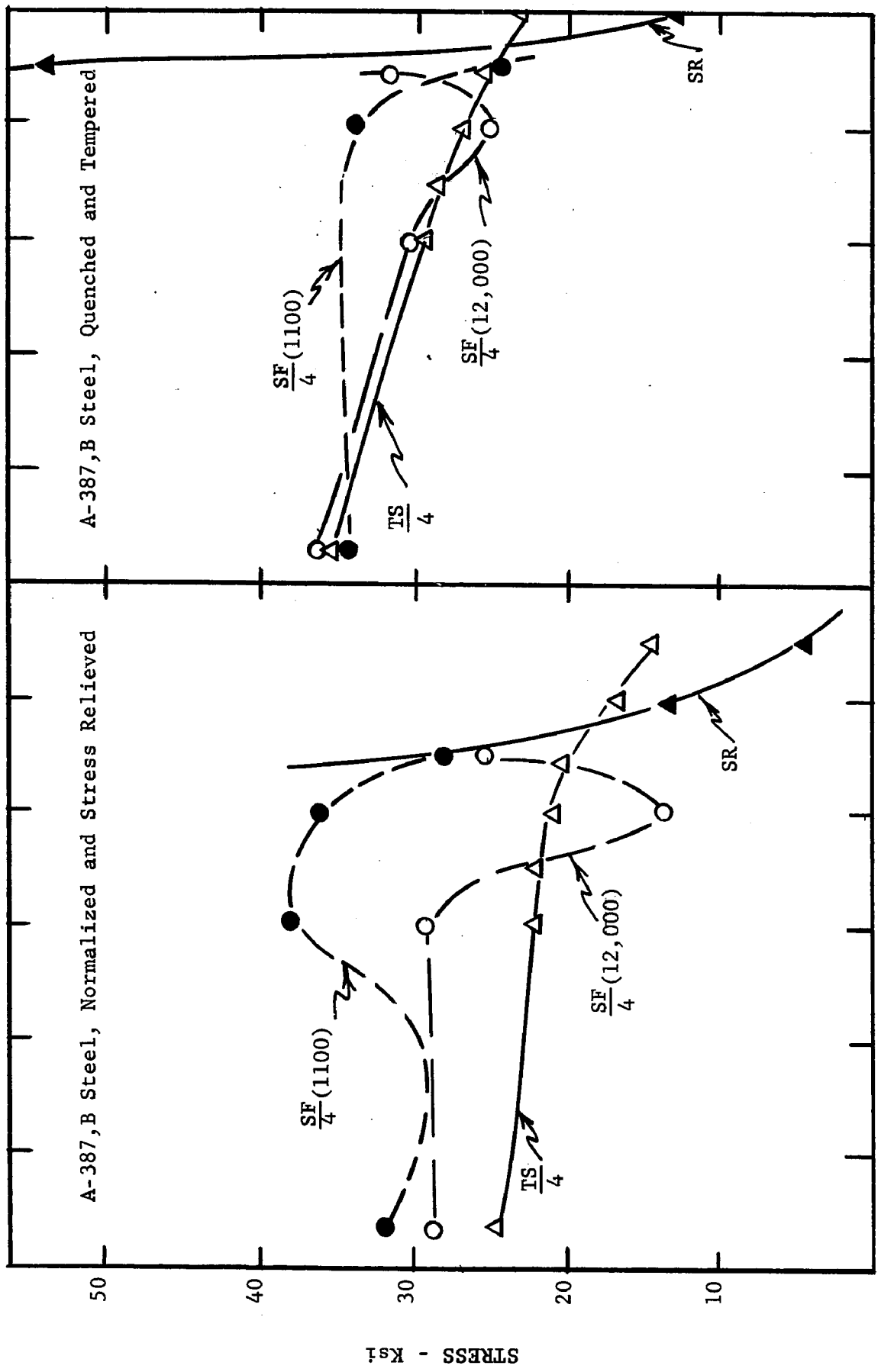

Figure A-3 - Relationship Between Various Design Criteria for A-387,B Steel

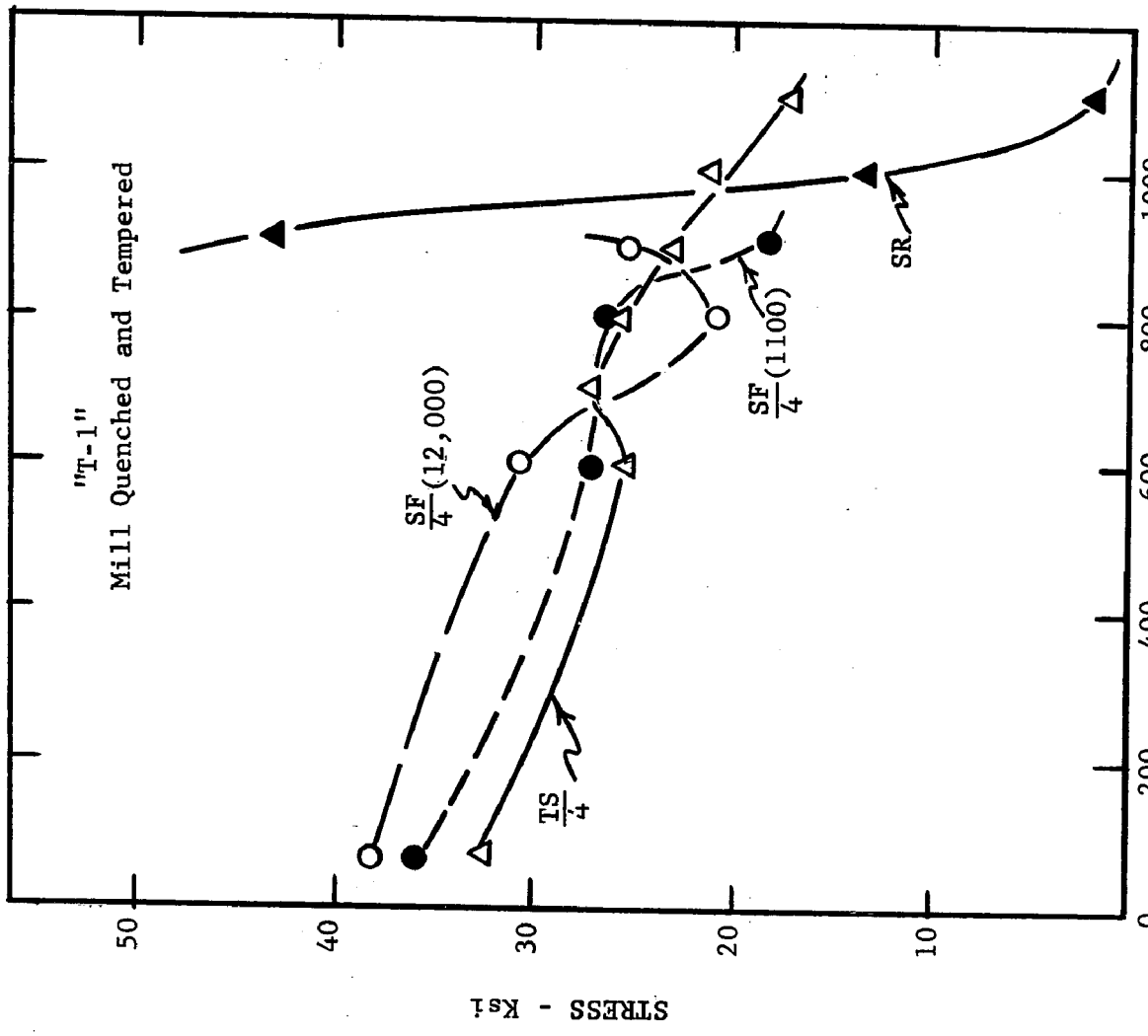

Figure A-4 - Relationship Between Various Design Criteria for "T-1" Steel

Table A-I

12,000 cph Fatigue Data

Steel, Condition and Testing Temp.	% Total Strain	% Plastic Strain	Cycles to Failure	Brinell Hardness No.
1-A-387,B; Q-T 80°F	.90	0.05	5,860	-
	.80	0.02	10,400	-
	.75	0.0	15,300	-
	.63	0.0	21,000	-
	.56	0.0	43,000	-
	.56	0.0	71,000	-
	.51	0.0	94,000	-
	.48	0.0	95,000	-
	.46	0.0	100,000	269
	.44	0.0	163,000	-
1-A-387,B; Q-T 600°F	1.20	-	5,100	-
	1.11	-	6,500	-
	.82	0.20	12,000	262
	.68	0.14	29,800	-
	.76	0.16	30,000	-
	.54	0.06	65,000	-
	.45	0.0	130,000	-
1-A-387,B; Q-T 800°F	1.02	-	1,860	-
	1.23	-	3,800	257
	.81	0.23	4,500	-
	.82	0.25	9,000	-
	.86	-	10,600	-
	.84	-	15,300	-
	.68	0.27	25,000	-
	.45	0.06	36,000	-
	.45	0.04	37,000	-
	.68	0.24	51,500	-
	.42	0.0	57,000	-
	.55	-	59,500	-
	.57	-	74,500	-
	.36	0.0	75,000	-
	.46	0.10	85,000	-
	.39	0.0	98,000	-

Table A-1 (cont'd)
12,000 cph Fatigue Data

Steel, Condition and Testing Temp.	% Total Strain	% Plastic Strain	Cycles to Failure	Brinell Hardness No.
1-A-387,B; Q-T 900°F	1.10	0.08	4,200	-
	1.34	0.135	4,600	-
	.88	0.065	11,600	-
	.87	0.05	12,500	-
	.65	0.0	29,500	-
	.69	0.0	33,400	-
	.66	0.0	50,000	-
	.54	0.0	56,000	-
	.66	0.0	83,000	229
	.62	0.0	206,000	-
	.43	0.0	260,000	-
1-A-387,B; N-SR 80°F	1.12	0.21	3,300	-
	.92	0.19	4,100	-
	.92	0.14	6,400	-
	.84	0.10	7,850	-
	.62	0.03	23,000	-
	.59	0.03	24,800	-
	.635	0.02	25,000	197
	.60	0.03	26,350	-
	.56	0.025	33,000	-
	.53	0.015	42,000	-
	.47	0.01	52,000	-
	.475	0.01	70,000	-
	.40	0.0	205,000	-
1-A-387,B; N-SR 600°F	1.72	0.0	3,600	-
	1.62	0.0	4,500	-
	1.17	-	6,775	-
	1.23	0.0	9,400	193
	1.07	-	11,100	-
	.94	0.0	11,500	-
	.84	-	18,000	-
	.66	0.0	40,000	-
	.53	0.0	61,000	-
	.63	-	67,000	-
	.40	0.0	145,000	-

Table A-1 (cont'd)
12,000 cph Fatigue Data

Steel, Condition and Testing Temp.	% Total Strain	% Plastic Strain	Cycles to Failure	Brinell Hardness No.
1-A-387,B; N-SR 800°F	1.31	-	1,980	-
	.725	0.085	2,850	-
	.685	0.085	4,000	-
	.92	-	7,000	-
	.54	0.0	12,500	-
	.415	0.0	19,700	-
	.425	-	23,800	-
	.40	0.0	28,000	-
	.37	0.0	31,000	-
	.22	0.0	70,000	207
	.24	0.0	72,000	-
	.235	0.0	125,000	-
	.22	-	204,000	-
1-A-387,B; N-SR 900°F	1.25	0.035	4,000	-
	1.04	0.0	4,800	-
	.81	0.0	8,200	-
	.93	0.0	12,600	-
	.64	0.0	19,000	152
	.62	0.0	20,500	-
	.49	0.0	30,600	-
	.51	0.0	34,500	-
	.57	0.0	66,900	-
	.60	0.0	84,000	-
	.46	0.0	97,500	-
	.22	0.0	204,000	212
1-"T-1"; Mill Q-T 80°F	1.14	-	4,350	235
	1.07	-	4,550	241
	.97	-	6,700	235
	.81	-	12,500	235
	.74	-	20,000	235
	.62	-	40,000	241
	.59	-	59,000	235
	.53	-	88,000	241
	.51	-	93,000	235
	.51	-	107,000	235
	.50	-	111,000	235
	.47	-	124,000	235
2-"T-1"; Mill Q-T 80°F	.88	0.04	6,400	248
	.775	0.02	10,100	244
	.705	0.0	18,900	244
	.55	0.0	64,500	252
	.47	0.0	119,500	245

Table A-1 (cont'd)
12,000 cph Fatigue Data

Steel, Condition and Testing Temp.	% Total Strain	% Plastic Strain	Cycles to Failure	Brinell Hardness No.
1-"T-1"; Mill Q-T 600°F	1.05	-	4,200	-
	.84	-	7,500	-
	.92	-	7,700	235
	.73	-	14,000	235
	.63	-	31,000	-
	.52	-	47,500	-
	.55	-	51,000	-
	.58	-	68,000	-
1-"T-1"; Mill Q-T 800°F	.75	-	3,400	-
	.88	-	4,300	248
	.88	-	4,500	248
	.93	-	5,280	255
	.83	-	5,640	248
	.72	0.06	13,800	248
	.70	0.05	29,500	255
	.59	0.05	49,500	241
	.62	0.05	50,000	241
	.41	0.05	57,000	235
	.34	0.05	66,700	-
	.46	0.05	72,600	248
	.44	0.05	73,000	-
	.43	-	80,000	255
	.32	0.05	110,000	255
2-"T-1"; Mill Q-T 800°F	1.01	0.05	3,300	252
	1.015	0.045	5,200	252
	.94	0.025	8,800	255
	.85	0.035	26,500	252
	.655	0.02	37,000	248
	.59	0.005	37,500	245
	.625	0.03	38,900	248
	.605	0.025	130,000	252
	.585	0.04	250,000	255
1-"T-1"; Mill Q-T 900°F	.92	0.04	4,700	-
	.96	0.0	5,600	-
	.83	0.055	10,200	-
	.72	0.0	15,500	-
	.68	0.0	20,500	-
	.76	0.0	24,000	-
	.71	0.0	45,600	-
	.47	0.0	50,500	-
	.42	0.0	100,300	-
	.45	0.0	156,000	-

Table A-1 (cont'd)
12,000 cph Fatigue Data

Steel, Condition and Testing Temp.	% Total Strain	% Plastic Strain	Cycles to Failure	Brinell Hardness No.
1-A-212,B; Q-T 80°F	1.16	0.41	4,900	-
	1.08	0.40	6,100	-
	.75	0.23	12,100	-
	.60	0.12	21,000	152
	.56	0.11	23,900	-
	.445	0.06	38,000	-
	.38	0.02	48,000	-
	.38	0.03	66,000	-
	.315	0.0	87,000	-
	.325	0.02	105,000	-
	.30	0.0	123,000	-
1-A-212,B; Q-T 600°F	1.075	0.205	4,850	-
	.81	0.20	6,400	-
	.85	0.20	7,100	-
	.71	0.12	16,000	-
	.45	0.0	26,000	-
	.56	0.015	34,000	-
	.545	0.0	36,800	-
	.32	0.0	124,500	-
	.37	0.0	130,000	-
1-A-212,B; Q-T 800°F	.66	0.185	3,860	-
	.64	0.10	6,000	-
	.52	0.075	10,000	-
	.55	0.065	18,500	-
	.51	0.06	25,000	-
	.38	0.0	73,400	-
	.45	0.0	73,600	-
1-A-212,B; Q-T 900°F	.675	0.12	12,600	140
	.515	0.065	24,500	-
	.445	0.075	61,700	140
	.24	0.0	285,000	137
1-A-212,B; N-SR 80°F	1.24	0.42	4,700	-
	1.19	0.39	4,900	-
	1.02	0.33	7,000	-
	.90	0.27	9,800	-
	.72	0.19	12,000	130
	.71	0.18	14,900	-
	.59	0.11	18,900	-
	.48	0.08	34,500	-
	.44	0.05	45,000	-
	.34	0.02	71,500	-
	.37	0.03	80,000	-
	.27	0.0	196,000	-

Table A-1 (cont'd)
12,000 cph Fatigue Data

Steel, Condition, and Testing Temp.	% Total Strain	% Plastic Strain	Cycles to Failure	Brinell Hardness No.
1-A-212,B; N-SR 600°F	1.44	0.38	2,750	-
	.99	0.189	6,500	128
	1.07	0.085	13,200	-
	.67	0.11	18,300	-
	.54	0.075	38,000	-
	.53	0.0	75,000	-
1-A-212,B; N-SR 800°F	1.02	0.195	3,800	-
	.81	0.32	5,900	-
	.86	0.20	6,500	-
	.89	0.055	6,800	-
	.64	0.10	11,400	-
	.55	0.075	25,000	128
	.53	0.055	50,000	-
	.35	0.0	51,500	-
	.42	0.0	96,900	-
	.26	0.0	165,000	-
1-A-212,B; N-SR 900°F	.865	0.205	4,950	127
	.615	0.115	8,000	131
	.54	0.01	31,000	131
	.43	0.03	95,000	127
	.18	0.0	140,000	128

Table A-II

1100 cph Fatigue Data

Steel, Condition and Testing Temp.	% Total Strain	% Plastic Strain	Cycles to Failure	Brinell Hardness No.
1-A-387,B; Q-T 80°F	1.085	0.09	2,870	241
	.98	0.065	4,100	255
	.80	0.02	9,550	241
	.57	0.01	22,000	262
	.61	0.01	35,200	235
	.53	0.01	47,000	250
	.56	0.01	50,000	242
	.46	0.0	151,000	244
2-A-387,B; Q-T 400°F	.90	0.08	8,500	-
	1.11	0.13	3,700	217
	.50	0.01	81,000	248
1-A-387,B; Q-T 600°F	1.33	0.145	2,250	255
	1.155	0.145	4,750	241
	.705	0.105	7,960	250
	.805	0.08	18,275	244
	.55	0.045	28,500	255
	.345	0.03	61,000	255
	.48	0.04	63,000	246
	.48	0.05	84,000	255
1-A-387,B; Q-T 800°F	1.125	0.07	2,500	-
	1.09	0.22	4,600	-
	.90	0.23	7,000	-
	.895	0.075	12,600	-
	.795	0.06	19,000	-
	.735	0.04	27,300	-
	.41	0.09	151,000	-
1-A-387,B; Q-T 900°F	.965	0.07	4,510	-
	.83	0.08	7,500	-
	.84	0.08	13,000	-
	.70	0.025	17,500	-
	.63	0.025	25,000	-
	.46	0.01	46,000	-
	.445	0.01	127,000	-

Table A-II (cont'd)
1100 cph Fatigue Data

Steel, Condition and Testing Temp.	% Total Strain	% Plastic Strain	Cycles to Failure	Brinell Hardness No.
1-A-387,B; N-SR 80°F	1.20	0.215	2,800	192
	1.00	0.14	4,550	183
	.80	0.09	9,200	187
	.65	0.055	14,300	170
	.56	0.03	31,100	179
	.47	0.0	48,950	179
	.445	0.0	53,600	187
	.41	0.0	131,000	197
2-A-387,B; N-SR 80°F	1.39	0.365	2,200	-
	.975	0.19	6,100	164
	.65	0.11	17,900	174
	.50	0.04	36,000	156
	.415	0.005	68,300	-
	.405	0.005	70,000	-
	.365	0.0	125,000	-
2-A-387,B; N-SR 400°F	.83	0.095	6,056	167
	.73	0.09	10,500	172
	.45	0.015	50,000	156
	.445	0.005	65,000	145
1-A-387,B; N-SR 600°F	1.315	0.205	2,500	192
	1.165	0.14	9,650	187
	.94	0.14	18,600	-
	.72	0.03	59,000	187
	.54	0.09	84,360	-
2-A-387,B; N-SR 800°F	1.22	0.07	2,300	157
	1.10	0.15	3,000	157
	1.045	0.09	3,250	-
	.925	0.115	8,000	172
	.885	0.14	14,000	159
	.765	0.045	20,000	170
	.55	0.035	50,700	169
	.56	-	160,000	157
	.64	0.025	202,000	180
2-A-387,B; N-SR 900°F	1.195	0.21	4,300	164
	.87	0.17	4,330	159
	.72	0.135	13,500	152
	.705	0.035	30,000	159
	.53	0.095	30,000	146
	.55	0.025	36,000	157
	.635	0.08	50,000	150
	.48	0.06	145,000	159

Table A-II (cont'd)
1100 cph Fatigue Data

Steel, Condition and Testing Temp.	% Total Strain	% Plastic Strain	Cycles to Failure	Brinell Hardness No.
1-"T-1"; Mill Q-T 80°F	1.39	0.24	2,600	235
	1.03	0.09	5,180	-
	.98	0.07	5,600	-
	.81	0.03	6,700	-
	.78	0.02	11,200	-
	.72	0.01	18,400	-
	.43	0.00	184,000	-
2-"T-1"; Mill Q-T 400°F	.45	0.015	116,000	262
	.97	0.07	8,100	257
	.91	0.05	7,640	257
	1.05	0,12	4,400	-
1-"T-1"; Mill Q-T 600°F	1.20	0.33	3,000	241
	1.21	0.29	3,250	-
	1.08	0.30	3,700	-
	.89	0.22	6,125	-
	.70	0.13	14,000	-
	.53	0.08	32,000	-
	.47	0.04	86,700	-
1-"T-1"; Mill Q-T 800°F	1.017	0.33	3,400	241
	.90	0.23	4,300	-
	.805	0.09	9,100	-
	.715	0.12	17,100	-
	.61	0.08	19,500	-
	.62	0.07	25,300	-
	.48	0.01	130,000	-
1-"T-1"; Mill Q-T 900°F	1.315	0.40	1,950	235
	1.095	0.36	2,500	-
	1.07	0.28	2,900	-
	.84	0.23	3,300	-
	.85	0.18	3,500	-
	.73	0.16	6,450	-
	.70	0.16	8,850	-
	.66	0.14	10,950	-
	.40	0.03	48,800	-
1-A-212,B; Q-T 80°F	1.75	0.57	1,825	140
	1.29	0.42	3,425	149
	.795	0.205	9,200	149
	.635	0.125	19,000	143
	.605	0.11	24,800	143
	.465	0.05	32,400	143
	.335	0.0	88,500	148

Table A-II (cont'd)
1100 cph Fatigue Data

Steel, Condition and Testing Temp.	% Total Strain	% Plastic Strain	Cycles to Failure	Brinell Hardness No.
2-A-212,B; Q-T 400°F	1.16	0.175	4,300	143
	.705	0.125	8,400	143
	.44	0.025	75,000	138
1-A-212,B; Q-T 600°F	1.345	0.365	2,300	157
	.915	0.185	5,800	141
	.52	0.145	18,200	148
	.395	0.03	21,000	144
	.50	0.09	26,000	157
	.38	0.0	190,000	144
2-A-212,B; Q-T 800°F	.735	0.08	4,500	137
	.75	0.095	5,000	134
	.53	0.03	20,000	-
	.35	0.075	54,000	131
	.35	0.065	80,000	137
	.31	0.03	105,500	134
1-A-212,B; Q-T 900°F	.685	0.05	4,500	133
	.67	0.155	4,800	131
	.385	0.09	24,000	141
	.23	0.025	62,000	131
	.22	0.02	113,000	-
1-A-212,B; N-SR 80°F	1.70	0.62	2,250	126
	.78	0.22	12,500	131
	.68	0.155	14,300	121
	.49	0.07	30,000	125
	.325	0.01	73,000	126
2-A-212,B; N-SR 80°F	1.14	0.405	6,200	-
	.865	0.23	12,200	131
	.64	0.145	18,500	135
	.46	0.055	38,000	-
	.405	-	47,000	-
	.31	0.0	113,500	132
2-A-212,B; N-SR 400°F	1.20	0.215	3,400	127
	.93	0.16	5,700	126
	.345	0.005	102,000	126

Table A-II (cont'd)
1100 cph Fatigue Data

Steel, Condition and Testing Temp.	% Total Strain	% Plastic Strain	Cycles to Failure	Brinell Hardness No.
1-A-212,B; N-SR 600°F	1.19	0.27	3,500	132
	1.255	0.28	3,900	131
	1.03	0.31	5,700	132
	.965	0.16	7,250	125
	.365	0.045	18,000	134
	.435	0.095	19,500	128
	.43	0.085	50,000	130
	.30	0.03	150,000	130
2-A-212,B; N-SR 800°F	.725	0.145	4,700	123
	.855	0.08	5,000	121
	.88	0.225	8,200	127
	.49	0.03	26,000	123
	.35	0.03	68,000	125
	.29	0.01	111,000	125
2-A-212,B; N-SR 900°F	.81	0.125	4,400	118
	.755	0.135	4,850	120
	.37	0.095	27,000	128
	.315	0.05	55,000	120
	.26	0.03	108,500	126

Table A-III

110 cph Fatigue Data

Steel, Condition and Testing Temp.	% Total Strain	% Plastic Strain	Cycles to Failure	Brinell Hardness No.
2-A-387,B; Q-T				
80°F	1.025	0.105	3,750	226
400°F	.93	0.135	7,400	235
600°F	1.02	0.08	3,400	235
800°F	.90	0.08	2,700	244
	.765	-	5,100	223
900°F	.975	0.075	3,400	217
2-A-387,B; N-SR	1.245	0.295	2,285	161
80°F	1.06	0.235	3,760	169
400°F	.87	0.075	7,000	149
	1.08	0.265	3,675	156
600°F	.945	0.065	2,800	149
	.99	0.19	4,000	152
800°F	.87	0.08	3,550	157
	.695	0.05	3,500	156
	.685	-	6,200	147
900°F	.775	0.05	4,600	149
2-"T-1"; Mill Q-T				
80°F	.925	0.03	5,600	241
400°F	1.11	0.13	6,250	248
600°F	.935	0.145	4,050	248
800°F	.915	0.10	2,500	255
	.87	0.035	4,600	253
900°F	.975	0.14	4,900	255
2-A-212,B; Q-T	1.315	0.445	3,600	131
80°F	.97	0.27	7,100	144
400°F	.92	0.17	11,000	137
	1.25	0.315	3,300	143
600°F	1.005	0.135	2,800	149
	.925	0.11	4,800	135
800°F	1.01	0.14	2,230	135
900°F	.93	0.10	2,300	130
2-A-212,B; N-SR	1.36	0.49	3,650	122
80°F	1.04	0.35	6,500	127
400°F	.865	0.18	6,700	126
600°F	.985	0.205	3,140	127
800°F	.935	0.13	2,700	132
900°F	.965	0.045	2,510	126

VITA

Robert Allen DePaul, son of Samuel and Emma M. DePaul, was born in Reading, Pennsylvania, on April 8, 1936. He graduated from Reading Senior High School in 1954, and entered a foundryman apprenticeship with Textile Machine Works in Wyomissing, Pennsylvania. As part of the apprentice training, he received a Certificate in Engineering Technology from The Wyomissing Polytechnic Institute in 1956. Robert was honored as an Outstanding Pennsylvania Apprentice in 1957 by the Pennsylvania Manufacturers' Association prior to receiving his Journeyman's Papers in 1958. At the completion of his apprenticeship, Robert was awarded a three-year scholarship by Textile Machine Works and entered Lehigh University in the Fall of 1958 with advanced standing as a metallurgical engineering student. While an undergraduate at Lehigh, Mr. DePaul was voted into Tau Beta Pi as a Junior and was awarded the Bradley Stoughton Student Award as a Senior. He was graduated with High Honors from Lehigh in 1961, receiving the degree of Bachelor of Science in Metallurgical Engineering.

Mr. DePaul entered the Graduate School of Lehigh in September, 1961, where he was subsequently elected to the Society of the Sigma Xi. While pursuing a program of graduate study he was engaged as a research assistant and instructor in the Department of Metallurgical Engineering.

In October of 1963, Mr. DePaul was awarded the degree Master of Science from Lehigh University. He has been a member of the American Society for Metals, the American Institute of Mining, Metallurgical, and Petroleum Engineers, the American Society for Testing and Materials, and faculty advisor to the Student Metallurgical Society while at Lehigh.